MODELING FLOW WITHIN A LIQUID DROP SLIDING ON A FLAT INCLINED SURFACE

A Thesis Submitted
in Partial Fulfilment of the Requirements
for the Degree of
Master of Technology

by

Amar Singh

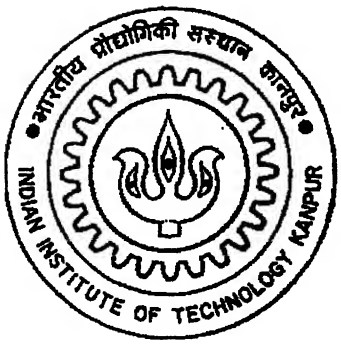

to the

NUCLEAR ENGINEERING AND TECHNOLOGY PROGRAMME
INDIAN INSTITUTE OF TECHNOLOGY KANPUR
INDIA

August 2003

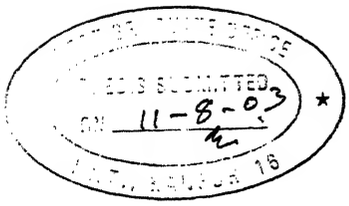

CERTIFICATE

It is certified that the work contained in the thesis entitled "**Modeling Flow within a Liquid Drop sliding on a Flat Inclined Surface**", by Amar Singh, has been carried out under our supervision and that this work has not been submitted elsewhere for a degree.

K. Muralidhar
Professor
Dept. of Mechanical Engineering
I.I.T. Kanpur 208016

L. M. Gantayet
Laser and Plasma Division
Bhabha Atomic Research Center
Mumbai 400085

August, 2003

To my parents ...

ACKNOWLEDGMENT

I feel immense pleasure and satisfaction by working with Prof. K. Muralidhar. the teacher with profound intellect and diverse interests whose brilliant guidance throughout the period of my M. Tech. thesis helped me to surpass all the obstacles smoothly. He introduced me to the subject of this thesis, guided and assisted me in difficult times and taught me the basics of research. His company not only enriches my knowledge but also widen my ways of thinking.

I would like to express my sincere gratitude to Dr. L. M. Gantayet for many invaluable suggestion, constant encouragement and generous help throughout the period of my research work.

I would like to express my sincere gratitude to Prof. P. K. Panigrahi for constant motivation and encouragement.

I am thankful to Mr. Malay Kumar Das for his generous help and motivation throughout my whole research.

I would like to thank Mr. Sushanta Dutta, Mr. Arvind Rao, Mr. Andalib Tariq, Mr. Joytirmay Banerjee, Mr. Atul Srivastava, Mr. Atanu Phukan, Mr. Pramod Pandey, Mr. Rajneesh Bhardwaj, Mr. Vinay Kumar, Mr. Shambhunath Sharma and Mr. Rajesh Singh for their pleasant company in the Laboratory.

I am thankful to all my NET classmates and friends for making my stay at IIT Kanpur enjoyable.

Amar Singh

Abstract

One of the areas of great emphasis in Bhabha Atomic Research Center (BARC) Mumbai is dropwise condensation of metal vapor on the lower side of the cooled substrate. In the present work, drop shapes are generated on and below the inclined plate. This is done for 4 different angles of inclination and 3 different liquids of different volumes. In the static case, stability analysis for the drop above and below the inclined plate is performed. Advancing and receding angles are calculated for the drop on and below the inclined plate. Center of gravity and moment calculations are performed for both configurations.

For the dynamic analysis of the drop movement, a semi-circular drop which is kept on a flat plate moving with uniform velocity is first modeled. Pressure and velocity values are calculated for the semi-circular drop, by solving the governing equations with appropriate boundary conditions. Grid independence test and code validation has also been carried out for the semi-circular drop. Coefficient of friction between the drop and plate is calculated. The assumptions taken for these calculations are that the flow is steady, incompressible and the Reynolds number is small enough for the creeping flow approximation to be valid.

The next step is grid generation for handling deformed drops. This approach is required when we have a complex geometry in the physical domain. We can transform the complex geometry from the physical to the computational domain by mapping each grid point in the physical domain to a convenient grid point in the computational domain. After the solution is obtained for all grid points in the computational domain, the solution is again mapped into the physical domain

through the transformation relations. The governing equations and boundary conditions are also transformed into the computational domain. In the present work, the physical domain is a deformed drop geometry while the computational domain is a semi-circular drop. Coefficient of friction has been calculated on the plate for the deformed drop in the physical domain. Results show that the coefficient of friction increases as Reynolds number and Weber number decreases. The effect of deformation is seen in the local pressure and velocity fields, but the overall impact on the coefficient of friction is small.

A proposal for solving high Reynolds number flows, energy equation, treatment of a cluster of drops and coalescence of adjacent drops has also been presented.

Contents

List of Figures

Nomenclature

Dimensional quantities

r^*	Radial distance, m
r_1	Characteristic length, m
u_0	Plate velocity, m/s
u^*	Fluid velocity in r direction, m/s
v^*	Fluid velocity in θ direction, m/s
t^*	Fluid inlet temperature, ^oC
p^*	Pressure inside the liquid drop, N/m^2

Greek Symbols

ρ	Fluid density, kg/m^3
ν	Kinematic viscosity of fluid, m^2/s
γ	Surface tension force per unit length, N/m
ψ	Contact angle
θ_c	Contact angle for a particular liquid
θ_p	Plate inclination angle
φ^*	Stream function m^2/s
ω^*	Vorticity /s

Non-dimensional quantities

r	r^*/r_1	Radial distance.
θ	θ	Angular distance.
ξ	ξ^*/ξ_1	Radial distance in computational domain.
η	η	Angular distance in computational domain.
u	u^*/u_0	Velocity in radial direction.
v	v^*/u_0	Velocity in angular direction.
p	$(p^* - p^*_{amb})/\rho u_0^2$	Pressure difference within the drop.
t	$t^* u_0/r_1$	Time.
φ	$\varphi^*/u_0 r_1$	Stream function.
ω	$\omega^* r_1/u_0$	Vorticity.
Re	$u_0 r_1/\nu$	Reynolds number.
Pr	ν/α	Prandtl number.
Fr	$u_0/\sqrt{(g r_1)}$	Froude number.
Pe	$u_0 r_1/\alpha$	Peclet number.
T	$(T^* - T^*_f)/(T^*_i - T^*_f)$	Computed non-dimensional fluid temperature.

Chapter 1

Introduction

Condensation of metallic vapor on the lower side of a cooled substrate, is one of the important areas of research in Bhabha Atomic Research Center (BARC), Mumbai. The process of vaporization and condensation takes place in a vacuum chamber, this is because the electron beam used to vaporize the metal from the crucible, does not interacts with any other material present, and thus efficiency achieved in vaporization is very high. In condensation, the condensation sites are either available on the substrate or on the dust particles suspended in the air, but as there is vacuum the process of condensation takes principally on the substrate.

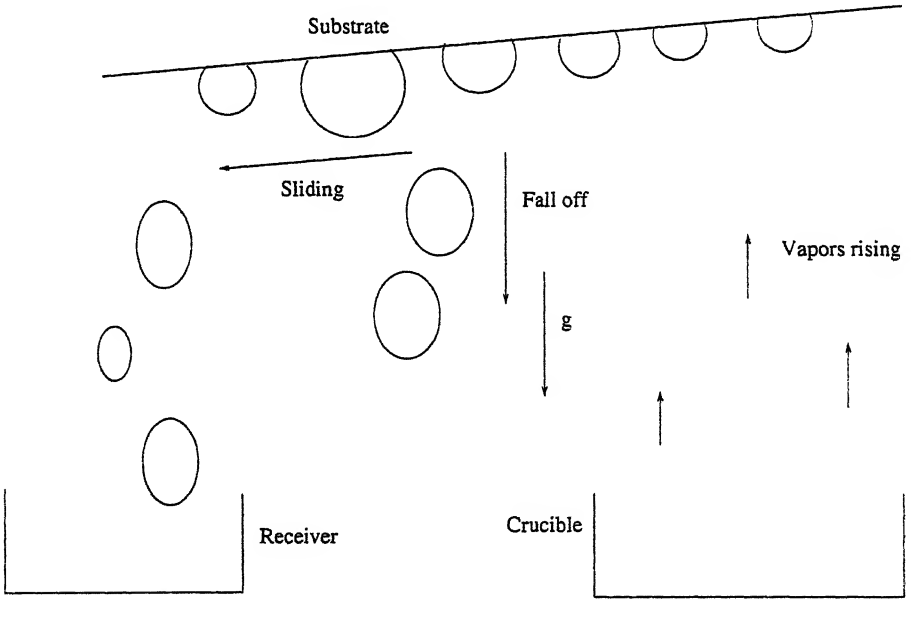

Figure 1.1: Typical arrangement involving condensation of metal vapor.

Arrangement involving condensation of metal vapor is shown in Figure 1.1. The metal material to be vaporized is kept in a water cooled crucible. The crucible material should be such that it should have limited or no solubility with the metal kept in it. The electron beam used to vaporize the metal from the crucible has a power rating of about 3kW and a peak value of 30kW. The electron beam. which is incident on the metal material in the crucible, makes an angle of 45^0 to the horizontal. Crucible is used because it facilitates the batch evaporation of the metal for a long period of time.

The stagnation temperature of the vapor is 1500K and the temperature of the substrate is 900K. So there is a large temperature gradient due to which condensation on the substrate is independent of the temperature difference. As the metal vapors rise in the vacuum chamber and reach the substrate, they are condensed on it.

The substrate should have such surface composition and thermo-physical properties that it permits dropwise condensation of metal vapors on it. It is tilted to $7-15^0$ to the horizontal to make the drainage of drops effective. Although the distribution of condensation sites is usually random, on an average, the density of nucleation sites is of the order of $10^4 sites/cm^2$. However the substrate surface can be made to have a preferred orientation.

When a drop is condensed on the substrate, its initial growth is due to the additional condensation of the vapor. But as time passes the drop size increases and inter-drop distance decreases. At a particular value of the drop radius and inter-drop distance the drop will coalesce with one or more drops around it. Condensation results in sudden increase in the radius of the drop and also its surface area. As the sum of the surface areas occupied by the drops individually before coalescence is greater than the surface area occupied by the single drop after coalescence, so the condensation is accelerated as now more surface is available for condensation.

After the process of condensation and coalescence have been initiated, at any instant of time, the substrate contains drops of various sizes. When a critical size of the drops is achieved, it can either fall-off or come down the substrate. When a drop comes down the substrate, it can slide or roll-down. But sliding motion is more prevalent than rolling motion in practical applications. As the drops slides down the substrate, they are collected in a receptor. Moreover, the

sliding process can further facilitate the coalescence.

Dropwise condensation is a complex process. In order to simulate the whole process from dropwise condensation till the drops are collected in a receptor, it is necessary to develop a model for an individual drop. Thus, the present work deals with the modeling of an individual drop.

This work starts from the simulation of drop shapes on an inclined surface, both above and below. Static drops involve estimation of threshold angle of inclination of the flat plate for which the drop will begin to slide. Then, when there is relative motion between the drop and the inclined plate, the velocity and pressure values inside the drop are numerically computed. The assumptions are that the flow within the drop is steady, incompressible and of low Reynolds number. The main purpose of studying the patterns of velocity and pressure inside the drop is to estimate the coefficient of friction between the flat plate and the drop. A proposal for obtaining pressure and velocity values for high Reynolds number flows, for the treatment of drop cluster and coalescence, and for obtaining unsteady temperature distribution inside the drop is also given.

1.1 Literature Review

A survey of the available literature has been presented below as per the following sections: (1) Threshold for movement of a drop down an inclined flat plate, (2) Droplet growth and coalescence.

1.1.1 Threshold for movement of a drop down an inclined flat plate

Furmidge (1961) studied the sliding of liquid drops on inclined solid surfaces and also gave a theory for spray retention. He did the study for spray liquids. He concluded that surface properties of the spray liquid/solid combination are among the most important factors controlling the retention of spray liquids on solid surfaces. The spray liquid he used was water and solutions of surfactants, while solid surfaces he used was wax and cellulose acetate surfaces. A theory, supported by experimental results, has been evolved by him in which he tried to explain the movement of drops in terms of the size of the drop, the angle of tilt of the surface, the air/liquid surface tension, and the advancing and receding

contact angles. Thus for a given liquid on a given surface.

$$\frac{mg\sin\alpha}{w} = H \tag{1.1}$$

where H is given by

$$H = \gamma_{AL}(\cos\theta_R - \cos\theta_A) \tag{1.2}$$

For a particular liquid/solid combination H may not be a constant.
m is the mass of the drop.
α is the angle of tilt of the surface necessary to produce sliding of the drop.
w is width of the drop on the solid surface.

Dimitrakopoulos and Higdon (1999) studied the yield conditions for the gravitational displacement of three-dimensional fluid droplets from inclined solid surfaces through a series of numerical computations. The study considers both sessile and pendant droplets and includes interfacial forces with constant surface tension. Their study seeks the optimal shape of the contact line which yields the maximum displacing force ($B_T = B_d \sin\beta$), B_d is the Bond number and β is the angle of inclination. This maximum displacing force is that for which a droplet can adhere to the surface.

Kim *et al.* (2002) have studied the sliding velocity of a liquid drop which partially wets a solid surface. This drop will slide down when the plane is tilted beyond a critical inclination. Experiments for measuring the steady sliding velocity of different liquids of drops were performed by them. Then they constructed a scaling law which predicts the sliding velocity given the physical properties, wetting characteristics, and size of the drop. When the sliding velocity is low and drop distortion due to inclination is small, the scaling law is shown to correctly model the functional dependency of the measured sliding velocity.

1.1.2 Droplet growth and coalescence

The formation of a distribution of various size droplets is a characteristic feature of many systems from thin films to fog and clouds. Family *et al.* (1989) have presented the results of their investigations of the kinetics of droplet growth and coalescence. In general, droplet formation occurs either by spontaneous nucleation or by growth from heterogeneously distributed nucleation centers, such as impurities. Two models have been introduced by them to describe these two

types of processes. In the homogeneous nucleation model droplets can form and grow anywhere in the system. The authors also introduce a heterogeneous nucleation model for studying processes in which droplets only form and grow at certain nucleation centers which are initially chosen at random. Simulations. scaling theory, and a kinetic equation approach for describing the two models have been presented by them. The theoretical predictions are found to be in excellent agreement with the simulations.

When two drops of radius R touch, surface tension drives an initially singular motion which joins them into a bigger drop with smaller surface area. The motion is always viscously dominated at early times. Eggers *et al.* (1999) have focused on the early-time behavior of the radius r_m of the small bridge between the two drops. They have also studied numerically the case of coalescence with an external viscous fluid analytically and the case of equal viscosities.

1.2 Scope of the Present Work

Earlier work primarily deals with generation of drop shapes above and below the inclined and horizontal flat plates. It has not included the stability analysis for a drop kept on an inclined plate or hanging below from an inclined plate. Modeling of flow inside the drop sliding down the flat inclined plate has also not been reported.

The present work is concerned with not only the generation of drop shapes above and below the inclined and horizontal plates, but also involves their stability analysis. Moreover, when the drop is in motion, detailed modeling (for steady, incompressible and low Reynolds number flow) is carried for obtaining velocity and pressure values inside the drop. The coefficient of friction is also estimated for the sliding motion of the drop.

A proposal for studying flow fields at high Reynolds numbers, solution of the unsteady energy equation, and treatment of a drop cluster and coalescence is also included in the thesis.

1.3 Objectives

The specific objectives of the present study are as follows:

1. The stability analysis for a sessile or pendant drop, kept on an inclined flat surface.
2. Solution for pressure and velocity in circular and deformed drops for Stokes flow.
3. Unsteady temperature distribution for the deformed drop.
4. The coefficient of friction for circular and deformed drops.

1.4 Thesis Organization

The present thesis has been organized in the following manner:

1. Chapter 1 presents introduction, literature review and scope of the present research.
2. Chapter 2 describes the determination of drop shapes on an inclined surface under static conditions, and stability analysis
3. Chapter 3 describes mathematical modeling of flow in a sliding semi-circular drop.
4. Chapter 4 presents numerical solution for flow in a sliding semi-circular drop.
5. Chapter 5 describes the grid generation methodology for a drop of a deformed shape.
6. Chapter 6 presents the derivation of pressure-velocity equations in transformed coordinates and boundary conditions.
7. Chapter 7 describes the numerical solution of the governing equations in transformed coordinates.

8. Chapter 8 is a proposal for studying flow fields at higher Reynolds numbers, solution of the energy equation, treatment of a drop cluster and drop coalescence.

9. Chapter 9 reports conclusions and scope for future work.

Chapter 2

Determination of drop shapes on an inclined surface under static conditions

Much work has been done on generating drop shapes on inclined surfaces. Extensive modeling and simulation has been reported for the relevant physical phenomena in static and moving drops.

2.1 Survey of approaches reported in the literature

Much literature is available on the shape of the drops on different configurations of the solid surface. Orr *et al.* (1975) determined interface shapes by using the surface representation $z = z(x, y)$ in Cartesian coordinates. Their representation was unsatisfactory because the function becomes multi-valued at certain tilt angle, specificall when the advancing angle exceeds 90^0. Multiple values should be avoided because they require the solution of coupled mathematical problems of considerably greater complexity. Brown *et al.* (1980) suggested the spherical coordinate system $r = f(\theta, \phi)$ to solve the Young-Laplace equation. They implemented a Galerkin finite element method to solve for the shape of a three-dimensional drop on an inclined plate. Drop shapes for different volumes and different tilt angles of the plate were simulated. It was observed that smaller drops deform less than larger ones, keeping other aspects same. Karmakar (2001) has also generated drop shapes both above and below a flat inclined surface. He generated the drop shapes on the inclined surface and then transformed them to

the horizontal.

2.2 Formulation

For generating static drop shapes, one has to implement the Laplace-Young equation. Let us consider a certain control volume that is occupied entirely by a fluid and is fixed in space. As the fluid flows, molecules enter and leave the control volume from all sides carrying momentum and thus imparting to the fluid that occupies the control volume, at a particular instant in time, a normal force. Furthermore, short-range intermolecular forces cause the molecules that are located on either side of the boundary of the control volume to be attracted, thereby generating an effective frictional force. The force exerted on an infinitesimal surface element of the boundary of the control volume is called the *surface stress* or *traction*, and will be denoted by $\mathbf{f}$. Clearly, the value of $\mathbf{f}$ will depend upon both the position and orientation of the infinitesimal surface element (Pozrikidis 1997).

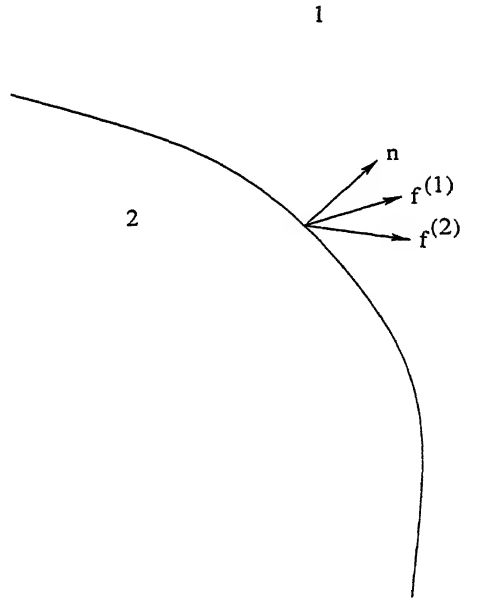

Figure 2.1: Schematic illustration of an interface between two fluids.

In general, the tractions exerted on the two sides of an interface between two fluids labeled 1 and 2 have two different values, with a corresponding discontinuity

$$\Delta\mathbf{f} \equiv \mathbf{f}^{(1)} - \mathbf{f}^{(2)} = (\sigma^{(1)} - \sigma^{(2)}) \cdot \mathbf{n} \tag{2.1}$$

where $\mathbf{n}$ is the unit normal vector *pointing into fluid 1*, as shown in Figure 2.1. and $\sigma^{(1)}$ and $\sigma^{(2)}$ are the stress tensors within the two fluids evaluated at the interface. The direction and magnitude of the discontinuity of the interfacial traction $\Delta\mathbf{f}$ depend upon the mechanical properties of the interface, which are determined by the physico-chemical properties of the fluids and molecular structure of the interface, and are therefore affected by the presence of surface-active substance es. An equation that relates $\Delta\mathbf{f}$ to the velocity field, the properties of the fluids, and the shape and thermodynamic properties of the interface, is called a *constitutive equation for the discontinuity in the interfacial traction.*

The most common type of interfacial behavior pertains to uncontaminated interfaces between two immiscible fluids characterized by isotropic surface tension γ, which may be regarded as a kind of energy per unit surface area or surface pressure. The physical origin of surface tension may be traced to differences in the attraction forces between the molecules of the two liquids. In general, the surface tension decreases as the temperature is raised, and vanishes when the temperature reaches the boiling point.

To derive the constitutive equation for $\Delta\mathbf{f}$, we assume that the interfacial stratum has negligible mass and write a force balance over a small section of th e interface D that is bounded by the contour C, as shown in Figure 2.2, requiring (Pozrikidis 1997),

$$\int_D \Delta\mathbf{f}\,dS + \int_C \gamma\mathbf{t}\times\mathbf{n}\,dl = \mathbf{0} \tag{2.2}$$

where $\mathbf{n}$ is the unit vector normal to D pointing into 1, $\mathbf{t}$ is the unit vector tangential to C, and $\mathbf{t}\times\mathbf{n}\equiv\mathbf{b}$ is the binormal vector as shown in Figure 2.2.

Furthermore, the domain of definition of the surface tension and normal vector can be extended from the interface into the whole space. The first extension can be done in an unrestricted manner, whereas the second extension is done by setting $\mathbf{n} = \nabla F/\mid\nabla F\mid$, where the equation $F(x,y,z) = 0$ describes the instantaneous location of the interface. A variation of Stokes's theorem states that for any arbitrary vector function $\mathbf{F}$,

$$\int_C \mathbf{F}\times\mathbf{t}\,dl = \int_D (\mathbf{n}\nabla\cdot\mathbf{F} - (\nabla\mathbf{F})\cdot\mathbf{n})\,dS \tag{2.3}$$

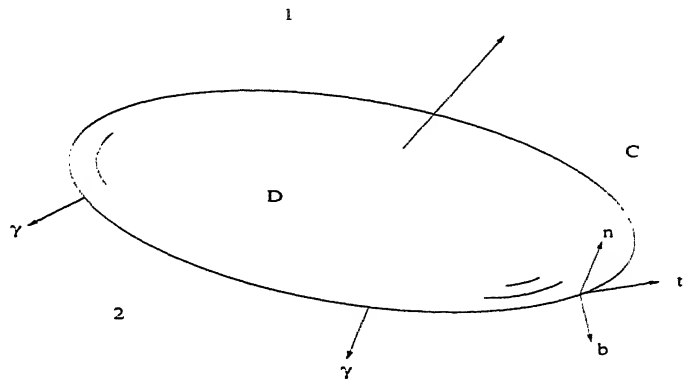

Figure 2.2: Surface tension acting along the edges of a test section of an interface.

Applying Equation (2.3) with $\mathbf{F} = \gamma\mathbf{n}$ and combining the resulting expression with Equation (2.2), we obtain

$$\int_D \Delta\mathbf{f}\, dS = \int_D [\mathbf{n}\nabla \cdot (\gamma\mathbf{n}) - (\nabla(\gamma\mathbf{n})) \cdot \mathbf{n}]\, dS \tag{2.4}$$

We now take the limit as D shrinks down to a point, expand out the derivatives within the integrand on the right-hand side, and thus obtain the desired constitutive equation

$$\Delta\mathbf{f} = \gamma\mathbf{n}\nabla \cdot \mathbf{n} - (\mathbf{n} \times \nabla\gamma) \times \mathbf{n} \tag{2.5}$$

The first and second terms in the right hand side of Equation (2.4) express, respectively, discontinuities in the normal and tangential directions. When the surface tension is uniform, the tangential component vanishes, and the jump in the interfacial traction points in the normal direction.

The divergence of the normal vector on the right-hand side of Equation (2.4) is equal to twice the mean curvature of the interface, denoted by κ_m,

$$\nabla \cdot \mathbf{n} = 2\kappa_m \tag{2.6}$$

By definition, the mean curvature is positive when the interface has a spherical shape with 2 lying inside and the normal vector pointing outward.

The normal component of the traction and thus the pressure undergo a discontinuity across an interface. To compute the jump in pressure in terms of the velocity, we resolve $\Delta\mathbf{f}$ into its normal and tangential components, and then we can have an expression for normal component as

$$\Delta\mathbf{f} = [-p_1 + p_2 + 2\mathbf{n}\cdot(\mu_1\nabla\mathbf{u}^{(1)} - \mu_2\nabla\mathbf{u}^{(2)})\cdot\mathbf{n}]\mathbf{n} + \mathbf{n}\times\Delta\mathbf{f}\times\mathbf{n} \tag{2.7}$$

Projecting Equation (2.7) onto the normal vector n produces the jump in interfacial pressure in terms of the normal component of $\Delta\mathbf{f}$ and the viscous normal stresses,

$$\Delta p \equiv p_1 - p_2 = -\Delta\mathbf{f}\cdot\mathbf{n} + 2\mathbf{n}\cdot(\mu_1\nabla\mathbf{u}^{(1)} - \mu_2\nabla\mathbf{u}^{(2)})\cdot\mathbf{n} \tag{2.8}$$

where $\Delta\mathbf{f}$ is given by an appropriate interfacial constitutive equation.

For example, when the fluids are stationary or inviscid, the second and third terms on the right-hand side of Equation (2.8) are absent. Assuming that the interface exhibits uniform isotropic tension, and using Equation (2.5), we find $\Delta p = -2\kappa_m\gamma$

The Navier-Stokes equation in an inertial frame of reference for a fluid that is stationary or translates with a uniform velocity $\mathbf{u} = \mathbf{U}(t)$ takes the simplified form

$$\rho\frac{d\mathbf{U}}{dt} = -\nabla p + \rho\mathbf{g} \tag{2.9}$$

Assuming that the density of the fluid is uniform and solving for the pressure, we obtain (Pozrikidis 1997)

$$p = \rho\left(\mathbf{g} - \frac{d\mathbf{U}}{dt}\right)\cdot\mathbf{x} + A(t) \tag{2.10}$$

where A(t) is a time-dependent constant whose value must be found by requiring an appropriate boundary condition.

Using the definition, Equation (2.1), the pressure distribution given in Equation (2.10) with vanishing acceleration, and the constitutive equation for the jump

in the interfacial traction given in Equation (2.5), we write

$$\Delta \mathbf{f} \equiv (\sigma^{(1)} - \sigma^{(2)}) \cdot \mathbf{n} = (p_2 - p_1)\mathbf{n} \tag{2.11}$$

where $\Delta\rho = \rho_2 - \rho_1$, A_1 and A_2 are two constants. $\mathbf{n}$ is the unit normal vector pointing into 1, and κ_m is the mean curvature of the interface. Rearranging Equation (2.11), we obtain the Laplace-Young equation

$$2\kappa_m = \frac{\Delta\rho}{\gamma}\mathbf{g} \cdot \mathbf{x} + B \tag{2.12}$$

where $B = (A_2 - A_1)/\gamma$ is a new constant with dimensions of inverse length.

For drop on an inclined surface the symmetricity of the drops is destroyed. Hence we need a two dimensional formulation that is applicable for unsymmetric interfaces. For a two dimensional surface the mean curvature is given by

$$\kappa_m = -\frac{1}{2}\frac{f''}{(1+f'^2)^{\frac{3}{2}}} \tag{2.13}$$

Using the Laplace-Young equation (2.12)

$$-\frac{1}{2}\frac{f''}{(1+f'^2)^{\frac{3}{2}}} = \frac{\Delta\rho}{\gamma}\mathbf{g} \cdot \mathbf{x} + B \tag{2.14}$$

This on simplification gives

$$f'' = \left(\frac{\Delta\rho}{\gamma}gy - B\right)(1+f'^2)^{\frac{3}{2}} \tag{2.15}$$

Substituting the capillary number $l = (\gamma/\Delta\rho g)^{1/2}$ in Equation (2.15), the governing equation is derived as

$$f'' = \left(\frac{y}{l^2} - B\right)(1+f'^2)^{\frac{3}{2}} \tag{2.16}$$

To solve Equation (2.16) numerically, we introduce the parameter ψ, which is defined by $\tan\psi = -f'$, and ranges from zero at the centerline of the drop to

the value of the contact angle α at the contact line. Performing the following calculations

$$\begin{aligned} f'' &= \frac{df'}{dx} = \frac{df'}{d\psi}\frac{d\psi}{dx} \\ &= \frac{d(-\tan\psi)}{d\psi}\frac{d\psi}{dx} = -\frac{1}{\cos^2\psi}\frac{d\psi}{dx} \end{aligned} \tag{2.17}$$

and

$$\frac{dy}{d\psi} = \frac{dy}{dx}\frac{dx}{d\psi} = -\tan\psi\frac{dx}{d\psi} \tag{2.18}$$

Substituting Equation (2.17) and Equation (2.18) in Equation (2.16), we get

$$-\frac{1}{\cos^2\psi}\frac{d\psi}{dx} = \left(\frac{y}{l^2} - B\right)(1+\tan^2\psi)^{\frac{3}{2}} \tag{2.19}$$

or

$$\begin{aligned} -\frac{1}{\cos^2\psi}\frac{d\psi}{dx} &= \left(\frac{y}{l^2} - B\right)\frac{1}{\cos^3\psi} \\ \frac{d\psi}{dx} &= -\left(\frac{y}{l^2} - B\right)\frac{1}{\cos\psi} \\ \frac{dx}{d\psi} &= -\frac{\cos\psi}{\left(\frac{y}{l^2} - B\right)} \end{aligned} \tag{2.20}$$

From Equation (2.18) and Equation (2.20), we get

$$\frac{dy}{d\psi} = \frac{\sin\psi}{\left(\frac{y}{l^2} - B\right)} \tag{2.21}$$

Hence, the first order system is derived as

$$\begin{aligned} \frac{dx}{d\psi} &= -\frac{\cos\psi}{w} \\ \frac{dy}{d\psi} &= \frac{\sin\psi}{w} \\ \text{where } w &= \left(\frac{y}{l^2} - B\right) \end{aligned} \tag{2.22}$$

2.3 Earlier Method

Equation (2.22) is to be solved with the boundary conditions

$$\begin{aligned} x(\alpha_A) &= x_0 \\ y(\alpha_A) &= 0 \\ \text{where } \psi &= \alpha_A \text{ to } -\alpha_R \end{aligned} \tag{2.23}$$

α_A is advancing angle and α_R is receding angle
The volume constraint is also applicable, namely

$$\begin{aligned} \int x^2 dy &= \frac{\text{Volume of the drop}}{\pi} \\ x(\alpha_A) &= x_0 \end{aligned} \tag{2.24}$$

where x_0 is the starting x coordinate of the drop as when kept on the horizontal plate. To solve the Equation (2.22), the following procedure was used by Karmakar (2001).

1. There are several unknowns. One is the radius of the drop and second is the constant B. In addition α_A and α_R are also unknown. To simplify the problem we assume that the contact line is pinned and does not change with inclination. Then we solve for zero inclination to get the radius of the drop.

2. Start the integration with the initial condition, Equation (2.23), and an assumed value of B. Integrate the equation using the 4^{th} order Runge-Kutta method till $\psi = \alpha$. Then we calculate the volume. If it matches the prescribed volume, terminate the iterations; otherwise change the value of B using the Newton-Raphson method.

3. After getting the value of B and radius, we start the integration with the initial condition $\psi = -\alpha$. Continue the integration till the angle equivalent to the plate inclination is reached. Reject all the points ahead and continue the integration till the curve (representing the drop) intersects the inclination line. Stop the integration.

4. Transform the inclined drop in normal plane. To satisfy the conditions, Equation (2.24), we need scaling. To satisfy the radius constraint we performed x scaling and to conserve the volume, the y coordinates were scaled.

2.4 Method Employed in the Present Work

Equation (2.22) is to be solved with the boundary conditions

$$\begin{aligned} x(\alpha_A) &= x_0 \\ y(\alpha_A) &= 0 \\ \text{where } \psi &= \alpha_A \text{ to } \alpha_R \end{aligned} \tag{2.25}$$

α_A is advancing angle and α_R is receding angle

$$\begin{aligned} \alpha_A &= \theta_c \\ \alpha_R &= \theta_p - \theta_c \end{aligned} \tag{2.26}$$

The volume constraint is also applicable, namely

$$\begin{aligned} \int x^2 dy &= \frac{\text{Volume of the drop}}{\pi} \\ x(\alpha_A) &= x_0 \end{aligned} \tag{2.27}$$

where x_0 is the starting x coordinate of the drop as when kept on the horizontal plate. The numerical algorithm is as follows

1. There are several unknowns. These are namely, constant B, α_A, θ_p, x_0, volume. These are provided as starting parameters for the problem, except constant B. To simplify the problem we assume that the contact line is pinned and does not change with inclination.

2. Start the integration with the initial condition, Equation (2.25), and an assumed value of B. Integrate the equation using the 4^{th} order Runge-Kutta method for $\psi = \alpha_A$ to $\psi = \alpha_R$. Then we calculate the volume. If it matches the prescribed volume, terminate the iterations; otherwise change the value of B using the Newton-Raphson method.

3. After getting the value of B, we start the integration with the initial condition $\psi = \alpha_A$ to $\psi = \alpha_R$. Stop the integration.

Karmakar (2001) generated the drop shapes above and below the inclined surface and transformed them to the horizontal. On the other hand the method employed in the present work, generates the drop shapes on the incline for different angles of inclination of the surface. This method gives a more clear picture of the drop shape on or below an inclined surface than method followed by Karmakar (2001). Also in experimental work the results can be easily related to the drop on or below the incline rather with the drop shape which has been transformed to the horizontal.

2.5 Numerical Technique

The numerical technique employed in solving the first order coupled ordinary differential equations, Equation (2.22) is the 4^{th} order Runge-Kutta method. For a single dependent variable, we have

$$\begin{aligned} \frac{dy}{dt} &= f(t,y) \\ y(t_n) &= y_n \end{aligned} \tag{2.28}$$

The 4^{th} order Runge-Kutta algorithm for solving Equation (2.28) is

$$\begin{aligned} y_{n+1} &= y_n + h\left(\frac{k_1}{6} + \frac{k_2}{3} + \frac{k_3}{3} + \frac{k_4}{6}\right) + O(h^5) \\ k_1 &= f(t_n, y_n) \\ k_2 &= f(t_n + \frac{h}{2}, y_n + h\frac{k_1}{2}) \\ k_3 &= f(t_n + \frac{h}{2}, y_n + h\frac{k_2}{2}) \\ k_4 &= f(t_n + h, y_n + hk_3) \end{aligned} \tag{2.29}$$

For Equation (2.22), there are two dependent variables x and y, and only one independent variable ψ.

2.6 Formulation for drop shape below a surface

The Laplace-Young equation for a pendant drop is

$$-\frac{1}{2}\frac{f''}{(1+f'^2)^{\frac{3}{2}}} = \frac{\Delta\rho}{\gamma}\mathbf{g}\cdot\mathbf{x} + B \tag{2.30}$$

when the drop is below an inclined flat plate

$$-\frac{1}{2}\frac{f''}{(1+f'^2)^{\frac{3}{2}}} = -\frac{\Delta\rho}{\gamma}gy + B \tag{2.31}$$

This on simplification gives

$$f'' = \left(-\frac{\Delta\rho}{\gamma}gy - B\right)(1+f'^2)^{\frac{3}{2}} \tag{2.32}$$

Substituting the capillary number $l = (\gamma/\Delta\rho g)^{1/2}$ in Equation (2.27), the governing equation is derived as

$$f'' = \left(-\frac{y}{l^2} - B\right)(1+f'^2)^{\frac{3}{2}} \tag{2.33}$$

To solve Equation (2.28) numerically, we introduce the parameter ψ, which is defined by $\tan\psi = -f'$, and ranges from zero at the centerline of the drop to the value of the contact angle α at the contact line. Performing the following calculations

$$\begin{aligned} f'' &= \frac{df'}{dx} = \frac{df'}{d\psi}\frac{d\psi}{dx} \\ &= \frac{d(-\tan\psi)}{d\psi}\frac{d\psi}{dx} = -\frac{1}{\cos^2\psi}\frac{d\psi}{dx} \end{aligned} \tag{2.34}$$

and

$$\frac{dy}{d\psi} = \frac{dy}{dx}\frac{dx}{d\psi} = -\tan\psi\frac{dx}{d\psi} \tag{2.35}$$

Substituting Equation (2.29) and Equation (2.30) in Equation (2.28). we get

$$-\frac{1}{\cos^2\psi}\frac{d\psi}{dx} = \left(-\frac{y}{l^2} - B\right)(1+\tan^2\psi)^{\frac{3}{2}} \tag{2.36}$$

or

$$\begin{aligned} -\frac{1}{\cos^2\psi}\frac{d\psi}{dx} &= \left(-\frac{y}{l^2} - B\right)\frac{1}{\cos^3\psi} \\ \frac{d\psi}{dx} &= -\left(-\frac{y}{l^2} - B\right)\frac{1}{\cos\psi} \\ \frac{dx}{d\psi} &= \frac{\cos\psi}{\left(\frac{y}{l^2} + B\right)} \end{aligned} \tag{2.37}$$

From Equation (2.30) and Equation (2.32), we get

$$\frac{dy}{d\psi} = -\frac{\sin\psi}{\left(\frac{y}{l^2} + B\right)} \tag{2.38}$$

Hence, the first order system is derived as

$$\begin{aligned} \frac{dx}{d\psi} &= \frac{\cos\psi}{w} \\ \frac{dy}{d\psi} &= -\frac{\sin\psi}{w} \\ \text{where } w &= \left(\frac{y}{l^2} + B\right) \end{aligned} \tag{2.39}$$

2.7 Earlier Method

Equation (2.39) is to be solved with the boundary conditions

$$\begin{aligned} x(\alpha_A) &= x_0 \\ y(\alpha_A) &= 0 \\ \text{where } \psi &= \alpha_A \text{ to } -\alpha_R \end{aligned} \tag{2.40}$$

α_A is advancing angle and α_R is receding angle The volume constraint is also applicable, namely

$$\begin{aligned} \int x^2 dy &= \frac{\text{Volume of the drop}}{\pi} \\ x(\alpha_A) &= x_0 \end{aligned} \tag{2.41}$$

where x_0 is the starting x coordinate of the drop as when kept on the horizontal plate. To solve the Equation (2.39), the following procedure was used by Karmakar (2001).

1. There are several unknowns. One is the radius of the drop and second is the constant B. In addition α_A and α_R are also unknown. To simplify the problem we assume that the contact line is pinned and does not change with inclination. Then we solve for zero inclination to get the radius of the drop.

2. Start the integration with the initial condition, Equation (2.40), and an assumed value of B. Integrate the equation using the 4^{th} order Runge-Kutta method till $\psi = \alpha$. Then we calculate the volume. If it matches the prescribed volume, terminate the iterations; otherwise change the value of B using the Newton-Raphson method.

3. After getting the value of B and radius, we start the integration with the initial condition $\psi = -\alpha$. Continue the integration till the angle equivalent to the plate inclination is reached. Reject all the points ahead and continue the integration till the curve (representing the drop) intersects the inclination line. Stop the integration.

4. Transform the inclined drop in normal plane. To satisfy the conditions (2.41) we need scaling. To satisfy the radius constraint we performed x scaling and to conserve the volume, the y coordinates were scaled.

2.8 Method Employed in the Present Work

Equation (2.39) is to be solved with the boundary conditions

$$\begin{aligned} x(\alpha_R) &= x_0 \\ y(\alpha_R) &= 0 \\ \text{where } \psi &= \alpha_R \text{ to } \alpha_A \end{aligned} \tag{2.42}$$

α_A is advancing angle and α_R is receding angle

$$\begin{aligned} \alpha_A &= \theta_p - \theta_c \\ \alpha_R &= \theta_c \end{aligned} \tag{2.43}$$

The volume constraint is also applicable, namely

$$\begin{aligned} \int x^2 dy &= \frac{\text{Volume of the drop}}{\pi} \\ x(\alpha_R) &= x_0 \end{aligned} \tag{2.44}$$

where x_0 is the starting x coordinate of the drop as when kept on the horizontal plate. The numerical algorithm is as follows.

1. There are several unknowns. These are namely, constant B, α_A, θ_c, θ_p, x_0, volume. These are provided as starting parameters for the problem, except constant B. To simplify the problem we assume that the contact line is pinned and does not change with inclination.

2. Start the integration with the initial condition, Equations (2.40), and an assumed value of B. Integrate the equation using the 4^{th} order Runge-Kutta method for $\psi = \alpha_R$ to $\psi = \alpha_A$. Then we calculate the volume. If it matches the prescribed volume, terminate the iterations; otherwise change the value of B using the Newton-Raphson method.

3. After getting the value of B, we start the integration with the initial condition $\psi = \alpha_R$ to $\psi = \alpha_A$. Stop the integration.

2.9 Numerical Technique

Numerical technique adopted for solving Equation (2.39) is 4^{th} order Runge-Kutta method of Section 2.5.

2.10 Stability Analysis

Properties of fluids used are as follows:

Table1. Properties of Fluids used.

S.No.	Fluid used	Density (kg/m^3)	Surface Tension (N/m)	Capillary Number (m)
1	Water	1000	0.07	0.0026752
2	Bismuth	10401.8	0.39557	0.0019699
3	Mercury	13545.9	0.486226	0.0019138

Stability analysis for the sessile drop above the incline and pendant drop below the incline, are separately carried out.

2.10.1 Sessile Drop

Center of gravity is calculated by taking the mass of any element as $\rho dxdy$. Then center of gravity coordinates (x_{cg}, y_{cg}) are given by

$$x_{cg} = \frac{\int\int x\rho dxdy}{\int\int \rho dxdy}$$
$$y_{cg} = \frac{\int\int y\rho dxdy}{\int\int \rho dxdy} \tag{2.45}$$

The advancing angle is calculated from the slope of the line joining the first and the second coordinate of the equation describing the drop shape. The receding angle calculation is done from the slope of the line joining the last and the last but one coordinate of the equation describing the drop shape.

Moment calculations for forces acting on a sessile drop, as shown in Figure 2.3, are given below:

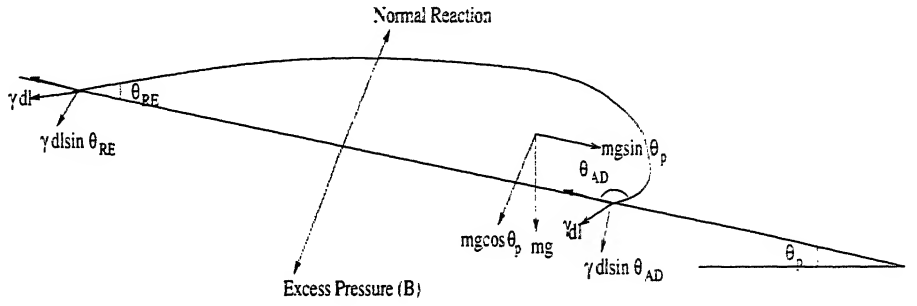

Figure 2.3: Force analysis for a sessile drop.

$$\text{Normal Reaction} = mgcos\theta_p + 2BR_1 + 2\gamma R_1[sin(\theta_{AD}) + sin(\theta_{RE})] \quad (2.46)$$

where mg is the magnitude of the weight force of the liquid, comprising the drop, B is the excess pressure term (difference between the ambient and pressure inside the drop), R_1 is the radius of the span which the drop covers on the flat inclined plate, γ is the surface tension, θ_{AD} is the advancing angle of the drop, θ_{RE} is the receding angle of the drop.
Taking moment about the advancing angle of the drop, we have

$$\begin{aligned} \text{Moment} &= (\text{Normal Reaction})R_1 + mgsin\theta_p[y_{cg}cos\theta_p - \mid x_1 - x_{cg} \mid sin\theta_p] \\ &\quad -mg(x_1 - x_{cg}) - BR_1 - 4\gamma R_1^2 sin\theta_{RE} \end{aligned} \quad (2.47)$$

where x_1 is the x coordinate of the advancing angle point of the drop.
On the other hand, considering only the forces which make the drop move along the incline, moment is calculated as follows:

$$\text{Moment1} = mgsin\theta_p[y_{cg}cos\theta_p - \mid x_1 - x_{cg} \mid sin\theta_p] - 4\gamma R_1^2 sin\theta_{RE} \quad (2.48)$$

For a three dimensional drop, only moment of those forces which make the drop move down the incline, as shown in Figure 2.4, is calculated as

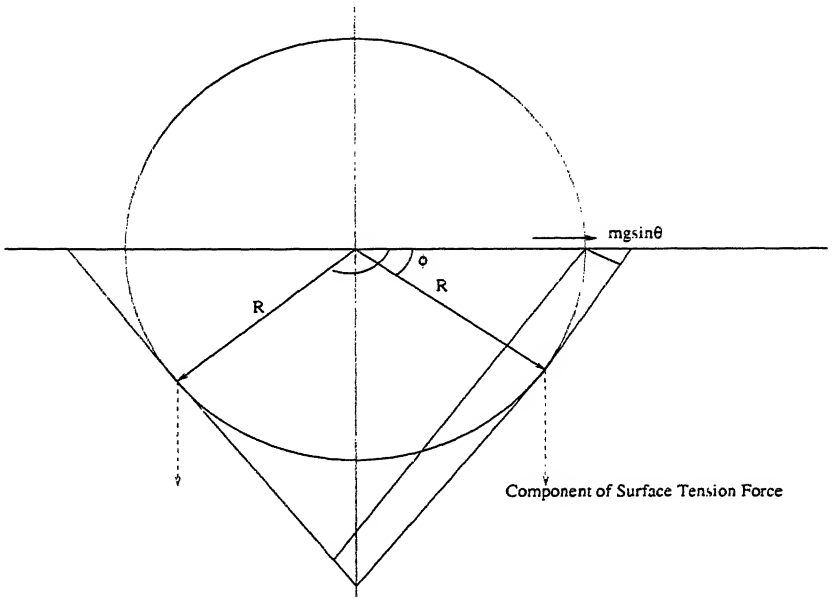

Figure 2.4: Base of a three dimensional drop representing forces, which make the drop move down the incline.

$$\begin{aligned} \text{Moment2} &= mgsin\theta_p[y_{cg}cos\theta_p - \mid x_1 - x_{cg} \mid sin\theta_p] \\ &\quad -4\gamma R_1^2 \int_{\phi=0}^{\phi=\pi/2} (1 - cos\phi) sin\left[\theta_{AD} - \frac{\theta_{AD} + \theta_{RE}}{h} i\right] d\phi \quad (2.49) \end{aligned}$$

where ϕ is the base angle (assuming to be a circle), ranges from 0 to π. Also h is the total no of steps in which $\theta_{AD} + \theta_{RE}$ is divided and i goes from 1 to $(h+1)/2$, if h is odd whereas i goes from 1 to $(h/2) + 1$ or 1 to $(h/2) - 1$, when h is even.

2.10.2 Pendant Drop

For pendant drop case (drop below a flat inclined surface), as shown in Figure 2.5, the stability calculations are as follows. The center of gravity is calculated by taking the mass of any element as $\rho dxdy$. Then center of gravity coordinates (x_{cg}, y_{cg}) are given by

$$x_{cg} = \frac{\int\int x\rho dxdy}{\int\int \rho dxdy}$$
$$y_{cg} = \frac{\int\int y\rho dxdy}{\int\int \rho dxdy} \tag{2.50}$$

The advancing angle is calculated from the slope of the line joining the last and the last but one coordinate of the equation describing the drop shape. The receding angle calculation is done from the slope of the line joining the first and the second coordinate of the equation describing the drop shape.

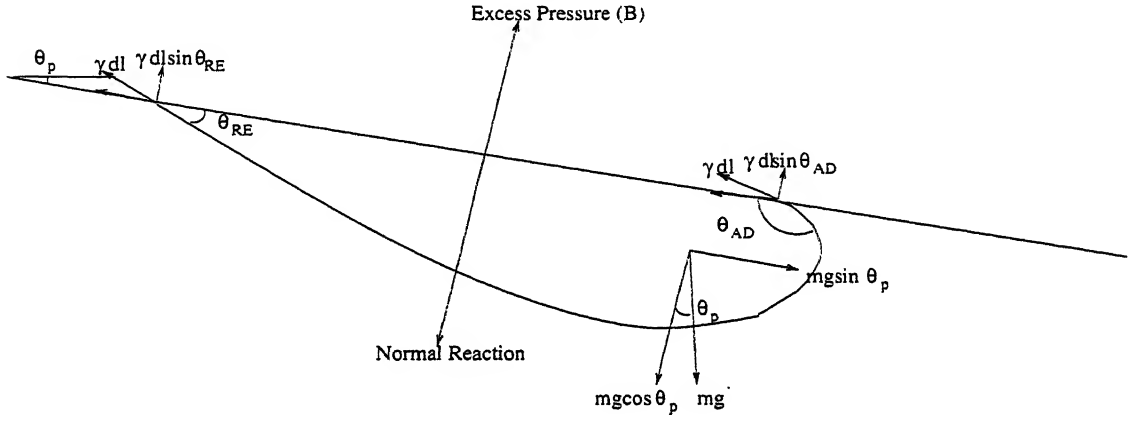

Figure 2.5: Force analysis for a pendant drop.

Moment calculations are given below:

$$\text{Normal Reaction} = 2BR_1 - mgcos\theta_p + 2\gamma R_1[sin(\theta_{AD}) + sin(\theta_{RE})] \tag{2.51}$$

where mg is the magnitude of the weight force of the liquid comprising the drop, B is the excess pressure term, R_1 is the radius of the span which the drop covers on the flat inclined plate, γ is the surface tension force, θ_{AD} is the advancing angle of the drop, θ_{RE} is the receding angle of the drop.

Taking moment about the advancing angle of the drop, we have

$$\begin{aligned}\text{Moment} &= (\text{Normal Reaction})R_1 + mgsin\theta_p[y_{cg}cos\theta_p - \mid x_1 - x_{cg} \mid sin\theta_p] \\ &\quad + mg \mid x_1 - x_{cg} \mid -BR_1 - 4\gamma R_1^2 sin\theta_{RE}\end{aligned} \tag{2.52}$$

On the other hand, considering only the forces which make the drop move along the incline, moment is calculated as follows:

$$\begin{aligned} \text{Moment1} &= mgsin\theta_p[y_{cg}cos\theta_p - \mid x_1 - x_{cg} \mid sin\theta_p] + mg \mid x_1 - x_{cg} \mid -BR_1 \\ &\quad -4\gamma R_1^2 sin\theta_{RE} \end{aligned} \tag{2.53}$$

For a three dimensional drop, only moment of those forces which make the drop move down the incline, as shown in Figure 2.3, is calculated as

$$\begin{aligned} \text{Moment2} &= mgsin\theta_p[y_{cg}cos\theta_p - \mid x_1 - x_{cg} \mid sin\theta_p] + mg \mid x_1 - x_{cg} \mid -BR_1 \\ &\quad -4\gamma R_1^2 \int_{\phi=0}^{\phi=\pi/2} (1 - cos\phi) sin\left[\theta_{AD} - \frac{\theta_{AD} + \theta_{RE}}{h} i\right] d\phi \end{aligned} \tag{2.54}$$

where ϕ is the base angle (assuming to be a circle), ranges from 0 to π. Also h is the total no of steps in which $\theta_{AD} + \theta_{RE}$ is divided and i goes from 1 to $(h+1)/2$, if h is odd whereas i goes from 1 to $(h/2) + 1$ or 1 to $(h/2) - 1$, when h is even.

2.11 Results and Discussion

Figures 2.6 and 2.7 show sessile and pendant drops respectively, generated by using axysymmetric formulation in the Laplace-Young equation. These drop shapes are for comparison with the two dimensional unsymmetric formulation for 0^0 plate inclination, shown in Figures 2.8 and 2.9. As in both two dimensional formulation and axysymmetric formulation, for 0^0 plate inclination, the drop shape should be the same. But as the plate inclination is different from 0^0, two dimensional formulation should be used to generate the drop shapes. Figure 2.6 is for 3 different liquids namely, mercury, bismuth and water, having contact angles 120^0, 135^0 and 60^0 respectively, with 2 different volumes 25 and 50mm^3. Similarly, Figure 2.7 is for the same parameters, except that bismuth and mercury volumes are 4 and 5mm^3, as for Figure 2.6, but former is for sessile drop case and latter is for pendant drop case.

Figure 2.8 shows the change in sessile drop shapes for 3 different liquids namely, mercury, bismuth and water, having volumes 25mm^3, 50mm^3, 50mm^3 and contact angles 120^0, 135^0, 60^0 respectively. It shows the change in drop shapes as plate inclination is changed from 0 to 30^0. As already discussed, the advancing angle and receding angle are $\theta_c - \theta_p$ and θ_c with respect to the inclined plate respectively. So, as the plate inclination increases, the advancing angle should decrease and receding angle should remain constant, with respect to the inclined plate.

Figure 2.9 shows the change in pendant drop shapes for 3 different liquids namely, mercury, bismuth and water, having volumes 25mm^3, 50mm^3, 50mm^3 and contact angles 120^0, 135^0, 60^0 respectively. It shows the change in drop shapes as plate inclination is changed from 0 to 30^0. As already discussed, the advancing angle and receding angle are θ_c and $\theta_c - \theta_p$ with respect to the inclined plate respectively. So, as the plate inclination increases, the advancing angle should remain constant and receding angle should decrease, with respect to the inclined plate.

Figures 2.10, 2.11, 2.12 shows for mercury, bismuth, water sessile drops respectively, variation of advancing angle, receding angle, moment and moment1 with respect to the plate inclination. Generally, advancing angle increases, receding angle decreases, moment and moment1 increases with respect to plate inclination. Here the drop shapes have been simulated with θ_c and $\theta_c - \theta_p$ as advancing angle and receding angle with respect to horizontal, but when calculated with respect to the incline flat plate they are $\theta_c - \theta_p$ and θ_c respectively.

Figures 2.13, 2.14, 2.15 shows for Mercury, Bismuth, Water pendant drops respectively, variation of advancing angle, receding angle, moment and moment1 with respect to the plate inclination. Generally, advancing angle increases, receding angle decreases, moment and moment1 increases with respect to plate inclination. Here the drop shapes have been simulated with $\theta_c - \theta_p$ and θ_c as advancing angle and receding angle with respect to horizontal, but when calculated with respect to the incline flat plate they are θ_c and $\theta_c - \theta_p$ respectively.

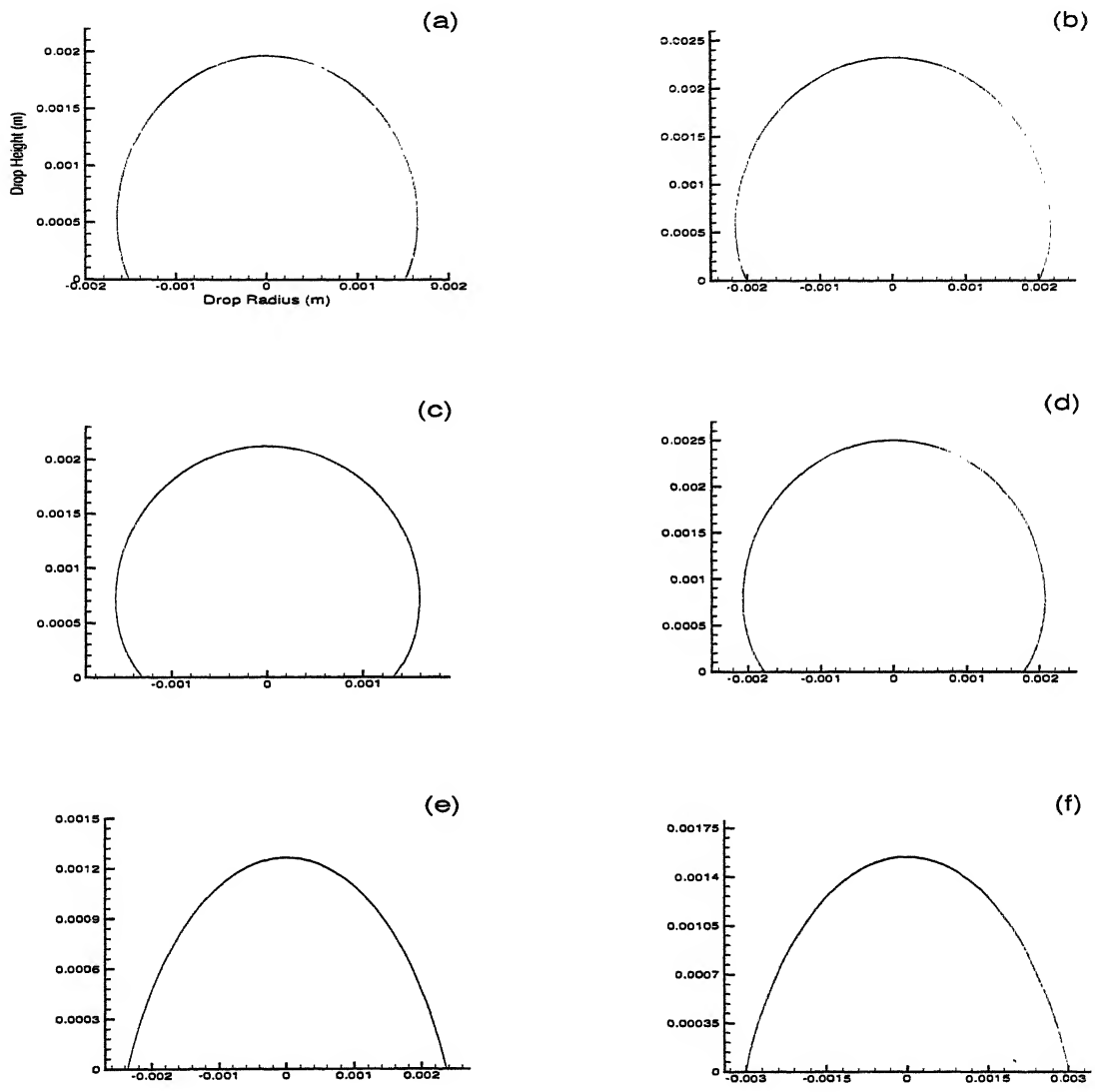

Figure 2.6: For zero plate inclination and axysymmetric formulation (a) mercury drop of volume 25mm^3 and contact angle 120^0 (b) mercury drop of volume 50mm^3 and contact angle 120^0 (c) bismuth drop of volume 25mm^3 and contact angle 135^0 (d) bismuth drop of volume 50mm^3 and contact angle 135^0 (e) water drop of volume 25mm^3 and contact angle 60^0 (f) water drop of volume 50mm^3 and contact angle 60^0.

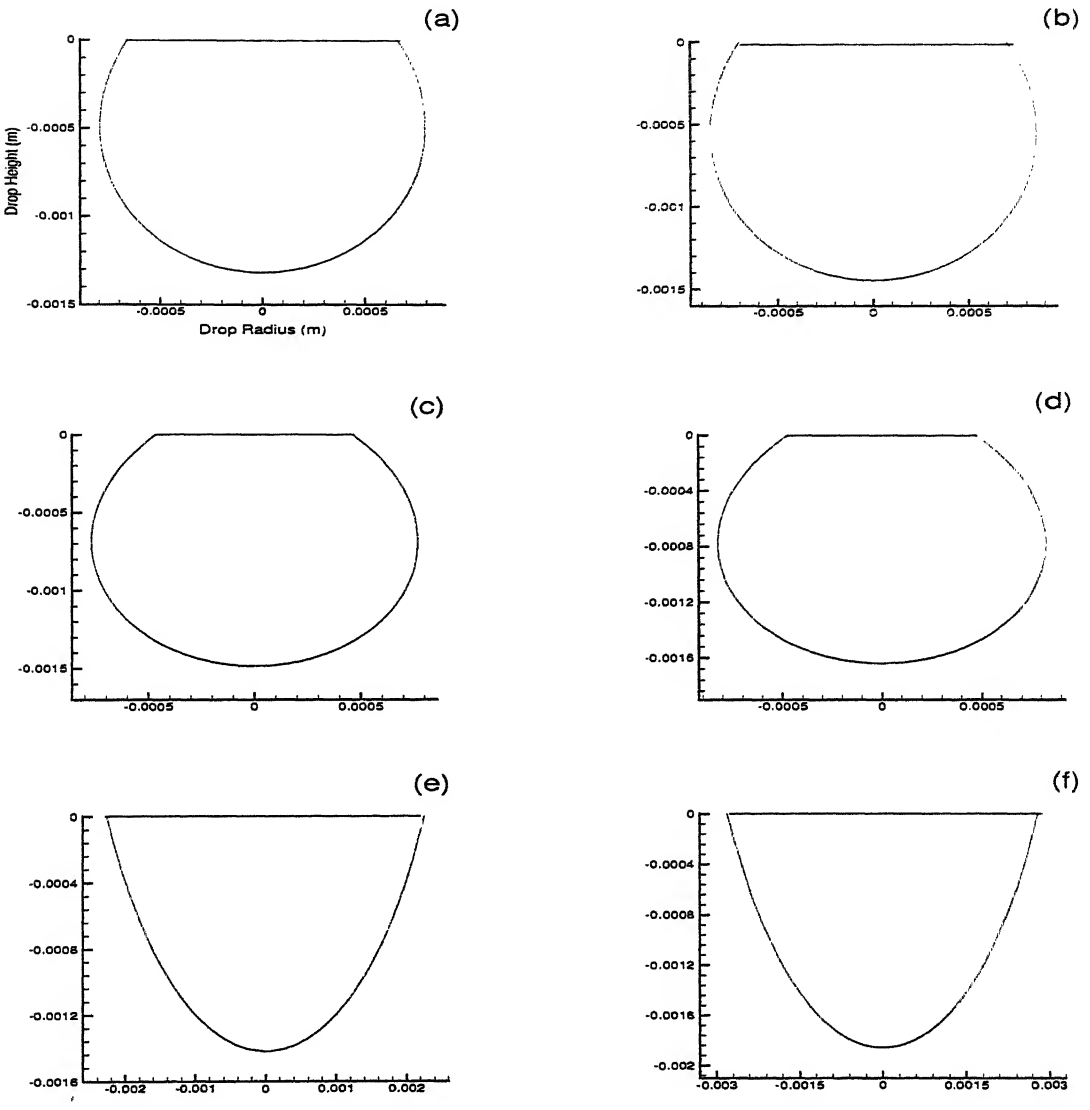

Figure 2.7: For zero plate inclination and axysymmetric formulation (a) mercury drop of volume 4mm^3 and contact angle 120^0, (b) mercury drop of volume 5mm^3 and contact angle 120^0, (c) bismuth drop of volume 4mm^3 and contact angle 135^0, (d) bismuth drop of volume 5mm^3 and contact angle 135^0, (e) water drop of volume 25mm^3 and contact angle 60^0, (f) water drop of volume 50mm^3 and contact angle 60^0.

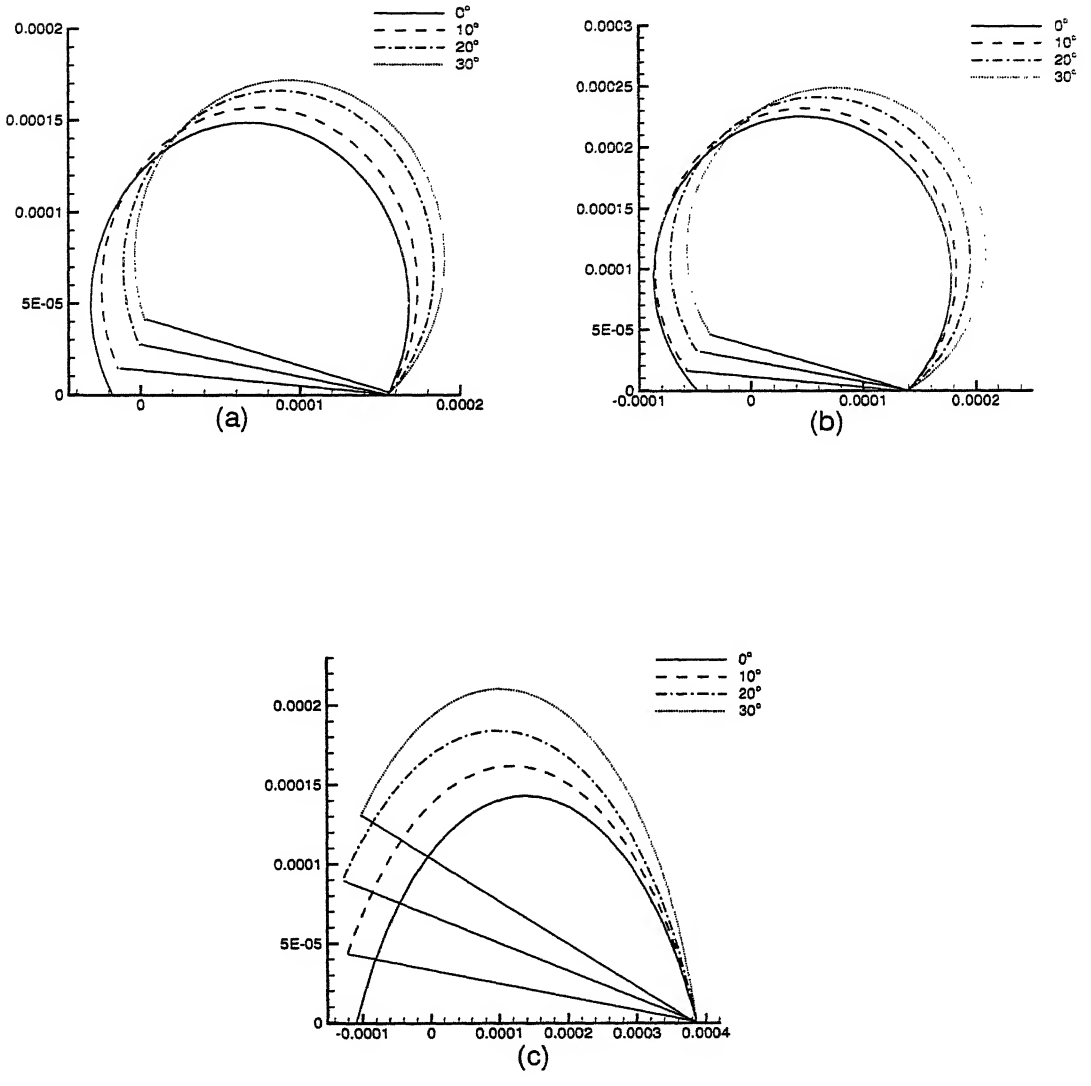

Figure 2.8: Sessile drop shapes for different plate inclinations from 0-30^0 of (a) mercury of volume 25mm^3 and contact angle 120^0, (b) bismuth of volume 50mm^3 and contact angle 135^0, (c) water of volume 50mm^3 and contact angle 60^0.

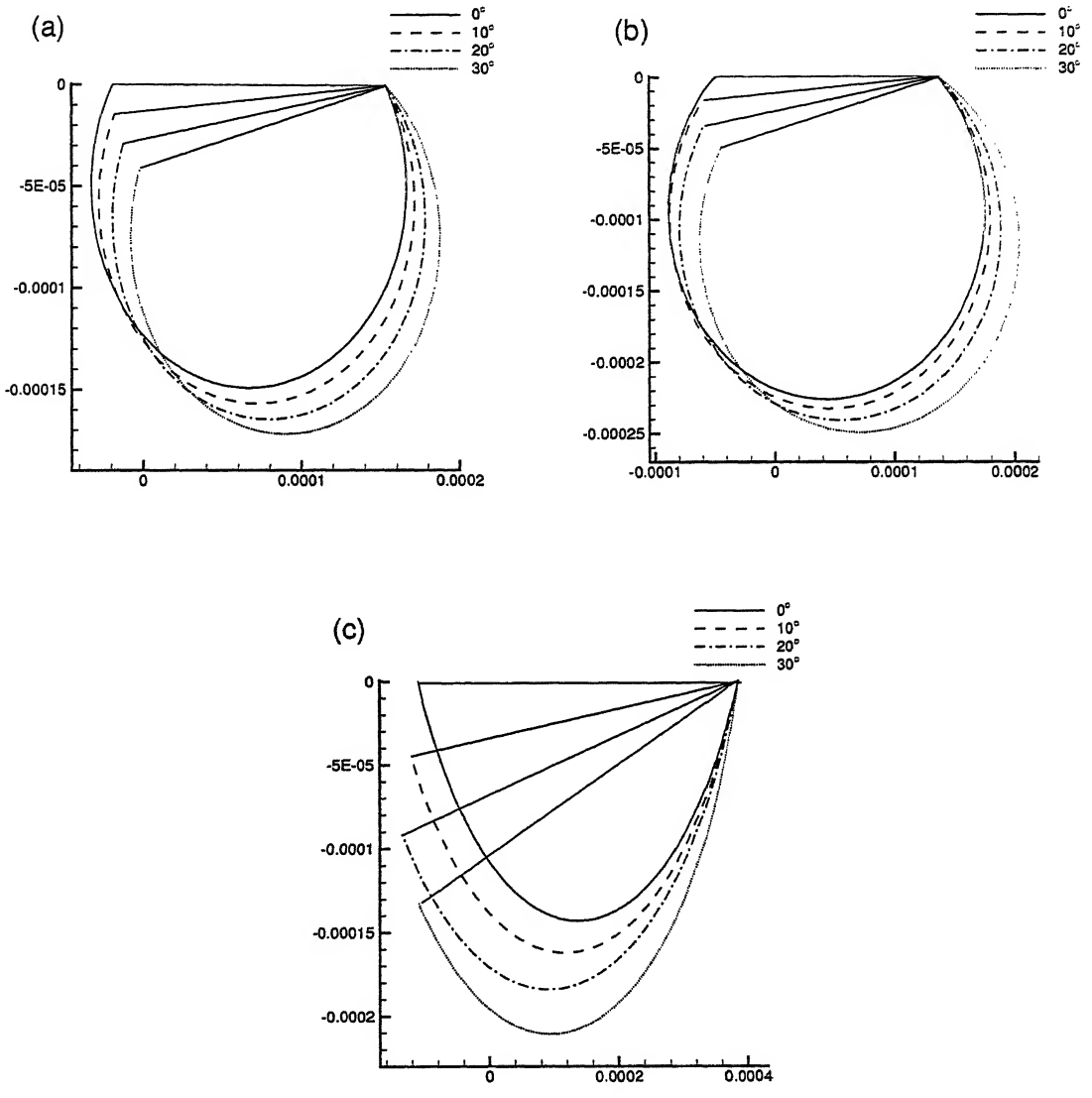

Figure 2.9: Pendant drop shapes for different plate inclinations from 0-30^0 of (a) mercury of volume 25mm^3 and contact angle 120^0, (b) bismuth of volume 50mm^3 and contact angle 135^0, (c) water of volume 50mm^3 and contact angle 60^0.

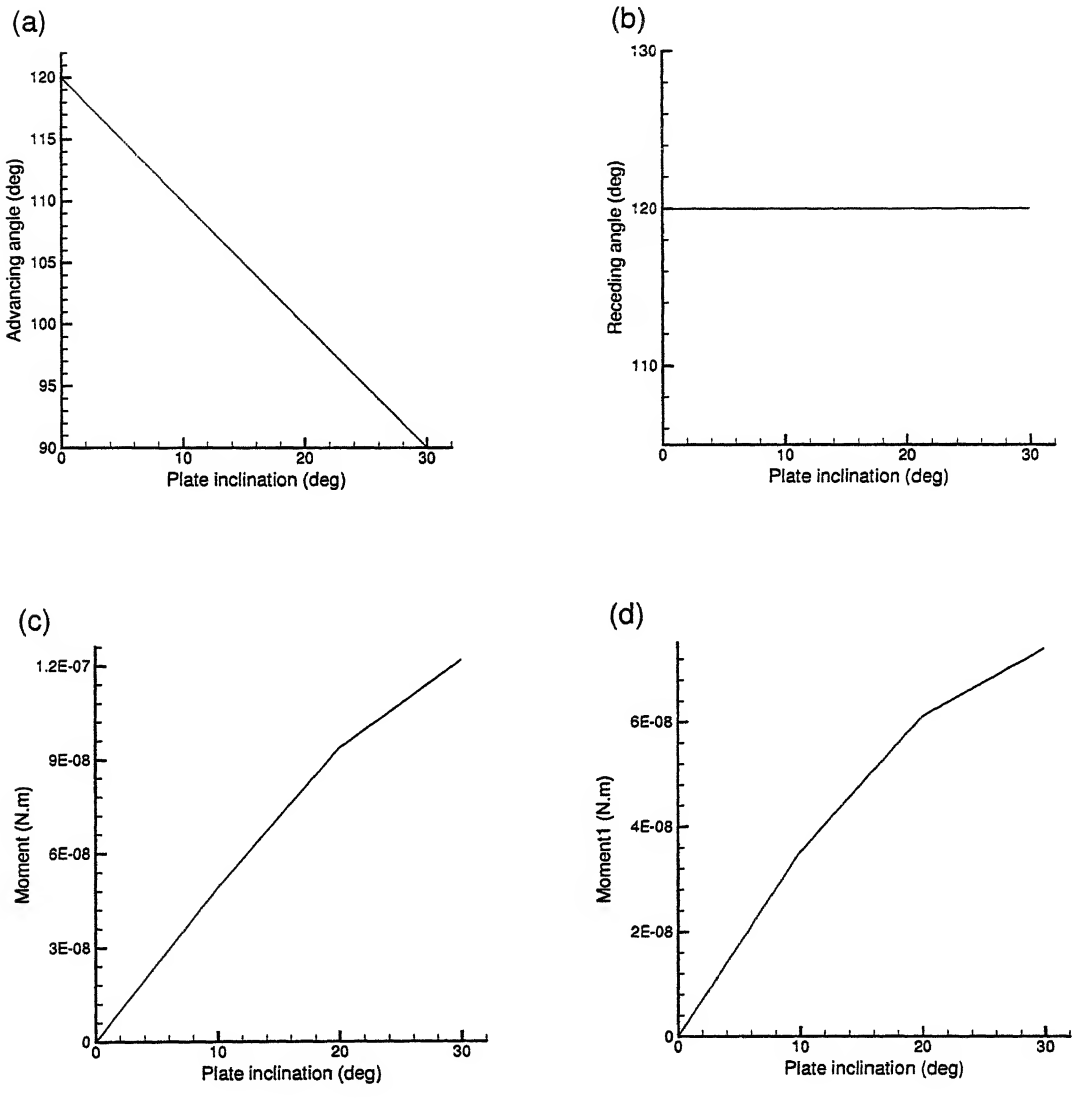

Figure 2.10: mercury sessile drop of volume 25mm^3, contact angle 120^0 (a) variation of advancing angle with respect to plate inclination, (b) variation of receding angle with respect to plate inclination, (c) variation of moment with respect to plate inclination, (d) variation of moment1 with respect to plate inclination.

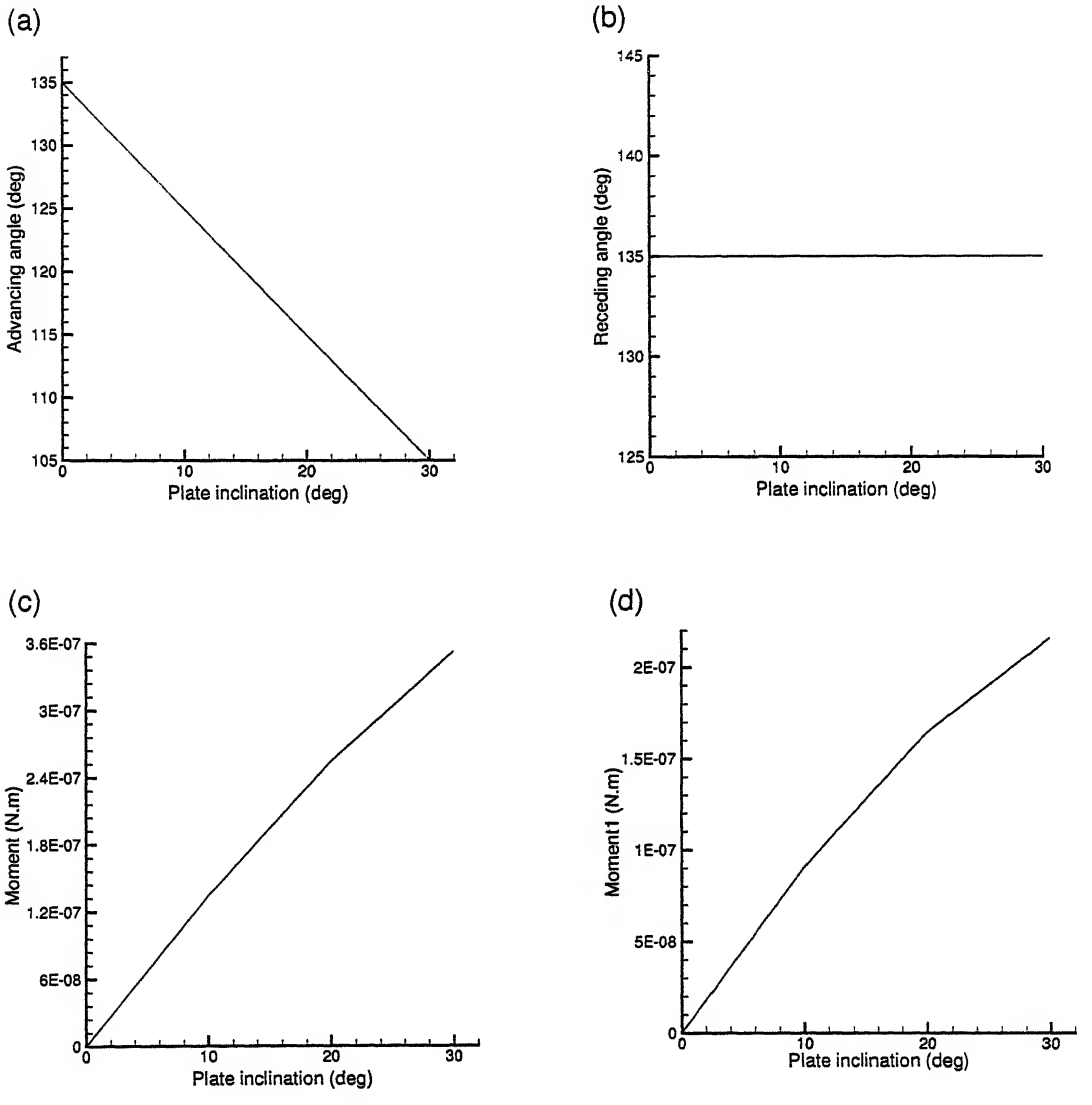

Figure 2.11: bismuth sessile drop of volume $50mm^3$, contact angle 135^0 (a) variation of advancing angle with respect to plate inclination, (b) variation of receding angle with respect to plate inclination, (c) variation of moment with respect to plate inclination, (d) variation of moment1 with respect to plate inclination.

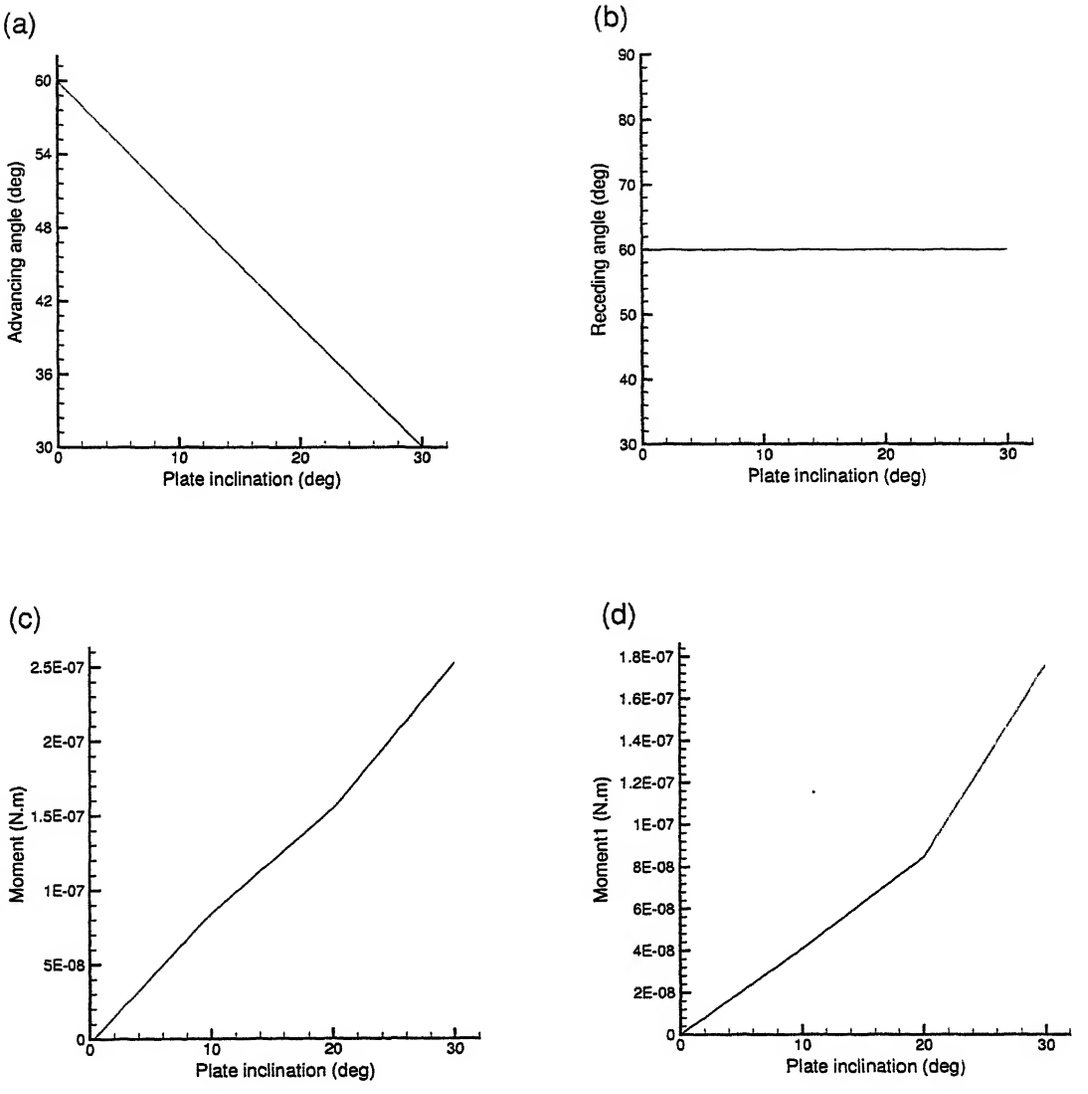

Figure 2.12: water sessile drop of volume $50mm^3$, contact angle 60^0 (a) variation of advancing angle with respect to plate inclination, (b) variation of receding angle with respect to plate inclination, (c) variation of moment with respect to plate inclination, (d) variation of moment1 with respect to plate inclination.

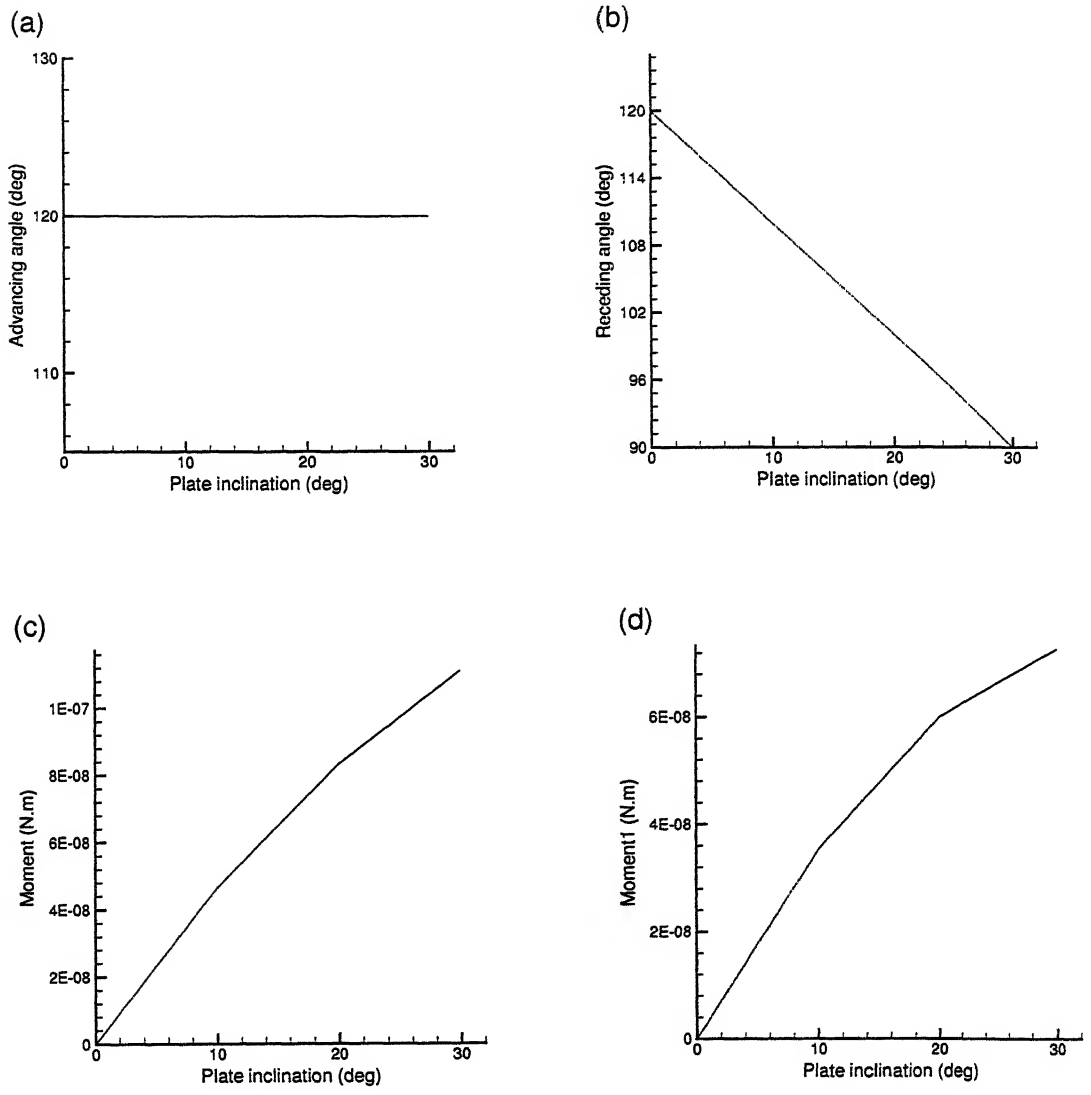

Figure 2.13: mercury pendant drop of volume 25mm^3, contact angle 120^0 (a) variation of advancing angle with respect to plate inclination, (b) variation of receding angle with respect to plate inclination, (c) variation of moment with respect to plate inclination, (d) variation of moment1 with respect to plate inclination.

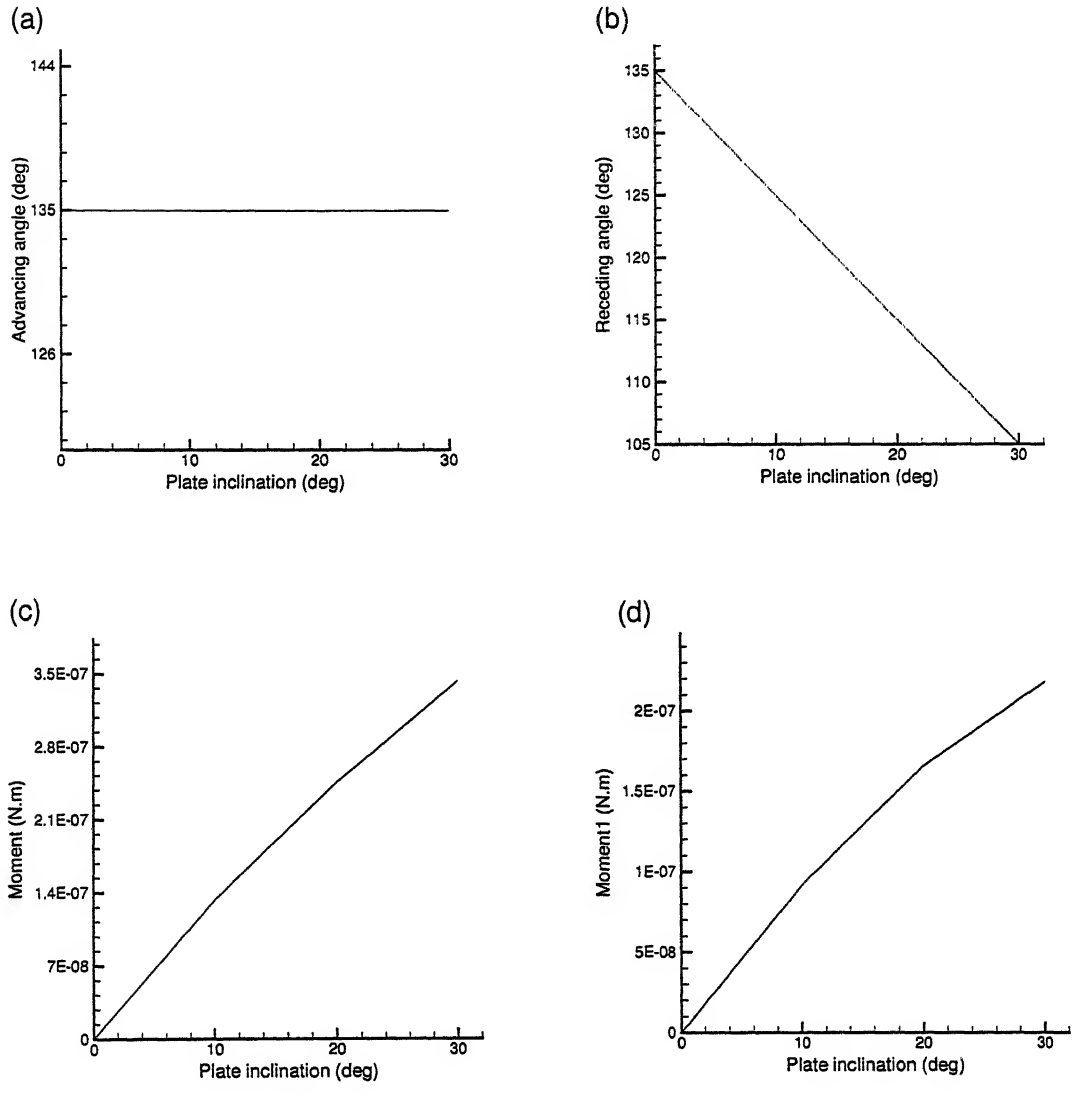

Figure 2.14: bismuth pendant drop of volume 50mm^3, contact angle 135^0 (a) variation of advancing angle with respect to plate inclination, (b) variation of receding angle with respect to plate inclination, (c) variation of moment with respect to plate inclination, (d) variation of moment1 with respect to plate inclination.

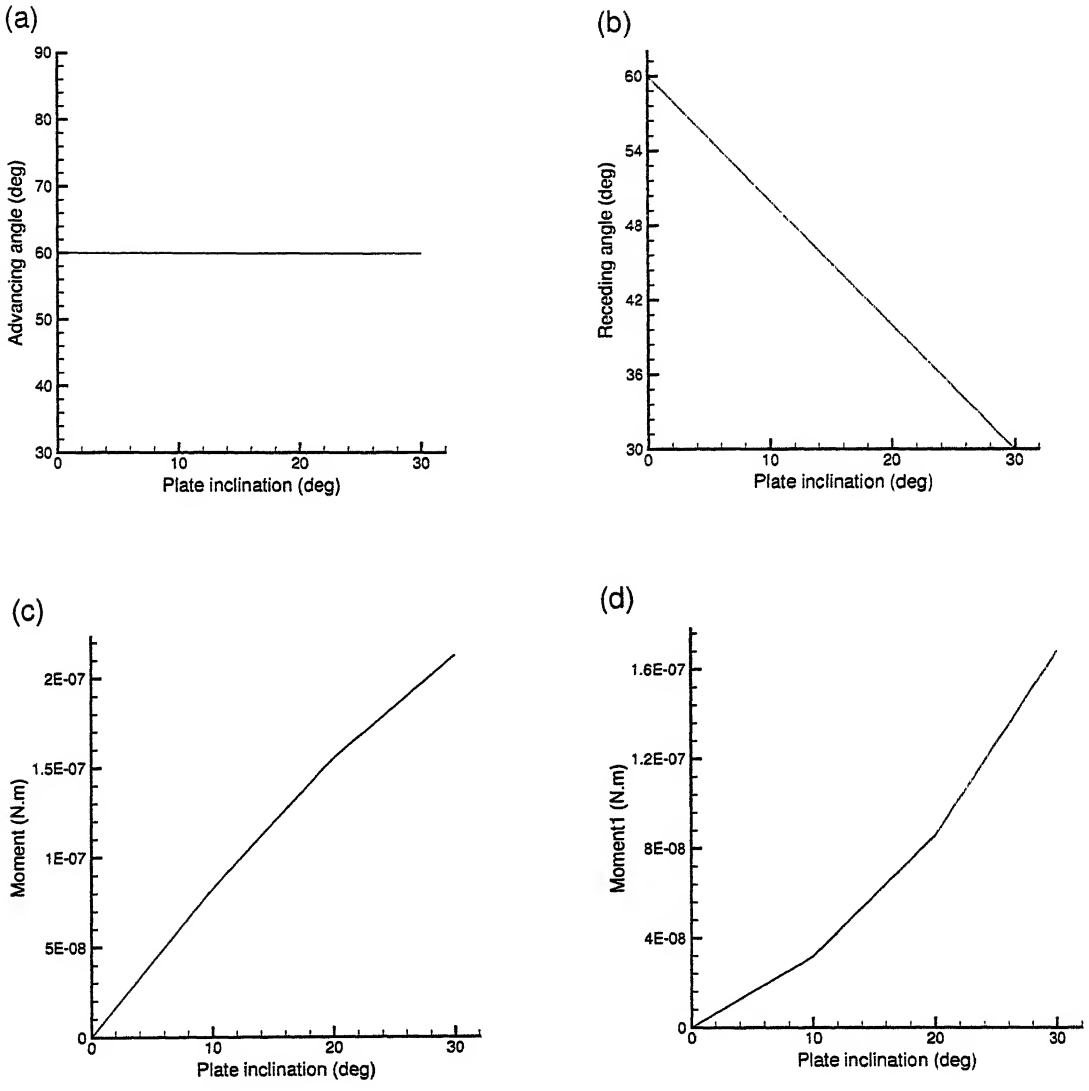

Figure 2.15: water pendant drop of volume $50mm^3$, contact angle 60^0 (a) variation of advancing angle with respect to plate inclination, (b) variation of receding angle with respect to plate inclination, (c) variation of moment with respect to plate inclination, (d) variation of moment1 with respect to plate inclination.

Chapter 3

Mathematical modeling of flow in a sliding semi-circular drop

The governing equations, namely continuity, momentum, and pressure equations for a semi-circular drop along with boundary conditions are presented below (Muralidhar *et al.* 1995).

3.1 Equations of Fluid Motion in a semi-circular region

The governing equations for fluid flow in r-θ coordinates are given below. The mass balance equation is

$$\frac{\partial \rho}{\partial t^\star} + \frac{\partial(\rho u^\star)}{\partial r^\star} + \frac{\rho u^\star}{r^\star} + \frac{1}{r^\star}\frac{\partial(\rho v^\star)}{\partial \theta} = 0 \tag{3.1}$$

where $u^\star$, and $v^\star$ are the components of velocity in $r^\star$ and θ direction respectively. The superscript $\star$ indicates that the respective quantities are in dimensional form. The momentum equations in component form are

$r^\star$ Component

$$\rho\left(\frac{du^\star}{dt^\star} - \frac{v^{\star 2}}{r^\star}\right) = X^\star - \frac{\partial p^\star}{\partial r^\star} + \mu\left[\nabla^2 u^\star - \frac{2}{r^{\star 2}}\left(\frac{\partial v^\star}{\partial \theta}\right) - \frac{u^\star}{r^{\star 2}}\right] \tag{3.2}$$

where $X^\star$, $Y^\star$ are the components of body force in $r^\star$ and θ direction respectively, μ is viscosity and $p^\star$ is pressure.

θ **Component**

$$\rho\left(\frac{dv^*}{dt^*}+\frac{u^*v^*}{r^*}\right)=Y^*-\frac{1}{r^*}\frac{\partial p^*}{\partial\theta}+\mu\left[\nabla^2 v^*+\frac{2}{r^{*2}}\left(\frac{\partial u^*}{\partial\theta}\right)-\frac{v^*}{r^{*2}}\right] \tag{3.3}$$

where

$$\frac{du^*}{dt^*}=\frac{\partial u^*}{\partial t^*}+u^*\left(\frac{\partial u^*}{\partial r^*}\right)+\frac{v^*}{r^*}\left(\frac{\partial u^*}{\partial\theta}\right) \tag{3.4}$$

$$\nabla^2 u^*=\frac{\partial^2 u^*}{\partial r^{*2}}+\frac{1}{r^*}\left(\frac{\partial u^*}{\partial r^*}\right)+\frac{1}{r^{*2}}\left(\frac{\partial^2 u^*}{\partial\theta^2}\right) \tag{3.5}$$

The following assumptions have been additionally enforced in the governing equations. The flow is of low Reynolds number (Re$<$ 1), steady, and incompressible. The body forces namely X^* and Y^* are neglected. The validity of these assumptions is based on the fact that the drop is physically small in size. For a small drop, surface forces are dominant in comparison to body forces. The mass balance equation, momentum equation, and pressure equation along with these assumptions and the boundary conditions for semi-circular drop placed on a flat horizontal surface are given below.

The mass balance equation in r^* θ coordinates is

$$\frac{\partial u^*}{\partial r^*}+\frac{u^*}{r^*}+\frac{1}{r^*}\left(\frac{\partial v^*}{\partial\theta}\right)=0 \tag{3.6}$$

The momentum equations in component form are

r^* **Component**

$$0=-\frac{\partial p^*}{\partial r^*}+\mu\left[\frac{\partial^2 u^*}{\partial r^{*2}}+\frac{1}{r^*}\left(\frac{\partial u^*}{\partial r^*}\right)+\frac{1}{r^{*2}}\left(\frac{\partial^2 u^*}{\partial\theta^2}\right)-\frac{2}{r^{*2}}\left(\frac{\partial v^*}{\partial\theta}\right)-\frac{u^*}{r^{*2}}\right] \tag{3.7}$$

θ **Component**

$$\begin{aligned}0 \;=\; & -\frac{1}{r^*}\left(\frac{\partial p^*}{\partial\theta}\right)+\mu\left[\frac{\partial^2 v^*}{\partial r^{*2}}+\frac{1}{r^*}\left(\frac{\partial v^*}{\partial r^*}\right)+\frac{1}{r^{*2}}\left(\frac{\partial^2 v^*}{\partial\theta^2}\right)+\frac{2}{r^{*2}}\left(\frac{\partial u^*}{\partial\theta}\right)\right.\\ & \left.-\frac{v^*}{r^{*2}}\right]\end{aligned} \tag{3.8}$$

From the mass balance and momentum equations. we obtain the governing equation for pressure as

$$\frac{\partial^2 p^\star}{\partial r^{\star 2}} + \frac{1}{r^\star}\left(\frac{\partial p^\star}{\partial r^\star}\right) + \frac{1}{r^{\star 2}}\left(\frac{\partial^2 p^\star}{\partial \theta^2}\right) = 0 \tag{3.9}$$

3.2 Dimensionless Governing Equations in the Physical Domain

Dimensionless governing equations in r and θ co-ordinates are given below, where superscript $\star$ denotes the dimensional quantities. the non-dimensional components of velocity are $u = u^\star/u_0$, $v = v^\star/u_0$ where u_0 is the plate velocity.

The non-dimensional radius, pressure are $r = r^\star/r_1$, $p = p^\star - p^\star_{amb}/\rho u_0^2$, where r_1 denotes the maximum radius of a data point in the physical domain, ρ is the density of fluid of the drop. $\mathrm{Re} = \rho u_0 r_1/\mu$, where Re is Reynolds number and μ is the viscosity of the liquid phase of the drop.

The mass balance equation in dimensionless form is

$$\frac{\partial u}{\partial r} + \frac{u}{r} + \frac{1}{r}\left(\frac{\partial v}{\partial \theta}\right) = 0 \tag{3.10}$$

The momentum equations in component form are given below

r Component

$$0 = -\frac{\partial p}{\partial r} + \frac{1}{\mathrm{Re}}\left[\frac{\partial^2 u}{\partial r^2} + \frac{1}{r}\left(\frac{\partial u}{\partial r}\right) + \frac{1}{r^2}\left(\frac{\partial^2 u}{\partial \theta^2}\right) - \frac{2}{r^2}\left(\frac{\partial v}{\partial \theta}\right) - \frac{u}{r^2}\right] \tag{3.11}$$

θ Component

$$0 = -\frac{1}{r}\left(\frac{\partial p}{\partial \theta}\right) + \frac{1}{\mathrm{Re}}\left[\frac{\partial^2 v}{\partial r^2} + \frac{1}{r}\left(\frac{\partial v}{\partial r}\right) + \frac{1}{r^2}\left(\frac{\partial^2 v}{\partial \theta^2}\right) + \frac{2}{r^2}\left(\frac{\partial u}{\partial \theta}\right) - \frac{v}{r^2}\right] \tag{3.12}$$

The boundary conditions for velocity are

For $\theta = 0$

$$u = 1, v = 0 \tag{3.13}$$

For $\theta = \pi$

$$u = -1, v = 0 \tag{3.14}$$

At fluid interface

$$\mathbf{u} \cdot \hat{\mathbf{n}} = 0 \tag{3.15}$$

and

$$\frac{\partial(\mathbf{u} \cdot \hat{\mathbf{t}})}{\partial \hat{\mathbf{n}}} = 0 \tag{3.16}$$

where $\mathbf{u}$ is velocity vector and $\hat{\mathbf{n}}$ is outward drawn unit normal vector on the drop surface and $\hat{\mathbf{t}}$ is the unit tangent vector on the drop surface. Let $F(x.y) = 0$ be the equation describing the drop shape, then $\hat{\mathbf{n}} = \nabla F / |\nabla F|$.
The pressure governing equation is

$$\frac{\partial^2 p}{\partial r^2} + \frac{1}{r}\left(\frac{\partial p}{\partial r}\right) + \frac{1}{r^2}\left(\frac{\partial^2 p}{\partial \theta^2}\right) = 0 \tag{3.17}$$

Pressure boundary conditions are:
At the fluid interface

$$p = 2k_m\gamma \tag{3.18}$$

where γ is surface tension and k_m is mean curvature of the drop in physical domain. Let $F(x, y) = 0$ or $y = f(x)$ be the equation describing the drop shape. Then k_m is defined as (Pozrikidis 1997)

$$k_m = -\frac{f''}{2(1 + f'^2)^{3/2}} \tag{3.19}$$

If $F(r, \theta) = 0$ be the equation of the drop, then k_m for a semi-circular geometry is

$$k_m = \frac{1}{2}\frac{1}{r_1} \tag{3.20}$$

For $\theta = 0$ and $\theta = \pi$ (at the plate), the pressure boundary conditions are

$$\frac{\partial p}{\partial \theta} = \frac{2r}{\mathrm{Re}}\left[\frac{\partial^2 v}{\partial r^2} + \frac{1}{r}\left(\frac{\partial v}{\partial r}\right) + \frac{1}{r^2}\left(\frac{\partial^2 v}{\partial \theta^2}\right) + \frac{2}{r^2}\left(\frac{\partial u}{\partial \theta}\right)\right] \tag{3.21}$$

As v is zero and u is constant at the plate $\theta = 0$ and $\theta = \pi$, the derivatives of v and u with respect to r are zero.

Chapter 4

Numerical solution of the Flow Equations for semi-circular drop

The dimensionless form of pressure governing equation is

$$\frac{\partial^2 p}{\partial r^2} + \frac{1}{r}\left(\frac{\partial p}{\partial r}\right) + \frac{1}{r^2}\left(\frac{\partial^2 p}{\partial \theta^2}\right) = 0 \tag{4.1}$$

The boundary condition for pressure are
For $\theta = 0$ and $\theta = \pi$ (at the plate):

$$\frac{\partial p}{\partial \theta} = \frac{2r}{\mathrm{Re}}\left[\frac{\partial^2 v}{\partial r^2} + \frac{1}{r}\left(\frac{\partial v}{\partial r}\right) + \frac{1}{r^2}\left(\frac{\partial^2 v}{\partial \theta^2}\right) + \frac{2}{r^2}\left(\frac{\partial u}{\partial \theta}\right)\right] \tag{4.2}$$

For $r = 0$

$$p = \text{average of all values at neighboring points} \tag{4.3}$$

For $r = 1$ (from Equation (3.18))

$$p = \frac{1}{\mathrm{We}} \tag{4.4}$$

where We is Weber number and is expressed as $\rho u_o^2 r_1/\gamma$.

For solving the governing equation for pressure along with boundary conditions, we adopt the finite difference technique. The radial distance of the cylindrical coordinates is discretized in to $n-1$ steps, with the index of discretization in radial direction being i. The angular length of π radians of the cylindrical co-ordinates is discretized in to $m-1$ steps, with the index of discretization in angular direction being j. There are m grid points in the radial direction and n grid points in the angular direction.
Equation (4.1) can be written in symbolic form as

$$A\frac{\partial^2 p}{\partial r^2} + B\frac{\partial p}{\partial r} + C\frac{\partial^2 p}{\partial \theta^2} = 0 \tag{4.5}$$

Discretizing this canonical form we get

$$\begin{aligned} &A\left[\frac{p_{i+1,j} - 2p_{i,j} + p_{i-1,j}}{(\Delta r)^2}\right] + B\left[\frac{p_{i+1,j} - p_{i-1,j}}{2\Delta r}\right] + \\ &C\left[\frac{p_{i,j+1} - 2p_{i,j} + p_{i,j-1}}{(\Delta\theta)^2}\right] = 0 \end{aligned} \tag{4.6}$$

or

$$\begin{aligned} p(i,j) \;=\; &\frac{1}{2[A(\Delta\theta)^2 + C(\Delta r)^2]}\left[\frac{(\Delta\theta)^2}{2}(2A + B\Delta r)p_{i+1,j} + \right. \\ &\left. p_{i-1,j}\frac{(\Delta\theta)^2}{2}(2A - B\Delta r) + C(\Delta r)^2(p_{i,j+1} + p_{i,j-1})\right] \end{aligned} \tag{4.7}$$

where

$$\begin{aligned} A &= 1 \\ B &= \frac{1}{r_{i,j}} \\ C &= \frac{1}{{r_{i,j}}^2} \end{aligned} \tag{4.8}$$

Discretizing the boundary conditions, we get
For $\theta = 0$

$$p_{i,1} = p_{i,2} - A\left(\frac{v_{i,1} - 2v_{i,2} + v_{i,3}}{\Delta\theta}\right) - B[u_{i,2} - u_{i,1}] \tag{4.9}$$

For $\theta = \pi$

$$p_{i,m} = p_{i,m-1} + A\left(\frac{v_{i,m} - 2v_{i,m-1} + v_{i,m-2}}{\Delta\theta}\right) + B[u_{i,m} - u_{i,m-1}] \tag{4.10}$$

For $r = 0$

$$p = \text{average of all values at neighboring points} \tag{4.11}$$

For $r = 1$

$$p_{n,j} = \frac{1}{\text{We}} \tag{4.12}$$

Dimensionless form of the r component of the momentum equation is

$$\frac{1}{\text{Re}}\left[\frac{\partial^2 u}{\partial r^2} + \frac{1}{r}\left(\frac{\partial u}{\partial r}\right) + \frac{1}{r^2}\left(\frac{\partial^2 u}{\partial \theta^2}\right) - \frac{2}{r^2}\left(\frac{\partial v}{\partial \theta}\right) - \frac{u}{r^2}\right] = \frac{\partial p}{\partial r} \tag{4.13}$$

The boundary conditions for r component of velocity are
For $\theta = 0$

$$u = 1 \tag{4.14}$$

For $\theta = \pi$

$$u = -1 \tag{4.15}$$

For $r = 0$

$$u = \text{linear interpolation between -1 and 1} \tag{4.16}$$

For $r = 1$

$$\mathbf{u} \cdot \hat{\mathbf{n}} = 0 \tag{4.17}$$

Equation (4.13) can be written as

$$A\frac{\partial^2 u}{\partial r^2} + B\frac{\partial u}{\partial r} + C\frac{\partial^2 u}{\partial \theta^2} + D\frac{\partial u}{\partial \theta} + Eu_{i,j} = F\frac{\partial p}{\partial r} \tag{4.18}$$

where

$$\begin{aligned} A &= 1 \\ B &= \frac{1}{r_{i,j}} \\ C &= \frac{1}{{r_{i,j}}^2} \\ D &= -\frac{2}{{r_{i,j}}^2} \\ E &= -\frac{1}{{r_{i,j}}^2} \\ F &= \text{Re} \end{aligned} \tag{4.19}$$

Discretizing Equation (4.18) by finite differences we get

$$\begin{aligned} &A\left[\frac{u_{i+1,j} - 2u_{i,j} + u_{i-1,j}}{(\Delta r)^2}\right] + B\left[\frac{u_{i+1,j} - u_{i-1,j}}{2\Delta r}\right] \\ &+C\left[\frac{u_{i,j+1} - 2u_{i,j} + u_{i,j-1}}{(\Delta \theta)^2}\right] + D\left[\frac{v_{i,j+1} - v_{i,j-1}}{\Delta \theta}\right] + Eu_{i,j} \\ &= F\left[\frac{p_{i+1,j} - p_{i-1,j}}{2\Delta r}\right] \end{aligned} \tag{4.20}$$

or

$$u_{i,j} = \frac{1}{[2A(\Delta\theta)^2 + 2C(\Delta r)^2 - E(\Delta\theta)^2(\Delta r)^2]} \left[u_{i+1,j}\frac{(\Delta\theta)^2}{2}(2A + B\Delta r) + (u_{i-1,j}\frac{(\Delta\theta)^2}{2}(2A - B\Delta r) + (u_{i,j-1} + u_{i,j+1})C(\Delta r)^2 + D\frac{\Delta\theta}{2}(\Delta r)^2(v_{i,j+1} - v_{i,j-1}) - F\frac{\Delta r}{2}(\Delta\theta)^2(p_{i+1,j} - p_{i-1,j}) \right] \quad (4.21)$$

Discretized boundary conditions are
For $\theta = 0$

$$u_{i,1} = 1 \quad (4.22)$$

For $\theta = \pi$

$$u_{i,m} = -1 \quad (4.23)$$

For $r = 0$

$$u_{1,j} = u_{2,1} + (j-1)\frac{u_{2,m} - u_{2,1}}{m-1} \quad (4.24)$$

For $r = 1$

$$u_{n,j} = 0 \quad (4.25)$$

The dimensionless form of the θ component of momentum equation, which is the θ component of velocity governing equation, is

$$\frac{1}{\mathrm{Re}}\left[\frac{\partial^2 v}{\partial r^2} + \frac{1}{r}\left(\frac{\partial v}{\partial r}\right) + \frac{1}{r^2}\left(\frac{\partial^2 v}{\partial \theta^2}\right) + \frac{2}{r^2}\left(\frac{\partial u}{\partial \theta}\right) - \frac{v}{r^2}\right] = \frac{1}{r}\left(\frac{\partial p}{\partial \theta}\right) \quad (4.26)$$

The boundary conditions for θ component of velocity are
For $\theta = 0$

$$v = 0 \tag{4.27}$$

For $\theta = \pi$

$$v = 0 \tag{4.28}$$

For $r = 0$

$$v = 0 \tag{4.29}$$

For $r = 1$

$$\frac{\partial(\mathbf{u} \cdot \hat{\mathbf{t}})}{\partial \hat{\mathbf{n}}} = 0 \tag{4.30}$$

Equation (4.26) can be written as

$$A\frac{\partial^2 v}{\partial r^2} + B\frac{\partial v}{\partial r} + C\frac{\partial^2 v}{\partial \theta^2} + D\frac{\partial u}{\partial \theta} - Ev_{i,j} = F\frac{\partial p}{\partial \theta} \tag{4.31}$$

where

$$\begin{aligned} A &= 1 \\ B &= \frac{1}{r_{i,j}} \\ C &= \frac{1}{{r_{i,j}}^2} \\ D &= \frac{2}{{r_{i,j}}^2} \\ E &= \frac{1}{{r_{i,j}}^2} \\ F &= \frac{\mathrm{Re}}{r_{i,j}} \end{aligned} \tag{4.32}$$

Discretizing Equation (4.31) by finite differences. we get

$$A\left[\frac{v_{i-1,j}-2v_{i,j}+v_{i+1,j}}{(\Delta r)^2}\right]+B\left[\frac{v_{i+1,j}-v_{i-1,j}}{2\Delta r}\right]+$$
$$C\left[\frac{v_{i,j-1}-2v_{i,j}+v_{i,j+1}}{(\Delta\theta)^2}\right]+D\left[\frac{u_{i,j+1}-u_{i,j-1}}{2\Delta\theta}\right]-Ev_{i,j}$$
$$=F\left[\frac{p_{i,j+1}-p_{i,j-1}}{2\Delta\theta}\right] \tag{4.33}$$

or

$$\begin{aligned} v_{i,j} = & \frac{1}{(2A(\Delta\theta)^2+2C(\Delta r)^2+E(\Delta r)^2(\Delta\theta)^2)} \\ & \left[v_{i-1,j}\frac{(\Delta\theta)^2}{2}(2A-B\Delta r)\right. \\ & +v_{i+1,j}\frac{(\Delta\theta)^2}{2}(2A+B\Delta r)+v_{i,j-1}\frac{(\Delta r)^2}{2}(2C-D\Delta\theta)+ \\ & \left.v_{i,j+1}\frac{(\Delta r)^2}{2}(2C+D\Delta\theta)-F\frac{\Delta\theta}{2}(\Delta r)^2(p_{i,j+1}-p_{i,j-1})\right] \end{aligned} \tag{4.34}$$

The discretized boundary conditions are

For $\theta = 0$

$$v_{i,1}=0 \tag{4.35}$$

For $\theta = \pi$

$$v_{i,m}=0 \tag{4.36}$$

For $r = 0$

$$v_{1,j}=0 \tag{4.37}$$

For $r = 1$

$$v_{n,j} = v_{n-1,j} \tag{4.38}$$

4.1 Iteration Algorithm

1. Grid points are generated in the physical domain. The pressure and momentum equations are coupled and are to be iteratively solved.
2. Initial guesses for u, v and p are taken to be zero.
3. Pressure equation is solved for zero initial values of u and v.
4. Numerical algorithm used for solving p, u and v is the Gauss-Seidel iterative method. Convergence criteria used is such that the ratio of the difference of the present and previous value, to the average value at each grid point is less than 10^{-5}.
5. Then u is solved with the present values of p and v.
6. Numerical algorithm and convergence criteria used for u is as in Step 4.
7. Next, v is solved with the present values of p and u.
8. Numerical algorithm and convergence criteria used for v is as in Step 4.
9. But as the governing equation for pressure contains the velocity terms, the velocity components should possess a unique value. Therefore the procedure from 5-8 is repeated until the convergence criteria for u and v at every grid point is met.
10. Next the coefficient of friction is calculated. It is defined as the ratio of average frictional force to the average normal force.
11. After we get a fixed value of u, v for a particular value of p at each grid point, these values of velocity components now serve as inputs for the next iteration for solving pressure.

12. Steps 5-10 are again repeated.

13. The above algorithm continues until convergence criterion for coefficient of friction is met. Convergence criteria for co-efficient of friction is as given in Step 4.

14. Lastly, we get the converged values of p, u, v and the coefficient of friction.

4.2 Code Validation

The code validation for Laplace equation in a semi-circular region has been carried out. The model problem has Dirichlet boundary conditions.
The governing differential equation is taken as

$$A\frac{\partial^2 p}{\partial r^2} + B\frac{\partial p}{\partial r} + C\frac{\partial^2 p}{\partial \theta^2} = 0 \tag{4.39}$$

where

$$\begin{aligned} A &= 1 \\ B &= \frac{1}{r_{i,j}} \\ C &= \frac{1}{{r_{i,j}}^2} \end{aligned} \tag{4.40}$$

with the boundary conditions are
For $\theta = 0$

$$p_{i,1} = 0 \tag{4.41}$$

For $\theta = \pi$

$$p_{i,m} = 0 \tag{4.42}$$

For $r = 0$

$$p_{1,j} = 0 \tag{4.43}$$

For $r = 1$

$$p_{n,j} = 1 \tag{4.44}$$

The analytical solution of the model problem is

$$p_{i,j} = \frac{4}{\pi}\left(\frac{r_{i,j}}{1}\sin(t_{i,j}) + \frac{{r_{i,j}}^3}{3}\sin(3t_{i,j}) + \frac{{r_{i,j}}^5}{5}\sin(5t_{i,j})\right) \tag{4.45}$$

The comparison of the numerical and analytical solutions is shown in Figure 4.1. The analytical and numerical results are similar. The dotted line shows the analytical solution and the solid line shows the numerical solution.

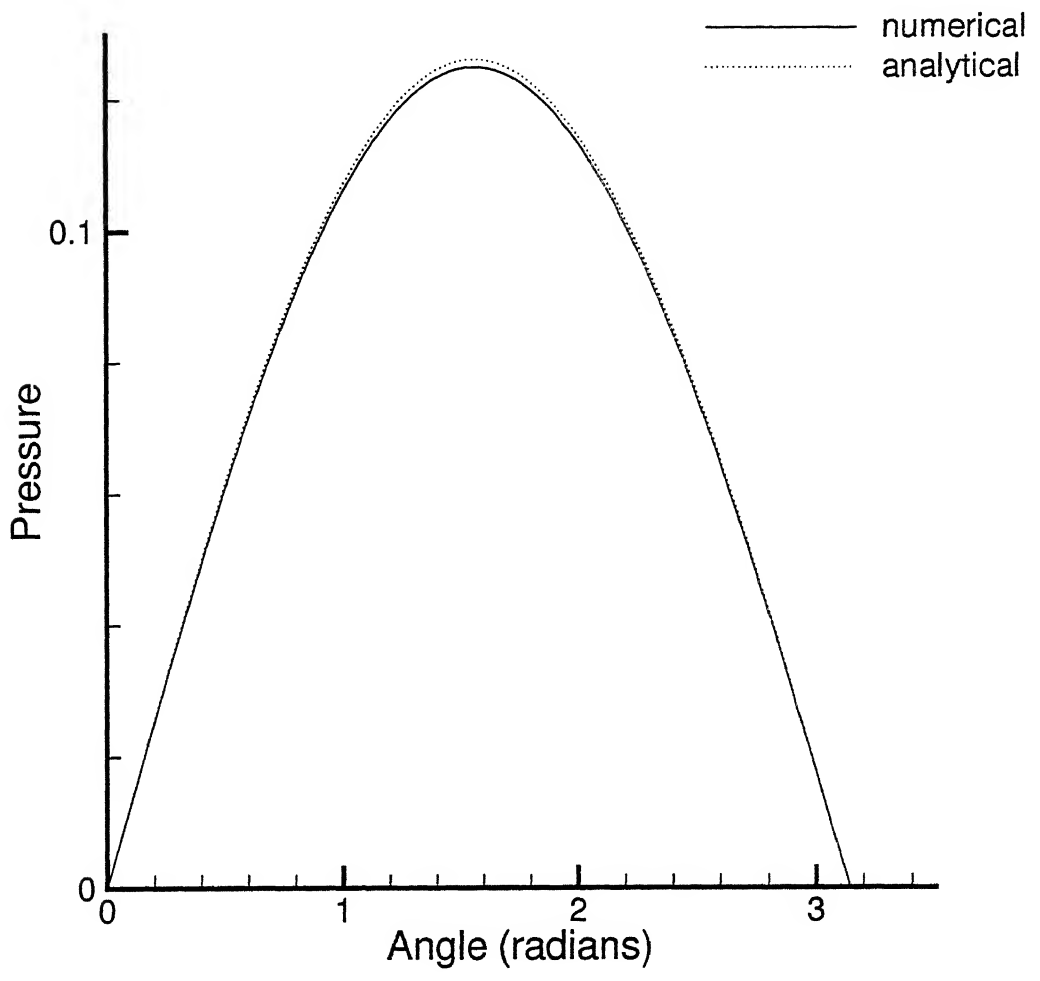

Figure 4.1: Code validation of Numerical Solution against the Analytical Solution.

4.3 Grid Independence

For $\theta = 72^0$, the profiles for pressure for all radii are compared for grids of Meaningful results 101×101 and 51×51. The results can be seen on the 51×51 grid in Figure 4.2. The nature of pressure values for 101×101 and 51×51 are same, hence all the calculations have been done for 51×51.

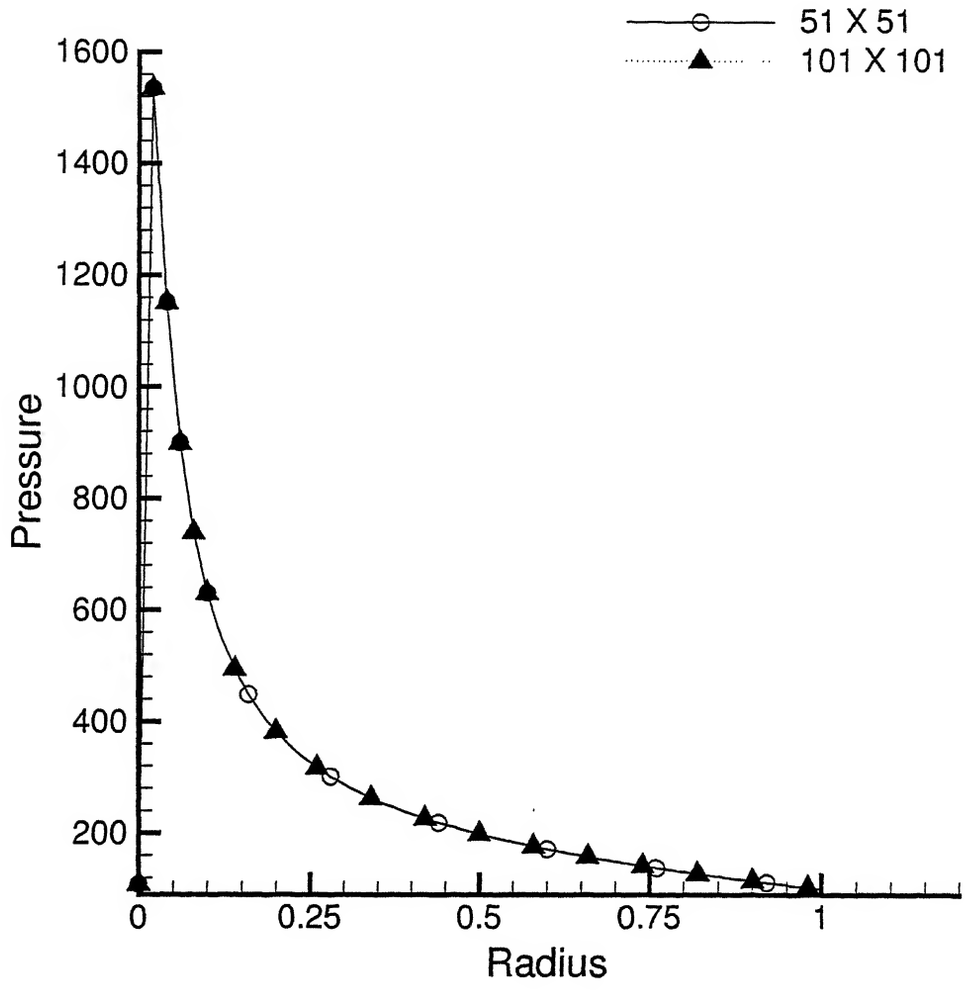

Figure 4.2: Grid independence test for 51×51 and 101×101.

4.4 Coefficient of Friction

The coefficient of friction expressed in terms of dimensional quantities is

$$\text{coefficient of friction} = \frac{\mu \int_{r^*=0}^{r^*=r_1} \frac{1}{r^*} \left(\frac{\partial u^*}{\partial \theta}\right) dr^* + \mu \int_{r^*=-r_1}^{r^*=0} \frac{1}{r^*} \left(\frac{\partial u^*}{\partial \theta}\right) dr^*}{\rho \left(\frac{\pi}{2} r_1^2\right) g + (p^* - p^*_{amb}) 2r_1} \tag{4.46}$$

When expressed in terms of non-dimensional form we get

$$\text{coefficient of friction} = \frac{\mu \int_{r=0}^{r=1} \frac{1}{rr_1} \left(\frac{\partial u}{\partial \theta}\right) dr(u_0 r_1) + \mu \int_{r=-1}^{r=0} \frac{1}{rr_1} \left(\frac{\partial u}{\partial \theta}\right) dr(u_0 r_1)}{\rho \left(\frac{\pi}{2} r_1^2\right) g + 2k_m \gamma (2r_1)} \tag{4.47}$$

where

$$2k_m = \nabla \cdot \left(\frac{\nabla F}{|\nabla F|}\right) \tag{4.48}$$

where $F(x, y) = 0$ is the equation of curve in Cartesian coordinates. If $F(r, \theta) = 0$ is the equation of the semi-circle then,

$$2k_m = \frac{1}{r_1} \tag{4.49}$$

Therefore, the expression for coefficient of friction for a semi-circular drop is

$$\text{coefficient of friction} = \frac{\mu \int_{r=0}^{r=1} \frac{1}{rr_1} \left(\frac{\partial u}{\partial \theta}\right) dr(u_0 r_1) + \mu \int_{r=-1}^{r=0} \frac{1}{rr_1} \left(\frac{\partial u}{\partial \theta}\right) dr(u_0 r_1)}{\rho \left(\frac{\pi}{2} r_1^2\right) g + \frac{1}{r_1} \gamma (2r_1)} \tag{4.50}$$

or

$$= \frac{\mu \int_{r=0}^{r=1} \frac{1}{r} \left(\frac{\partial u}{\partial \theta}\right) dr + \mu \int_{r=-1}^{r=0} \frac{1}{r} \left(\frac{\partial u}{\partial \theta}\right) dr}{\left(\frac{\rho \pi r_1^2 g}{2\mu u_0}\right) + \left(\frac{2\gamma \rho u_0 r_1}{\mu u_0^2 \rho r_1}\right)} \tag{4.51}$$

$$= \frac{\mu \int_{r=0}^{r=1} \frac{1}{r} \left(\frac{\partial u}{\partial \theta}\right) dr + \mu \int_{r=-1}^{r=0} \frac{1}{r} \left(\frac{\partial u}{\partial \theta}\right) dr}{\text{Rey} \left(\frac{\pi}{2\text{Fr}^2} + \frac{2}{\text{We}}\right)} \tag{4.52}$$

where

$$\begin{aligned} \text{Rey} &= \frac{\rho u_0 r_1}{\mu} \\ \text{Fr} &= \frac{u_0}{\sqrt{(g r_1)}} \\ \text{We} &= \frac{\rho u_0^2 r_1}{\gamma} \end{aligned} \tag{4.53}$$

For $10mm^3$ drop and u_0 =1m/s, Fr is 35.7434.
The table for coefficient of friction for a semi-circular drop, with We and Re varied over three orders of magnitudes, can be seen on the next page. The coefficient of friction increases with decreasing Reynolds number because of an increase in viscosity. It decreases with decreasing Weber number (increasing surface tension) because of an increase in the bulk pressure of the drop.

Table2. Variation of Coefficient of Friction with Re and We.

S.No.	We	Re	Coefficient of Friction
1	0.01	0.01	2.789
2	0.1	0.01	27.961
3	1.0	0.01	279.457
4	0.01	0.1	0.291
5	0.1	0.1	2.789
6	1.0	0.1	27.946
7	0.01	1.0	0.003
8	0.1	1.0	0.291
9	1.0	1.0	2.787

4.5 Results and Discussion

Figure 4.3 shows pressure contours and velocity vectors in a semi-circular drop. The boundary has a constant pressure. Inside the drop, the pressure must be positive, except where it is negative. This negative pattern are due to recirculation. The boundary condition for velocity is that there is no flow in the direction of the normal vector to the bounadry and there is no shear stress at the boundary. The velocity vectors are computed with respect to the plate. Similarly Figures 4.2 to 4.9 have the same boundary condition for pressure and velocity, except in all these figures Weber number and Reynolds number vary over three orders of magnitude.

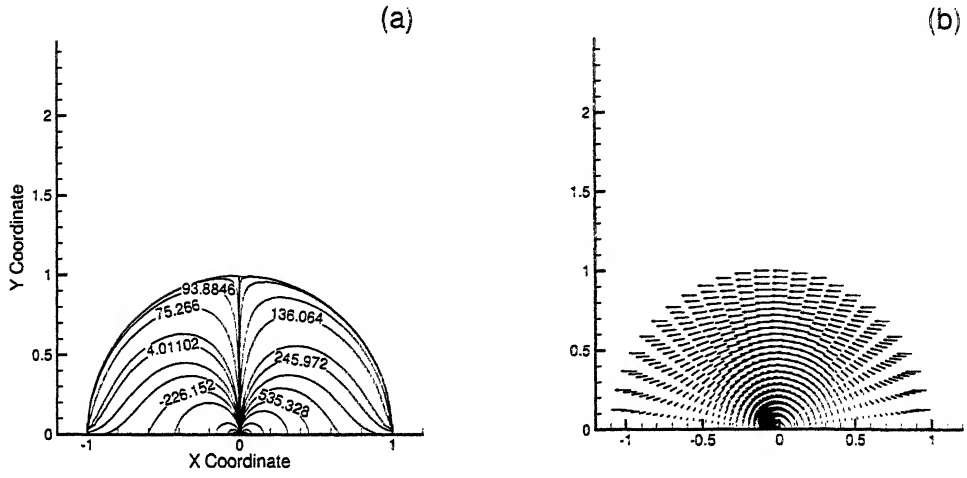

Figure 4.3: For We=0.01 and Re=0.01 (a) pressure contours (b) velocity vectors relative to the plate.

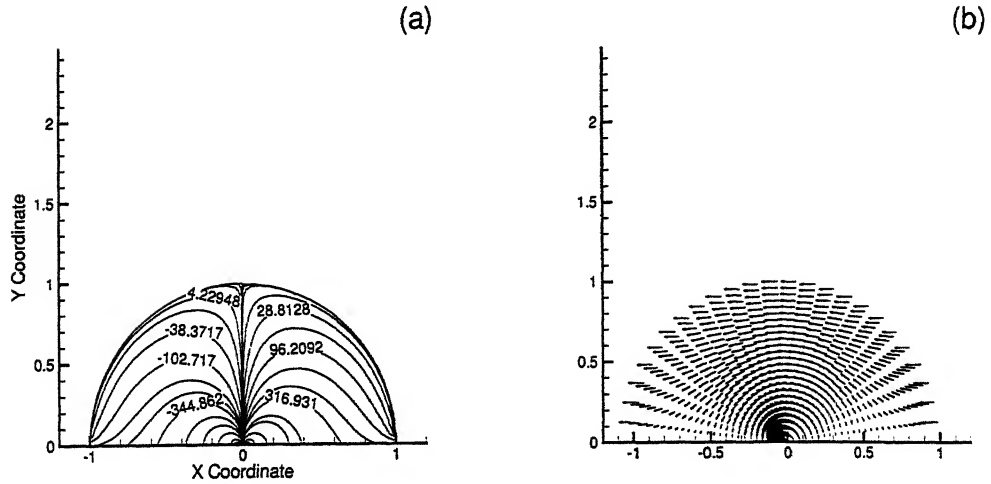

Figure 4.4: For We=0.1 and Re=0.01 (a) pressure contours (b) velocity vectors relative to the plate.

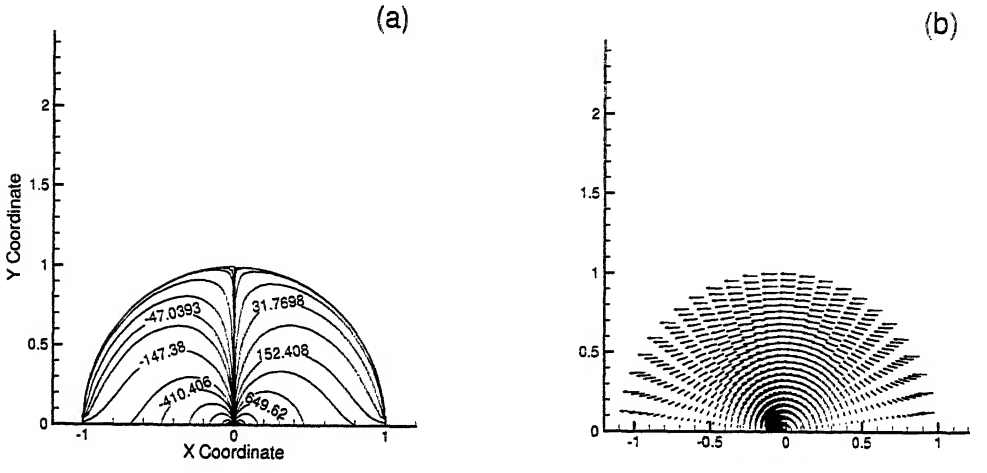

Figure 4.5: For We=1.0 and Re=0.01 (a) pressure contours (b) velocity vectors relative to the plate.

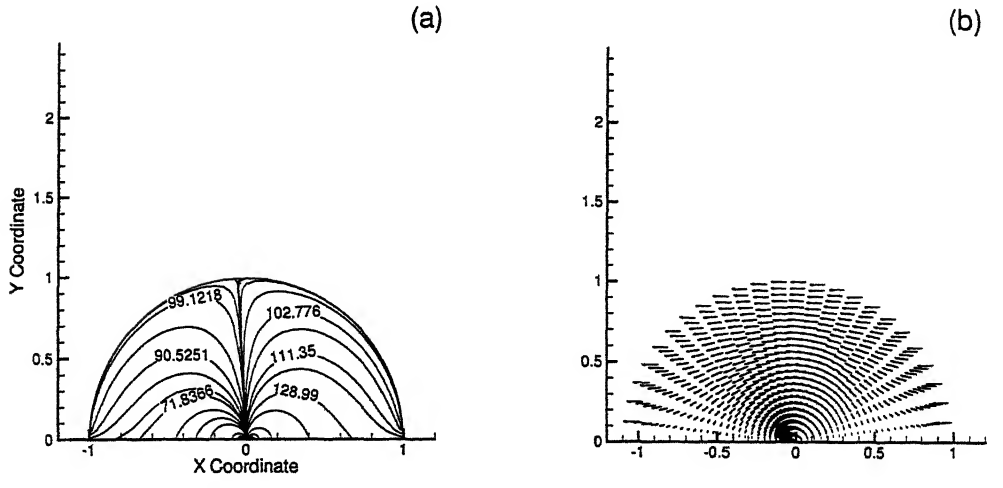

Figure 4.6: For We=0.01 and Re=0.1 (a) pressure contours (b) velocity vectors relative to the plate.

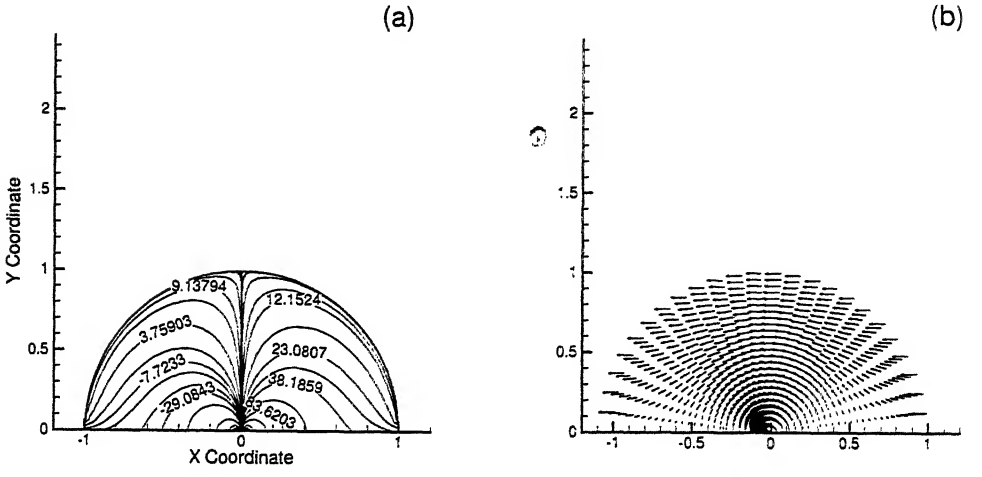

Figure 4.7: For We=0.1 and Re=0.1 (a) pressure contours (b) velocity vectors relative to the plate.

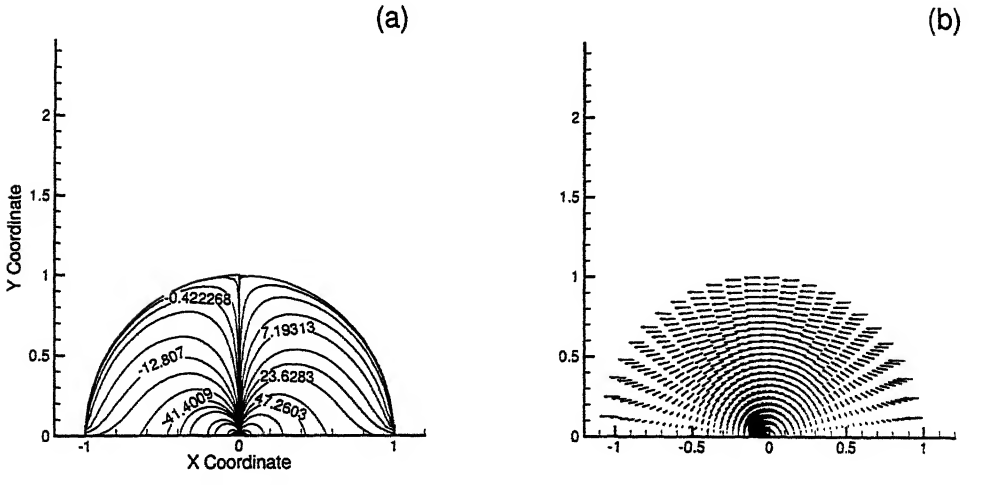

Figure 4.8: For We=1.0 and Re=0.1 (a) pressure contours (b) velocity vectors relative to the plate.

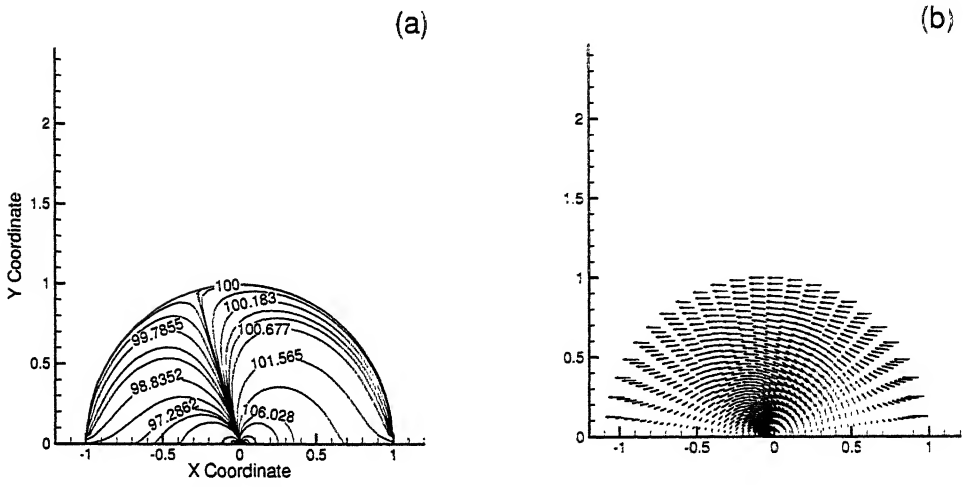

Figure 4.9: For We=0.01 and Re=1.0 (a) pressure contours (b) velocity vectors relative to the plate.

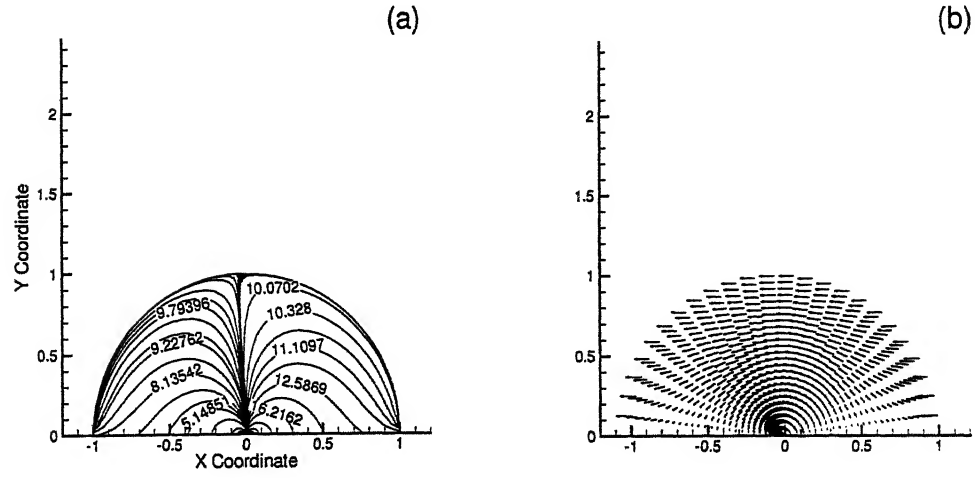

Figure 4.10: For We=0.1 and Re=1.0 (a) pressure contours (b) velocity vectors relative to the plate.

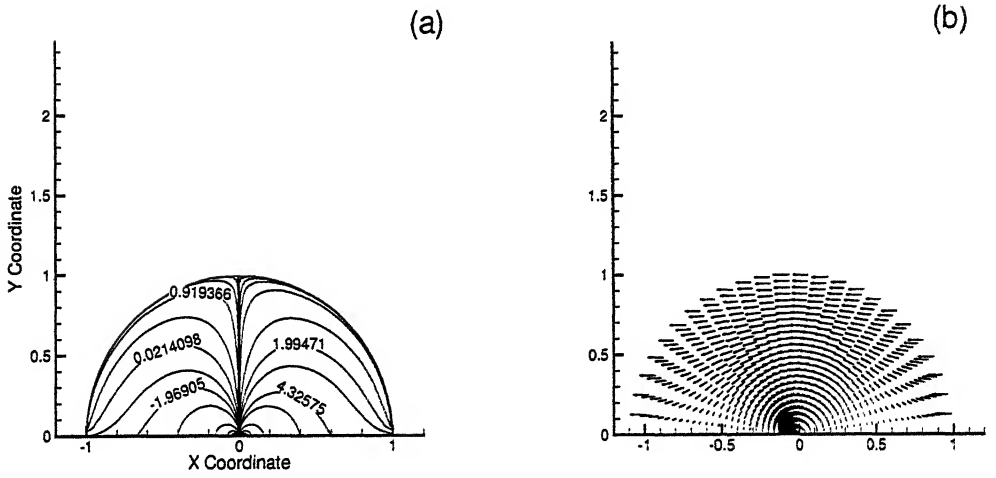

Figure 4.11: For We=1.0 and Re=1.0 (a) pressure contours (b) velocity vectors relative to the plate.

Chapter 5

Grid Generation

The grid generation procedure that transforms the deformed drop geometry to a semi-circular geometry is described in the present chapter. Figure 5.1 shows mapping of physical domain (deformed drop) to computational domain (semi-circular region). Let the body-fitting coordinate transformation be of the form

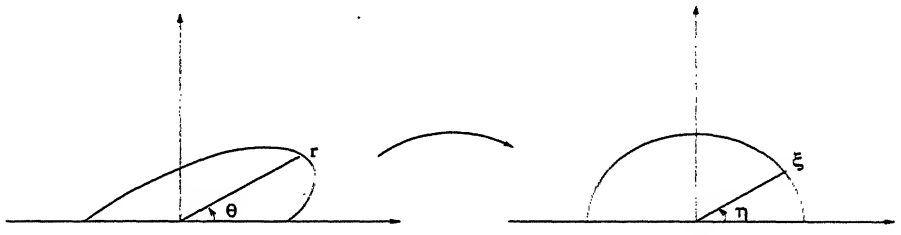

Figure 5.1: Physical domain (deformed drop) is mapped to computational domain (semi-circular region)

$\xi = \xi(r, \theta)$ and $\eta = \eta(r, \theta)$. From chain rule

$$\begin{Bmatrix} d\xi \\ d\eta \end{Bmatrix} = \begin{bmatrix} \xi_r dr & + & \xi_\theta d\theta \\ \eta_r dr & + & \eta_\theta d\theta \end{bmatrix} = \begin{bmatrix} \xi_r & \xi_\theta \\ \eta_r & \eta_\theta \end{bmatrix} \begin{Bmatrix} dr \\ d\theta \end{Bmatrix} \tag{5.1}$$

where (ξ_r, ξ_θ), (η_r, η_θ) are partial derivatives of ξ and η with respect to r and θ respectively. In a similar way, considering $r = r(\xi, \eta)$ and $\theta = \theta(\xi, \eta)$, we obtain

$$\begin{Bmatrix} dr \\ d\theta \end{Bmatrix} = \begin{bmatrix} r_\xi & r_\eta \\ \theta_\xi & \theta_\eta \end{bmatrix} \begin{Bmatrix} d\xi \\ d\eta \end{Bmatrix} \tag{5.2}$$

Combining Equations (5.1) and (5.2)

$$\begin{Bmatrix} dr \\ d\theta \end{Bmatrix} = \begin{bmatrix} r_\xi & r_\eta \\ \theta_\xi & \theta_\eta \end{bmatrix} \begin{bmatrix} \xi_r & \xi_\theta \\ \eta_r & \eta_\theta \end{bmatrix} \begin{Bmatrix} dr \\ d\theta \end{Bmatrix} \tag{5.3}$$

or

$$\begin{bmatrix} \xi_r & \xi_\theta \\ \eta_r & \eta_\theta \end{bmatrix} = \begin{bmatrix} r_\xi & r_\eta \\ \theta_\xi & \theta_\eta \end{bmatrix}^{-1} = \frac{1}{|J|} \begin{bmatrix} \theta_\eta & -r_\eta \\ -\theta_\xi & r_\xi \end{bmatrix} \tag{5.4}$$

where $|J| = r_\xi \theta_\eta - \theta_\xi r_\eta$, is the determinant of the Jacobian matrix

$$[J] = \begin{bmatrix} r_\xi & r_\eta \\ \theta_\xi & \theta_\eta \end{bmatrix} \tag{5.5}$$

For one-to-one mapping to exist, the determinant $|J|$ should be finite and non-zero. From Equation (5.4), it is clear that the partial derivatives of ξ and η are related to those of r and θ through the relations

$$\begin{aligned} \xi_r &= \theta_\eta / |J| ; & \xi_\theta &= -r_\eta / |J| ; \\ \eta_r &= -\theta_\xi / |J| : & \eta_\theta &= r_\xi / |J| . \end{aligned} \tag{5.6}$$

5.1 Grid Generation Technique

For regular geometries, the grid generation can be done analytically through suitable algebraic transformation. For irregular geometries, obtaining transformation functions is difficult; also, there is no guarantee that the particular transformation employed may produce an acceptable grid. A more general procedure for the algebraic generation of grids is based on interpolation. Here, the coordinates of the interior nodes are obtained by interpolation between the prescribed boundary data. A very useful technique for this purpose is the Transfinite Interpolation. As given by Muralidhar *et al.* (1995), the general algorithm of transfinite interpolation can be stated as:

1. Place grid points on the boundaries of the domain as desired.

2. Apply unidirectional interpolation in ξ-direction (or η-direction) between the boundary grid data given on the curves $\xi = 0$ and $\xi = 1$ (or $\eta = 0$ and $\eta = 1$) and obtain the coordinates for every interior and boundary point.

3. Calculate the mismatch between the interpolated and the actual coordinates on the $\eta = 0$ and $\eta = 1$ (or $\xi = 0$ and $\xi = 1$) boundaries.

4. Linearly interpolate the difference in the boundary point coordinates and find the correction to be applied to the coordinates of every interior point.

5. For each point, final coordinate value is equal to uni-directionally interpolated value - correction.

The transfinite interpolation is a very simple and powerful numerical procedure. The main weakness of this procedure is that the slope discontinuities at the boundary propagate to the interior and spoil grid smoothness. However, since the metric derivatives are also evaluated numerically, the effect of a slope discontinuity is not severe, as in the case of analytical transformation.

Figure 5.2 shows the mapping procedure for grid points from physical domain (deformed drop) to computational domain (semi-circular region).

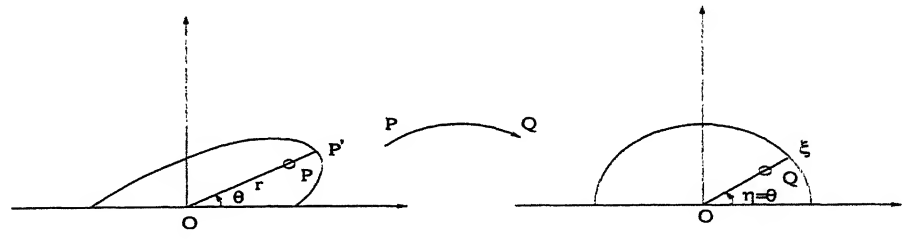

Figure 5.2: Mapping procedure for grid points from physical domain (deformed drop) to computational domain (semi-circular region)

This procedure is described as follows:

$$\eta = \theta \tag{5.7}$$

Then $\xi = \xi(r, \theta)$ is determined for each θ.

If P is any grid point in the physical domain and P$'$ is the grid point where line

joining origin (O) to P when extended meets the boundary. Q is the corresponding grid point on the line joining origin (O) to Q. OQ is given by

$$OQ = \frac{OP}{OP'} \tag{5.8}$$

Chapter 6

Governing equations in transformed coordinates

Dimensionless form of the governing pressure equation in transformed coordinates can be derived to be of the form:

$$A\frac{\partial^2 p}{\partial \xi^2} + B\frac{\partial^2 p}{\partial \eta^2} + E\frac{\partial^2 p}{\partial \xi \partial \eta} + C\frac{\partial p}{\partial \xi} + D1\frac{\partial p}{\partial \eta} = 0 \tag{6.1}$$

where

$$\begin{aligned} A &= \xi_r^2 + \frac{\xi_\theta^2}{r^2} \\ B &= \eta_r^2 + \frac{\eta_\theta^2}{r^2} \\ E &= 2\left(\xi_r \eta_r + \frac{\xi_\theta \eta_\theta}{r^2}\right) \\ C &= \xi_{rr} + \frac{\xi_r}{r} + \frac{\xi_{\theta\theta}}{r^2} \\ D1 &= \eta_{rr} + \frac{\eta_r}{r} + \frac{\eta_{\theta\theta}}{r^2} \end{aligned} \tag{6.2}$$

There boundary conditions in ξ-η coordinates are
For $\eta = 0$ and $\eta = \pi$

$$\frac{\partial p}{\partial \eta} = \frac{r}{\mathrm{Re}}\left(A\frac{\partial^2 v}{\partial \xi^2} + B\frac{\partial^2 v}{\partial \eta^2} + C\frac{\partial^2 v}{\partial \eta \partial \xi} + D\frac{\partial v}{\partial \xi} + E\frac{\partial v}{\partial \eta}\right) - \xi_\theta p_\xi \tag{6.3}$$

where

$$\begin{aligned} A &= \frac{\xi_\theta^2}{r^2} \\ B &= \frac{\eta_\theta^2}{r^2} \\ C &= 2\frac{\xi_\theta \eta\theta}{r^2} \\ D &= \frac{\xi_{\theta\theta}}{r^2} \\ E &= \frac{\eta_{\theta\theta}}{r^2} \\ F &= 2\frac{\xi_\theta}{r^2} \\ G &= 2\frac{\eta_\theta}{r^2} \end{aligned} \tag{6.4}$$

For $\xi = 0$

$$p = \text{Average of pressure values at surrounding grid points} \tag{6.5}$$

For $\xi = 1$

$$p = \frac{1}{\text{We}} \tag{6.6}$$

Dimensionless form of the governing equation for r component of velocity is

$$\begin{aligned} &A\frac{\partial^2 u}{\partial \xi^2} + B\frac{\partial^2 u}{\partial \eta^2} + C\frac{\partial^2 u}{\partial \xi \partial \eta} + D\frac{\partial u}{\partial \xi} + E\frac{\partial u}{\partial \eta} + F\frac{\partial v}{\partial \xi} + G\frac{\partial v}{\partial \eta} + Hu \\ &= AA\frac{\partial p}{\partial \xi} + BB\frac{\partial p}{\partial \eta} \end{aligned} \tag{6.7}$$

where

$$\begin{aligned} A &= \xi_r^2 + \frac{\xi_\theta^2}{r^2} \\ B &= \eta_r^2 + \frac{\eta_\theta^2}{r^2} \\ C &= 2\left(\xi_r\eta_r - \frac{\xi_\theta\eta_\theta}{r^2}\right) \\ D &= \xi_{rr} + \frac{\xi_r}{r} + \frac{\xi_{\theta\theta}}{r^2} \\ E &= \eta_{rr} + \frac{\eta_r}{r} + \frac{\eta_{\theta\theta}}{r^2} \\ F &= -2\frac{\xi_\theta}{r^2} \\ G &= -2\frac{\eta_\theta}{r^2} \\ H &= -\frac{1}{r^2} \\ AA &= \mathrm{Re}(\xi_r) \\ BB &= \mathrm{Re}(\eta_r) \end{aligned} \tag{6.8}$$

The boundary conditions are
For $\eta = 0$

$$u_{i,1} = 1 \tag{6.9}$$

For $\eta = \pi$

$$u_{i,m} = -1 \tag{6.10}$$

For $\xi = 0$

$$u_{1,j} = u_{2,1} + (j-1)\frac{u_{2,m} - u_{2,1}}{m-1} \tag{6.11}$$

For $\xi = 1$

$$u_{n,j} = \frac{v_{n,j}}{r_{n,j}} \left(\frac{r_{n,j-1} - r_{n,j-1}}{2\Delta\eta} \right) \tag{6.12}$$

The dimensionless form of the governing equation for θ component of velocity is

$$\begin{aligned} &A\frac{\partial^2 v}{\partial \xi^2} + B\frac{\partial^2 v}{\partial \eta^2} + C\frac{\partial^2 v}{\partial \eta \partial \xi} + D\frac{\partial v}{\partial \xi} + E\frac{\partial v}{\partial \eta} + F\frac{\partial u}{\partial \xi} + G\frac{\partial u}{\partial \eta} + Hv \\ &= Co1\frac{\partial p}{\partial \xi} + Co2\frac{\partial p}{\partial \eta} \end{aligned} \tag{6.13}$$

where

$$\begin{aligned} A &= \xi_r^2 + \frac{\xi_\theta^2}{r^2} \\ B &= \eta_r^2 + \frac{\eta_\theta^2}{r^2} \\ C &= 2\left(\xi_r \eta_r + \frac{\xi_\theta \eta_\theta}{r^2} \right) \\ D &= \xi_{rr} + \frac{\xi_r}{r} + \frac{\xi_{\theta\theta}}{r^2} \\ E &= \eta_{rr} + \frac{\eta_r}{r} + \frac{\eta_{\theta\theta}}{r^2} \\ F &= 2\frac{\xi_\theta}{r^2} \\ G &= 2\frac{\eta_\theta}{r^2} \\ H &= -\frac{1}{r^2} \\ Co1 &= \mathrm{Re}\left(\frac{\xi_\theta}{r} \right) \\ Co2 &= \mathrm{Re}\left(\frac{\eta_\theta}{r} \right) \end{aligned} \tag{6.14}$$

The boundary conditions are

For $\eta = 0$

$$v_{i,1} = 0 \tag{6.15}$$

For $\eta = \pi$

$$v_{i,m} = 0 \tag{6.16}$$

For $\xi = 0$

$$v_{1,j} = 0 \tag{6.17}$$

For $\xi = 1$

$$v_{n,j} = \frac{\sqrt{\left[1+\left(\eta_\theta \frac{r_{n,j+1}-r_{n,j-1}}{2r_{n,j}\Delta\eta}\right)^2\right]}}{2}\left(\frac{\eta_\theta \frac{u_{n-1,j}r_{n-1,j+1}-r_{n-1,j-1}}{2r_{n-1,j}\Delta\eta}+v_{n-1,j}}{\sqrt{\left[1+\left(\eta_\theta \frac{r_{n-1,j+1}-r_{n-1,j-1}}{2r_{n-1,j}\Delta\eta}\right)^2\right]}}+\right.$$
$$\left.\frac{\eta_\theta \frac{u_{n-1,j-1}r_{n-1,j}-r_{n-1,j-2}}{2r_{n-1,j-1}\Delta\eta}+v_{n-1,j-1}}{\sqrt{\left[1+\left(\eta_\theta \frac{r_{n-1,j}-r_{n-1,j-2}}{2r_{n-1,j-1}\Delta\eta}\right)^2\right]}}\right)-\eta_\theta \frac{u_{n,j}r_{n,j+1}-r_{n,j-1}}{2r_{n,j}\Delta\eta} \tag{6.18}$$

Simplifying all equations for the case where $\eta = \theta$ and only ξ_r (or r_ξ) is non-zero, we obtain the following equations:
Dimensionless form of the governing pressure equation in transformed coordinates can be derived to be of the form:

$$A\frac{\partial^2 p}{\partial \xi^2}+B\frac{\partial^2 p}{\partial \eta^2}+E\frac{\partial^2 p}{\partial \xi \partial \eta}+C\frac{\partial p}{\partial \xi}+D1\frac{\partial p}{\partial \eta}=0 \tag{6.19}$$

where

$$\begin{aligned} A &= 0 \\ B &= \frac{1}{r^2} \\ E &= 0 \\ C &= \frac{\xi_r}{r} \\ D1 &= 0 \end{aligned} \tag{6.20}$$

There boundary conditions in ξ-η coordinates are
For $\eta = 0$ and $\eta = \pi$

$$\frac{\partial p}{\partial \eta} = \frac{r}{\mathrm{Re}} \left(A\frac{\partial^2 v}{\partial \xi^2} + B\frac{\partial^2 v}{\partial \eta^2} + C\frac{\partial^2 v}{\partial \eta \partial \xi} + D\frac{\partial v}{\partial \xi} + E\frac{\partial v}{\partial \eta} \right) - \xi_\theta p_\xi \tag{6.21}$$

where

$$\begin{aligned} A &= 0 \\ B &= \frac{1}{r^2} \\ C &= 0 \\ D &= 0 \\ E &= 0 \\ F &= 0 \\ G &= \frac{2}{r^2} \end{aligned} \tag{6.22}$$

For $\xi = 0$

$$p = \text{Average of pressure values at surrounding grid points} \tag{6.23}$$

For $\xi = 1$

$$p = \frac{1}{\mathrm{We}} \tag{6.24}$$

Dimensionless form of the governing equation for r component of velocity is

$$A\frac{\partial^2 u}{\partial \xi^2} + B\frac{\partial^2 u}{\partial \eta^2} + C\frac{\partial^2 u}{\partial \xi \partial \eta} + D\frac{\partial u}{\partial \xi} + E\frac{\partial u}{\partial \eta} + F\frac{\partial v}{\partial \xi} + G\frac{\partial v}{\partial \eta} - Hu$$
$$= AA\frac{\partial p}{\partial \xi} + BB\frac{\partial p}{\partial \eta} \tag{6.25}$$

where

$$\begin{aligned} A &= \xi_r^2 \\ B &= \frac{1}{r^2} \\ C &= 0 \\ D &= \frac{\xi_r}{r} \\ E &= 0 \\ F &= 0 \\ G &= -\frac{2}{r^2} \\ H &= -\frac{1}{r^2} \\ AA &= \mathrm{Re}(\xi_r) \\ BB &= 0 \end{aligned} \tag{6.26}$$

The boundary conditions are
For $\eta = 0$

$$u_{i,1} = 1 \tag{6.27}$$

For $\eta = \pi$

$$u_{i,m} = -1 \tag{6.28}$$

For $\xi = 0$

$$u_{1,j} = u_{2,1} + (j-1)\frac{u_{2,m} - u_{2,1}}{m-1} \tag{6.29}$$

For $\xi = 1$

$$u_{n,j} = \frac{v_{n,j}}{r_{n,j}}\left(\frac{r_{n,j+1} - r_{n,j-1}}{2\Delta\theta}\right) \tag{6.30}$$

The dimensionless form of the governing equation for θ component of velocity is

$$\begin{aligned} &A\frac{\partial^2 v}{\partial \xi^2} + B\frac{\partial^2 v}{\partial \eta^2} + C\frac{\partial^2 v}{\partial \eta \partial \xi} + D\frac{\partial v}{\partial \xi} + E\frac{\partial v}{\partial \eta} + F\frac{\partial u}{\partial \xi} + G\frac{\partial u}{\partial \eta} + Hv \\ &= Co1\frac{\partial p}{\partial \xi} + Co2\frac{\partial p}{\partial \eta} \end{aligned} \tag{6.31}$$

where

$$\begin{aligned} A &= \xi_r^2 \\ B &= \frac{\eta_\theta^2}{r^2} \\ C &= 0 \\ D &= \frac{\xi_r}{r} \\ E &= 0 \\ F &= 0 \\ G &= \frac{2}{r^2} \\ H &= -\frac{1}{r^2} \\ Co1 &= 0 \\ Co2 &= \mathrm{Re}\left(\frac{1}{r}\right) \end{aligned} \tag{6.32}$$

The boundary conditions are

For $\eta = 0$

$$v_{i,1} = 0 \tag{6.33}$$

For $\eta = \pi$

$$v_{i,m} = 0 \tag{6.34}$$

For $\xi = 0$

$$v_{1,j} = 0 \tag{6.35}$$

For $\xi = 1$

$$v_{n,j} = \frac{\sqrt{\left[1+\left(\frac{r_{n,j+1}-r_{n,j-1}}{2r_{n,j}\Delta\theta}\right)^2\right]}}{2}\left(\frac{\frac{u_{n-1,j}r_{n-1,j+1}-r_{n-1,j-1}}{2r_{n-1,j}\Delta\theta}+v_{n-1,j}}{\sqrt{\left[1+\left(\frac{r_{n-1,j+1}-r_{n-1,j-1}}{2r_{n-1,j}\Delta\theta}\right)^2\right]}}+\frac{\frac{u_{n-1,j-1}r_{n-1,j}-r_{n-1,j-2}}{2r_{n-1,j-1}\Delta\theta}+v_{n-1,j-1}}{\sqrt{\left[1+\left(\frac{r_{n-1,j}-r_{n-1,j-2}}{2r_{n-1,j-1}\Delta\theta}\right)^2\right]}}\right)-\frac{u_{n,j}r_{n,j+1}-r_{n,j-1}}{2r_{n,j}\Delta\theta} \tag{6.36}$$

Chapter 7

Numerical solution of the governing equations in transformed coordinates

Dimensionless form of the governing pressure equation in transformed coordinates, with i being the index of variation in the radial direction (r or ξ), both in physical and computational domains, and j being the index of variation in the angular direction (θ or η), both in physical and computational domains.

$$A\frac{\partial^2 p}{\partial \xi^2} + B\frac{\partial^2 p}{\partial \eta^2} + E\frac{\partial^2 p}{\partial \xi \partial \eta} + C\frac{\partial p}{\partial \xi} + D1\frac{\partial p}{\partial \eta} = 0 \tag{7.1}$$

where

$$\begin{aligned} A &= \xi_r^2 + \frac{\xi_\theta^2}{r^2} \\ B &= \eta_r^2 + \frac{\eta_\theta^2}{r^2} \\ E &= 2\left(\xi_r \eta_r + \frac{\xi_\theta \eta_\theta}{r^2}\right) \\ C &= \xi_{rr} + \frac{\xi_r}{r} + \frac{\xi_{\theta\theta}}{r^2} \\ D1 &= \eta_{rr} + \frac{\eta_r}{r} + \frac{\eta_{\theta\theta}}{r^2} \end{aligned} \tag{7.2}$$

scretizing the governing differential equation for pressure. we get

$$A\left[\frac{p_{i-1,j}-2p_{i,j}+p_{i+1,j}}{(\Delta\xi)^2}\right]+B\left[\frac{p_{i,j-1}-2p_{i,j}+p_{i,j-1}}{(\Delta\eta)^2}\right]+$$
$$E\left[\frac{p_{i+1,j+1}-p_{i+1,j-1}-p_{i-1,j-1}+p_{i-1,j-1}}{4(\Delta\xi)(\Delta\eta)}\right]+C\left[\frac{p_{i+1,j}-p_{i-1,j}}{2\Delta\xi}\right]$$
$$+D1\left[\frac{p_{i,j+1}-p_{i,j-1}}{2\Delta\eta}\right]=0 \tag{7.3}$$

$$\begin{aligned} p_{i,j} = \frac{1}{[2A(\Delta\eta)^2+2B(\Delta\xi)^2]}\Bigg[&p_{i-1,j}\frac{\Delta\eta^2}{2}(2A-C\Delta\xi)+\\ &p_{i+1,j}\frac{\Delta\eta^2}{2}(2A+C\Delta\xi)+p_{i,j+1}\frac{\Delta\xi^2}{2}(2B+D1\Delta\eta)+\\ &p_{i,j-1}\frac{\Delta\xi^2}{2}(2B-D1\Delta\eta)+\\ &E\frac{(\Delta\xi)(\Delta\eta)}{4}\{p_{i+1,j+1}-p_{i+1,j-1}-p_{i-1,j+1}+p_{i-1,j-1}\}\Bigg] \end{aligned} \tag{7.4}$$

e boundary conditions are

r $\eta=0$

$$\begin{aligned} p_{i,1} = p_{i,2}-\frac{\Delta\eta}{\eta_\theta}\Bigg[&\frac{r}{\mathrm{Re}}\left(A\frac{\partial^2 v}{\partial\xi^2}+B\frac{\partial^2 v}{\partial\eta^2}+C\frac{\partial^2 v}{\partial\eta\partial\xi}+D\frac{\partial v}{\partial\xi}+E\frac{\partial v}{\partial\eta}\right)\\ &-\xi_\theta\frac{\partial p}{\partial\xi}\Bigg] \end{aligned} \tag{7.5}$$

ere A, B, C, D, E, F, G have been defined in Equation (6.4).

: $\eta=\pi$

$$\begin{aligned} p_{i,m} = p_{i,m-1}+\frac{\Delta\eta}{\eta_\theta}\Bigg[&\frac{r}{\mathrm{Re}}\left(A\frac{\partial^2 v}{\partial\xi^2}+B\frac{\partial^2 v}{\partial\eta^2}+C\frac{\partial^2 v}{\partial\eta\partial\xi}+D\frac{\partial v}{\partial\xi}+E\frac{\partial v}{\partial\eta}\right)\\ &-\xi_\theta\frac{\partial p}{\partial\xi}\Bigg] \end{aligned} \tag{7.6}$$

For $\xi = 0$

$$p = \text{Average of pressure values at surrounding grid points} \tag{7.7}$$

For $\xi = 1$

$$p = \frac{1}{We} \tag{7.8}$$

Dimensionless form of the governing equation for r component of velocity is

$$\begin{aligned} &A\frac{\partial^2 u}{\partial \xi^2} + B\frac{\partial^2 u}{\partial \eta^2} + C\frac{\partial^2 u}{\partial \xi \partial \eta} + D\frac{\partial u}{\partial \xi} + E\frac{\partial u}{\partial \eta} + F\frac{\partial v}{\partial \xi} + G\frac{\partial v}{\partial \eta} + Hu \\ &= AA\frac{\partial p}{\partial \xi} + BB\frac{\partial p}{\partial \eta} \end{aligned} \tag{7.9}$$

where

$$\begin{aligned} A &= \xi_r^2 + \frac{\xi_\theta^2}{r^2} \\ B &= \eta_r^2 + \frac{\eta_\theta^2}{r^2} \\ C &= 2\left(\xi_r \eta_r + \frac{\xi_\theta \eta_\theta}{r^2}\right) \\ D &= \xi_{rr} + \frac{\xi_r}{r} + \frac{\xi_{\theta\theta}}{r^2} \\ E &= \eta_{rr} + \frac{\eta_r}{r} + \frac{\eta_{\theta\theta}}{r^2} \\ F &= -2\frac{\xi_\theta}{r^2} \\ G &= -2\frac{\eta_\theta}{r^2} \\ H &= -\frac{1}{r^2} \\ AA &= \mathrm{Re}(\xi_r) \\ BB &= \mathrm{Re}(\eta_r) \end{aligned} \tag{7.10}$$

Discretizing by finite difference. we get

$$A\left[\frac{u_{i-1,j}-2u_{i,j}+u_{i-1,j}}{(\Delta\xi)^2}\right]+B\left[\frac{u_{i,j-1}-2u_{i,j}+u_{i,j+1}}{(\Delta\eta)^2}\right]+$$
$$C\left[\frac{u_{i+1,j+1}-u_{i+1,j-1}-u_{i-1,j+1}+u_{i-1,j-1}}{4(\Delta\eta)(\Delta\xi)}\right]-D\left[\frac{u_{i+1,j}-u_{i-1,j}}{2(\Delta\xi)}\right]+$$
$$E\left[\frac{u_{i,j+1}-u_{i,j-1}}{2(\Delta\eta)}\right]+F\left[\frac{v_{i+1,j}-v_{i-1,j}}{2(\Delta\xi)}\right]+G\left[\frac{v_{i,j+1}-v_{i,j-1}}{2(\Delta\eta)}\right]+$$
$$Hu_{i,j}=AA\left[\frac{p_{i-1,j}-p_{i-1,j}}{2(\Delta\xi)}\right]+BB\left[\frac{p_{i,j+1}-p_{i,j-1}}{2(\Delta\eta)}\right] \tag{7.11}$$

or

$$\begin{aligned}u_{i,j} = {} & \frac{1}{[2A\Delta\eta^2+2B\Delta\xi^2-H\Delta\xi^2\Delta\eta^2]}\left[u_{i-1,j}\frac{\Delta\eta^2}{2}(2A-D\Delta\xi)+\right.\\
& u_{i+1,j}\frac{\Delta\eta^2}{2}(2A+D\Delta\xi)+u_{i,j-1}\frac{\Delta\xi^2}{2}(2B-E\Delta\eta)+\\
& u_{i,j+1}\frac{\Delta\xi^2}{2}(2B+E\Delta\eta)+\\
& C\frac{(\Delta\xi)(\Delta\eta)}{4}(u_{i+1,j+1}-u_{i+1,j-1}-u_{i-1,j+1}+u_{i-1,j-1})+\\
& F\frac{(\Delta\eta)^2(\Delta\xi)}{2}(v_{i+1,j}-v_{i-1,j})+G\frac{(\Delta\xi)^2(\Delta\eta)}{2}(v_{i,j+1}-v_{i,j-1})-\\
& AA\frac{(\Delta\eta)^2(\Delta\xi)}{2}(p_{i+1,j}-p_{i-1,j})\\
& \left.-BB\frac{(\Delta\xi)^2(\Delta\eta)}{2}(p_{i,j+1}-p_{i,j-1})\right]\end{aligned} \tag{7.12}$$

The boundary conditions are

For $\eta = 0$

$$u_{i,1}=1 \tag{7.13}$$

For $\eta = \pi$

$$u_{i,m} = -1 \tag{7.14}$$

For $\xi = 0$

$$u_{1,j} = u_{2,i} + (j-1)\frac{u_{2,m} - u_{2,i}}{m-1} \tag{7.15}$$

For $\xi = 1$

$$u_{n,j} = \frac{v_{n,j}}{r_{n,j}}\left(\frac{r_{n,j+1} - r_{n,j-1}}{2\Delta\eta}\right) \tag{7.16}$$

Dimensionless form of the governing equation for θ component of velocity is

$$\begin{aligned} &A\frac{\partial^2 v}{\partial \xi^2} + B\frac{\partial^2 v}{\partial \eta^2} + C\frac{\partial^2 v}{\partial \eta \partial \xi} + D\frac{\partial v}{\partial \xi} + E\frac{\partial v}{\partial \eta} + F\frac{\partial u}{\partial \xi} + G\frac{\partial u}{\partial \eta} + Hv \\ &= Co1\frac{\partial p}{\partial \xi} + Co2\frac{\partial p}{\partial \eta} \end{aligned} \tag{7.17}$$

where

$$\begin{aligned} A &= \xi_r^2 + \frac{\xi_\theta^2}{r^2} \\ B &= \eta_r^2 + \frac{\eta_\theta^2}{r^2} \\ C &= 2\left(\xi_r \eta_r + \frac{\xi_\theta \eta_\theta}{r^2}\right) \\ D &= \xi_{rr} + \frac{\xi_r}{r} + \frac{\xi_{\theta\theta}}{r^2} \\ E &= \eta_{rr} + \frac{\eta_r}{r} + \frac{\eta_{\theta\theta}}{r^2} \\ F &= 2\frac{\xi_\theta}{r^2} \\ G &= 2\frac{\eta_\theta}{r^2} \end{aligned}$$

$$
\begin{aligned}
H &= -\frac{1}{r^2} \\
Co1 &= \mathrm{Re}\frac{\xi_\theta}{r} \\
Co2 &= \mathrm{Re}\frac{\eta_\theta}{r}
\end{aligned} \tag{7.18}
$$

Discretizing by finite differences. we get

$$
\begin{aligned}
&A\left[\frac{v_{i+1,j}-2v_{i,j}+v_{i-1,j}}{(\Delta\xi)^2}\right]+B\left[\frac{v_{i,j+1}-2v_{i,j}+v_{i,j-1}}{(\Delta\eta)^2}\right]+ \\
&C\left[\frac{v_{i+1,j+1}-v_{i+1,j-1}-v_{i-1,j+1}+v_{i-1,j-1}}{4(\Delta\eta)(\Delta\xi)}\right]+D\left[\frac{v_{i-1,j}-v_{i-1,j}}{2(\Delta\xi)}\right]+ \\
&E\left[\frac{v_{i,j+1}-v_{i,j-1}}{2(\Delta\eta)}\right]+F\left[\frac{u_{i+1,j}-u_{i-1,j}}{2(\Delta\xi)}\right]+G\left[\frac{u_{i,j+1}-u_{i,j-1}}{2(\Delta\eta)}\right]+ \\
&Hv_{i,j}=Co1\left[\frac{p_{i+1,j}-p_{i-1,j}}{2(\Delta\xi)}\right]+Co2\left[\frac{p_{i,j+1}-p_{i,j-1}}{2(\Delta\eta)}\right]
\end{aligned} \tag{7.19}
$$

or

$$
\begin{aligned}
v_{i,j} = \frac{1}{[2A(\Delta\eta)^2+2B(\Delta\xi)^2-H(\Delta\eta)^2(\Delta\xi)^2]}\Bigg[&v_{i+1,j}\frac{(\Delta\eta)^2}{2}(2A+D\Delta\xi) \\
&+v_{i-1,j}\frac{(\Delta\eta)^2}{2}(2A-D\Delta\xi)+v_{i,j+1}\frac{(\Delta\xi)^2}{2}(2B+E\Delta\eta)+ \\
&v_{i,j-1}\frac{(\Delta\xi)^2}{2}(2B-E\Delta\eta)+ \\
&C(\Delta\xi)(\Delta\eta)\frac{v_{i+1,j+1}-v_{i+1,j-1}-v_{i-1,j+1}+v_{i-1,j-1}}{4}+ \\
&F(u_{i+1,j}-u_{i-1,j})\frac{\Delta\eta^2(\Delta\xi)}{2}+G(u_{i,j+1}-u_{i,j-1})\frac{(\Delta\xi)^2(\Delta\eta)}{2}- \\
&Co1(p_{i+1,j}-p_{i-1,j})\frac{(\Delta\eta)^2(\Delta\xi)}{2} \\
&-Co2(p_{i,j+1}-p_{i,j-1})\frac{(\Delta\xi)^2(\Delta\eta)}{2}\Bigg]
\end{aligned} \tag{7.20}
$$

The boundary conditions are

For $\eta = 0$

$$v_{i,1} = 0 \tag{7.21}$$

For $\eta = \pi$

$$v_{i,m} = 0 \tag{7.22}$$

For $\xi = 0$

$$v_{1,j} = 0 \tag{7.23}$$

For $\xi = 1$

$$v_{n,j} = \frac{\sqrt{\left[1+\left(\eta_\theta \frac{r_{n,j+1}-r_{n,j-1}}{2r_{n,j}\Delta\eta}\right)^2\right]}}{2}\left(\frac{\eta_\theta \frac{u_{n-1,j}r_{n-1,j+1}-r_{n-1,j-1}}{2r_{n-1,j}\Delta\eta}+v_{n-1,j}}{\sqrt{\left[1+\left(\eta_\theta \frac{r_{n-1,j+1}-r_{n-1,j-1}}{2r_{n-1,j}\Delta\eta}\right)^2\right]}}+\right.$$
$$\left.\frac{\eta_\theta \frac{u_{n-1,j-1}r_{n-1,j}-r_{n-1,j-2}}{2r_{n-1,j-1}\Delta\eta}+v_{n-1,j-1}}{\sqrt{\left[1+\left(\eta_\theta \frac{r_{n-1,j}-r_{n-1,j-2}}{2r_{n-1,j-1}\Delta\eta}\right)^2\right]}}\right)-\eta_\theta \frac{u_{n,j}r_{n,j+1}-r_{n,j-1}}{2r_{n,j}\Delta\eta} \tag{7.24}$$

7.1 Coefficient of Friction

Coefficient of friction for the deformed drop can be calculated as

$$\text{coefficient of friction} = \frac{\mu\int_{r=0}^{r=1}\frac{1}{r}\left(\frac{\partial u}{\partial\theta}\right)dr+\mu\int_{r=-1}^{r=0}\frac{1}{r}\left(\frac{\partial u}{\partial\theta}\right)dr}{\text{Rey}\left(\frac{\pi}{2\text{Fr}^2}+\frac{2}{\text{We}}\right)} \tag{7.25}$$

where

$$\begin{aligned} \text{Re}_Y &= \frac{\rho u_0 r_1}{\mu} \\ \text{Fr} &= \frac{u_0}{\sqrt{(g r_1)}} \\ \text{We} &= \frac{\rho u_0^2 r_1}{\gamma} \end{aligned} \tag{7.26}$$

For 10mm^3 drop and u_0=1m/s. Fr is 35.7434.
Below is table for coefficient of friction for a deformed drop. with We and Re varied over three orders of magnitudes. The coefficient of friction increases with decreasing Reynolds number because of an increase in viscosity. It decreases with decreasing Weber number (increasing surface tension) because of an increase in the bulk pressure of the drop.

Table3. Variation of Coefficient of Friction with Re and We.

S.No.	We	Re	Coefficient of Friction
1	0.01	0.01	1.912
2	0.1	0.01	19.441
3	1.0	0.01	201.124
4	0.01	0.1	0.272
5	0.1	0.1	1.931
6	1.0	0.1	19.434
7	0.01	1.0	0.019
8	0.1	1.0	0.288
9	1.0	1.0	1.924

It can be noted that drop deformation does not have a major influence on coefficient of friction, when compared to that for a semi-circular drop.

7.2 Results and Discussion

Figure 7.1 shows pressure contours and velocity vectors in semi-circular region (computational domain) and deformed drop (physical domain), for Weber number 0.01 and Reynolds number 0.01. The boundary has a constant pressure. Inside

the drop, the pressure must be greater than that on the boundary. The boundary condition for velocity is that there is no flow in the direction of the normal vector to the boundary and there is no shear stress at the boundary. The velocity vectors are computed with respect to the plate. Similarly Figures 7.2 to 7.9 show pressure contours and velocity vectors in semi-circular region (computational domain) and deformed drop (physical domain), for the same boundary condition for pressure and velocity, except in all these figures Weber number and Reynolds number vary over three orders of magnitude. As Weber number increases from 0.01 to 1.0, the values of pressure contours decreases. With increasing Reynolds number, velocity is increased.

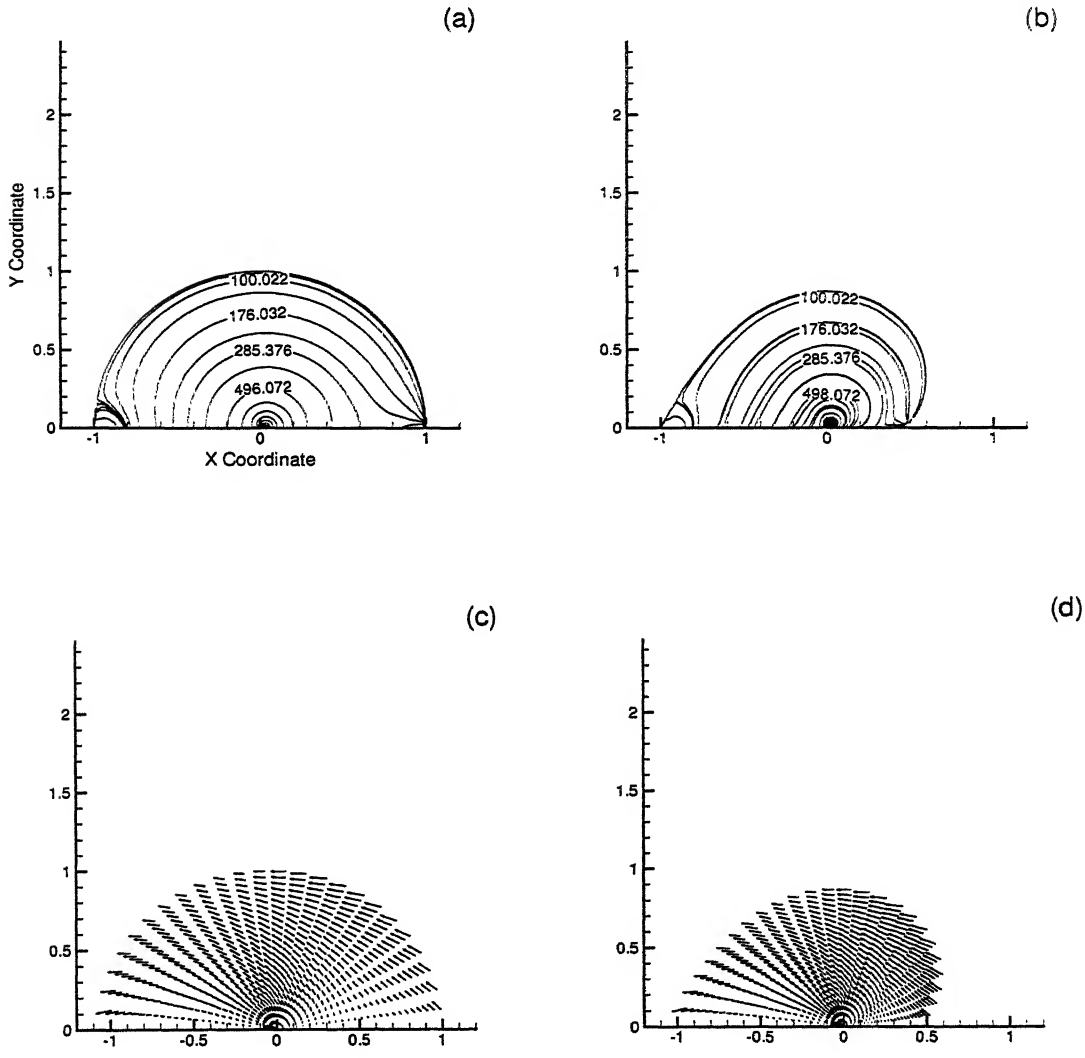

Figure 7.1: Pressure contours and velocity vectors (relative to the plate) for We=0.01 and Re=0.01. (a), (c): computational domain; (b), (d): physical domain.

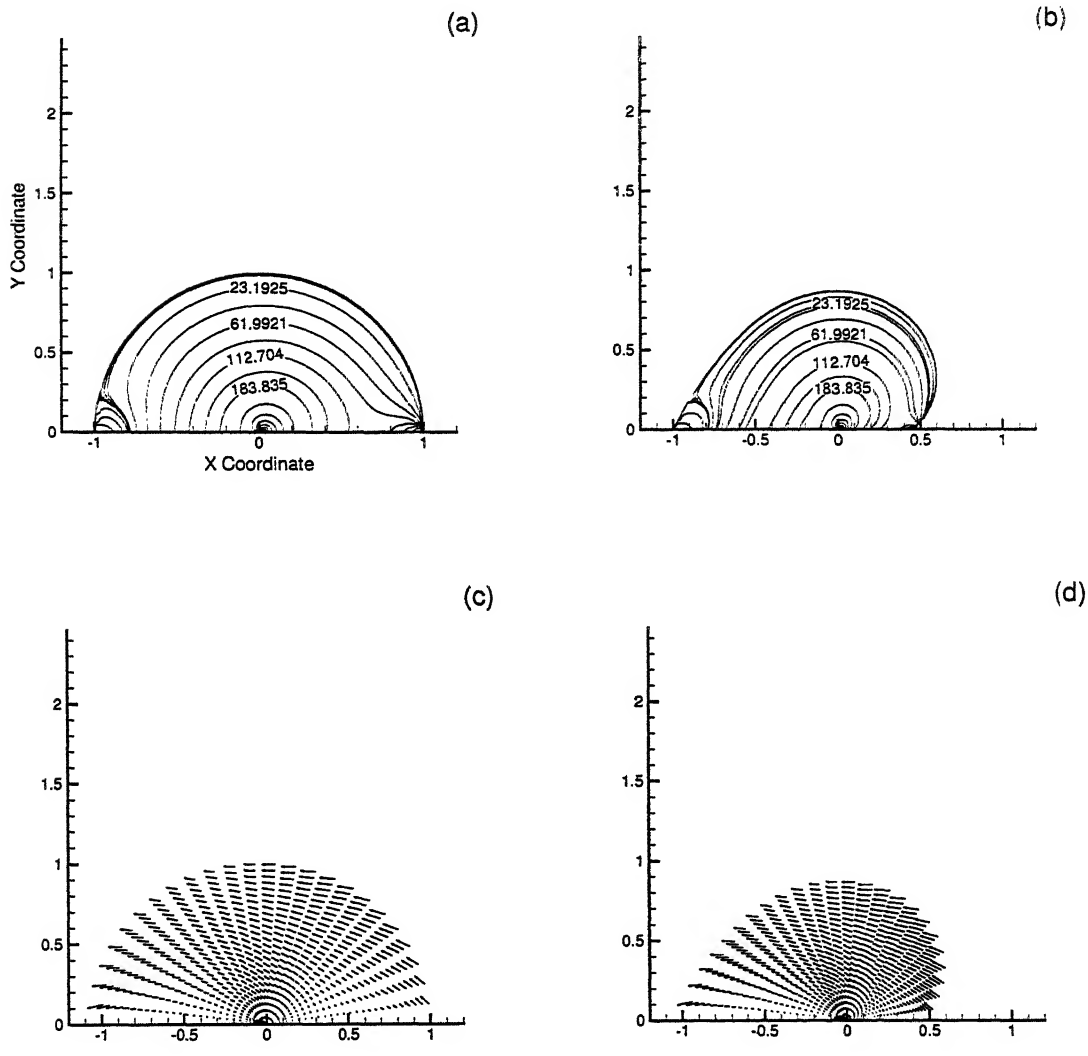

Figure 7.2: Pressure contours and velocity vectors for We=0.1 and Re=0.01. (a), (c): computational domain; (b), (d): physical domain.

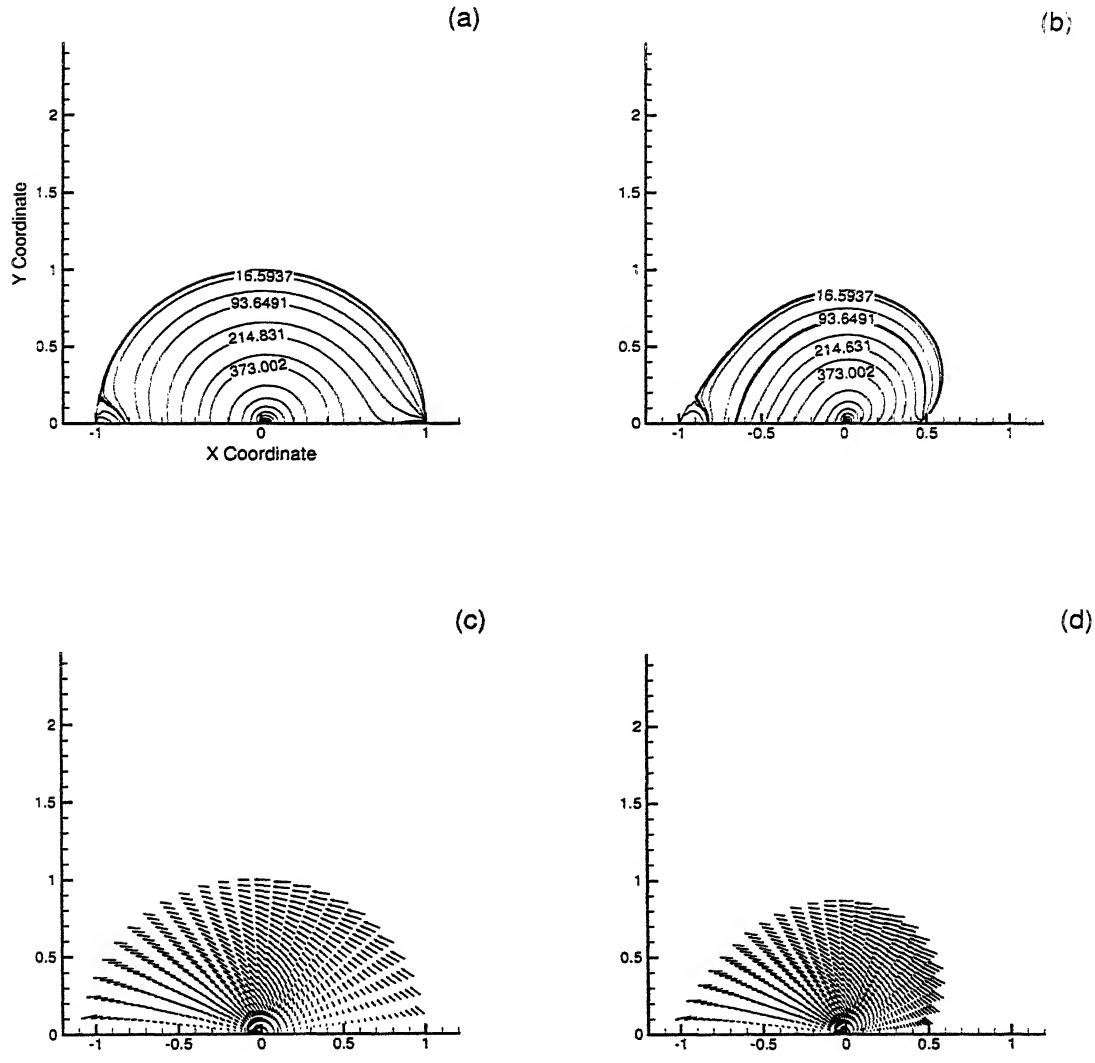

Figure 7.3: Pressure contours and velocity vectors (relative to the plate) for We=1.0 and Re=0.01. (a), (c): computational domain; (b), (d): physical domain.

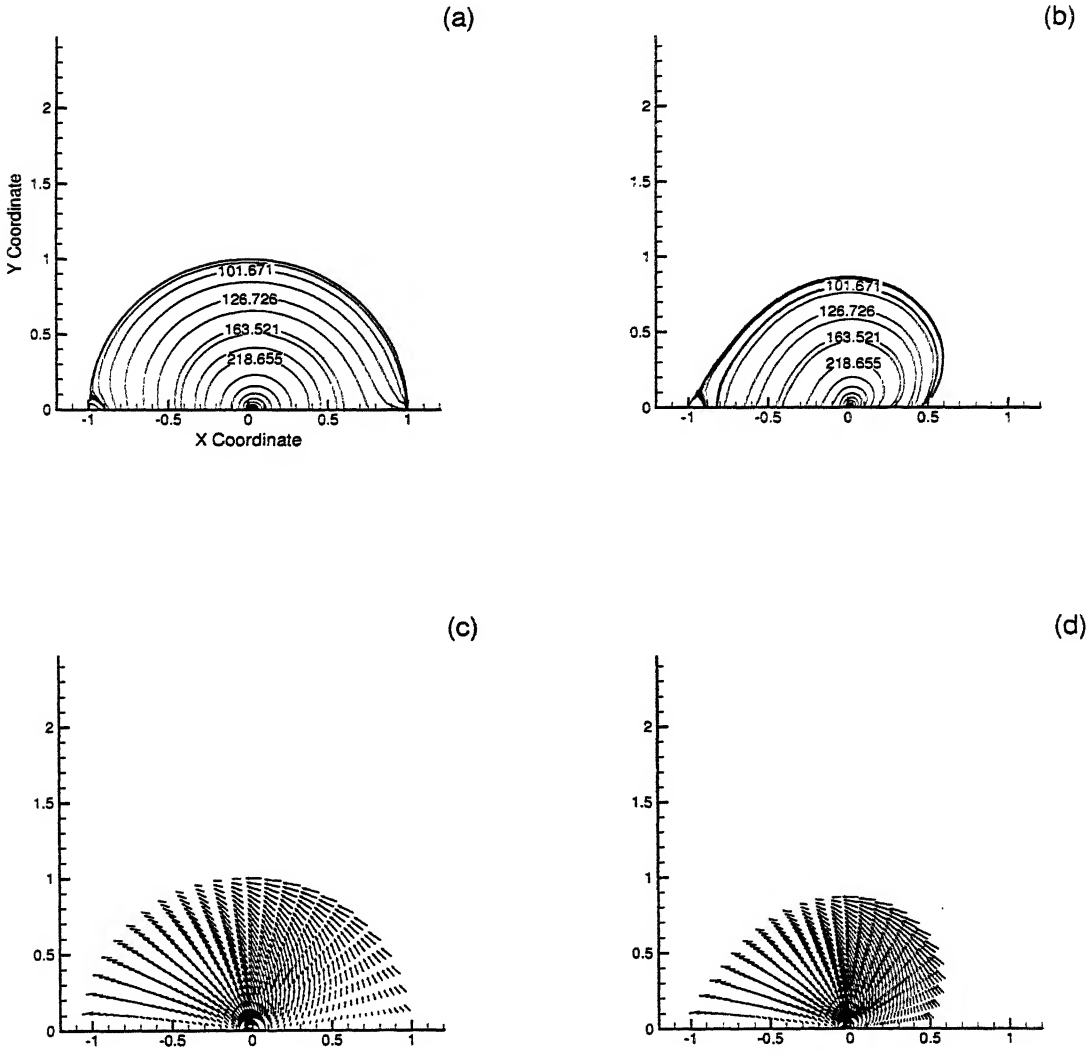

Figure 7.4: Pressure contours and velocity vectors (relative to the plate) for We=0.01 and Re=0.1. (a), (c): computational domain; (b), (d): physical domain.

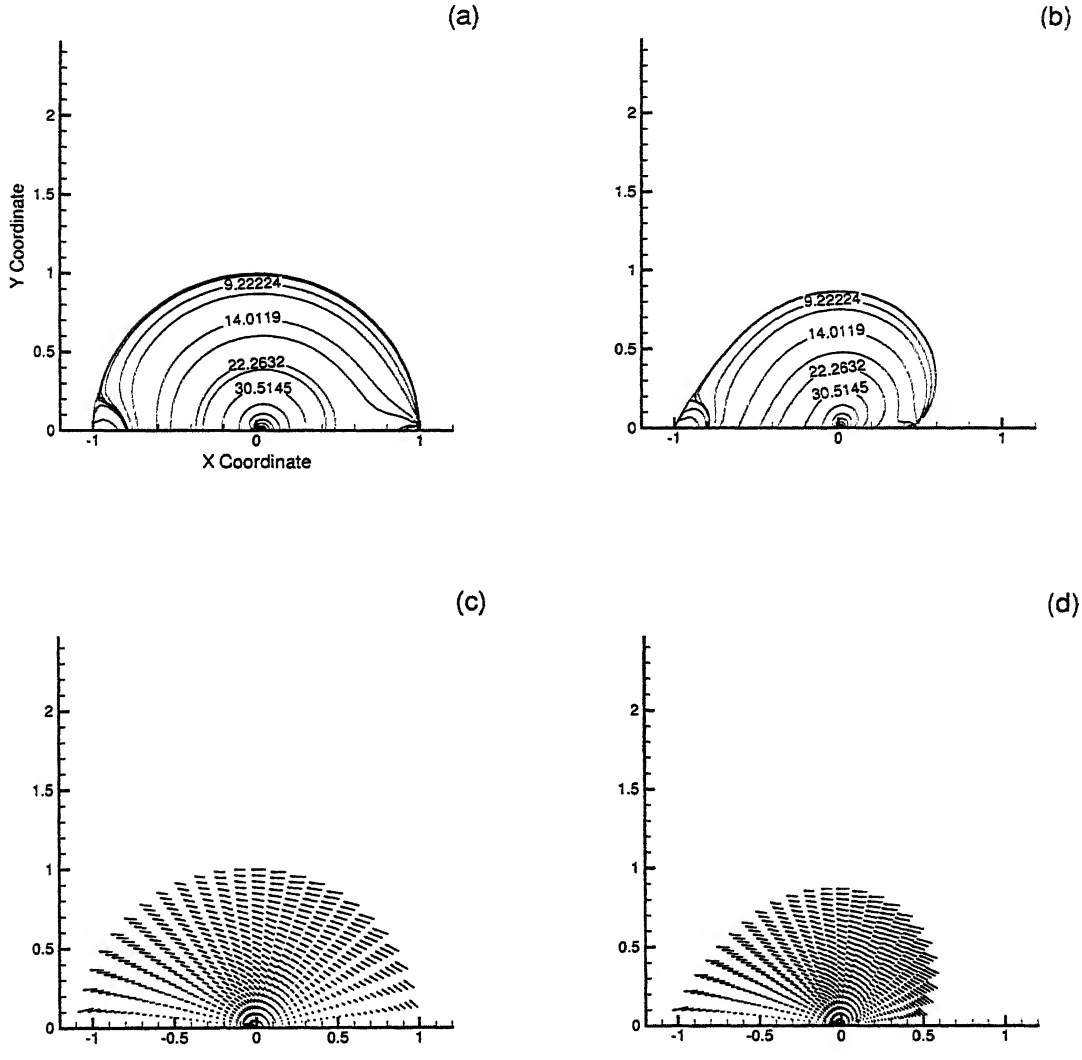

Figure 7.5: Pressure contours and velocity vectors (relative to the plate) for We=0.1 and Re=0.1. (a), (c): computational domain; (b), (d): physical domain.

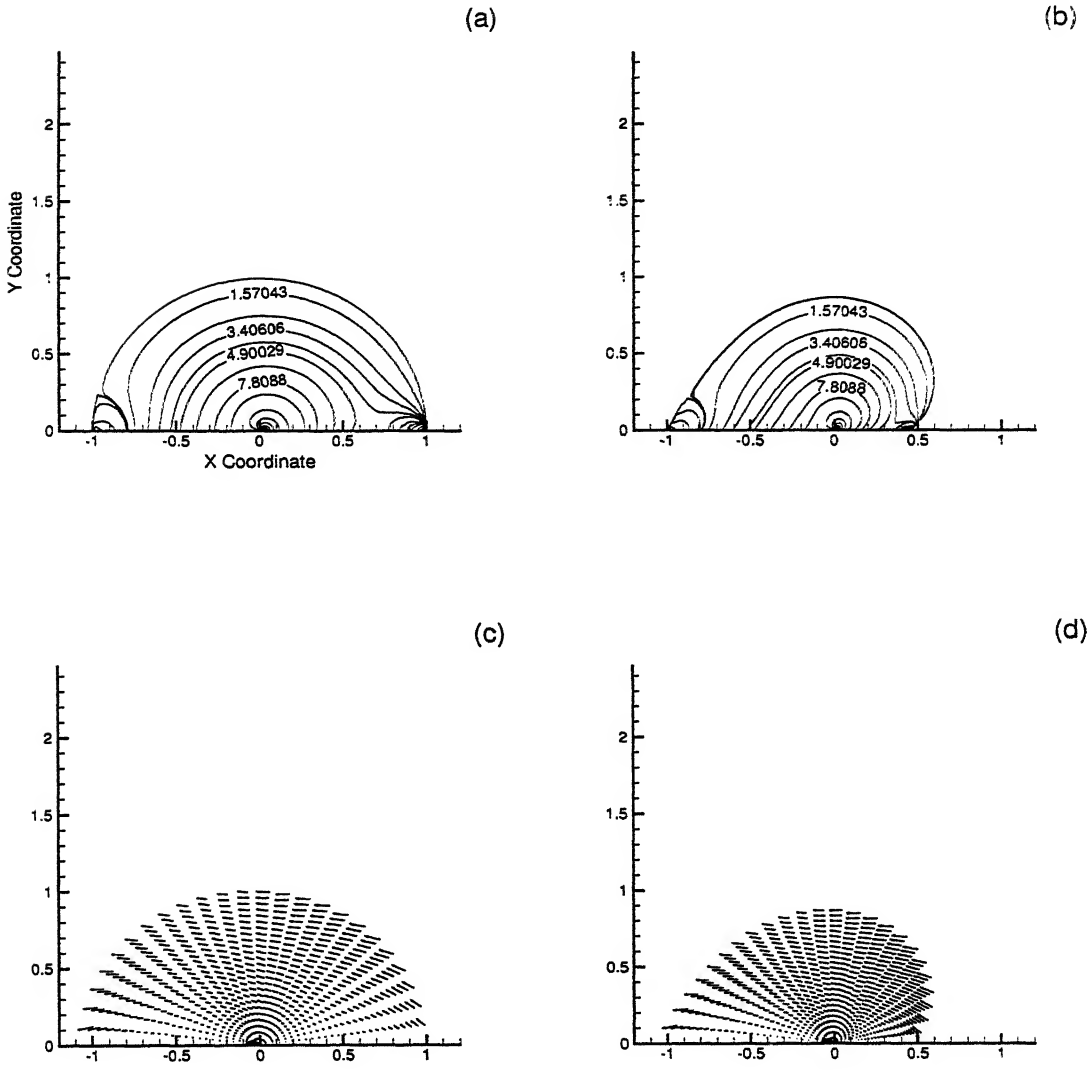

Figure 7.6: Pressure contours and velocity vectors (relative to the plate) for We=1.0 and Re=0.1. (a), (c): computational domain; (b), (d): physical domain.

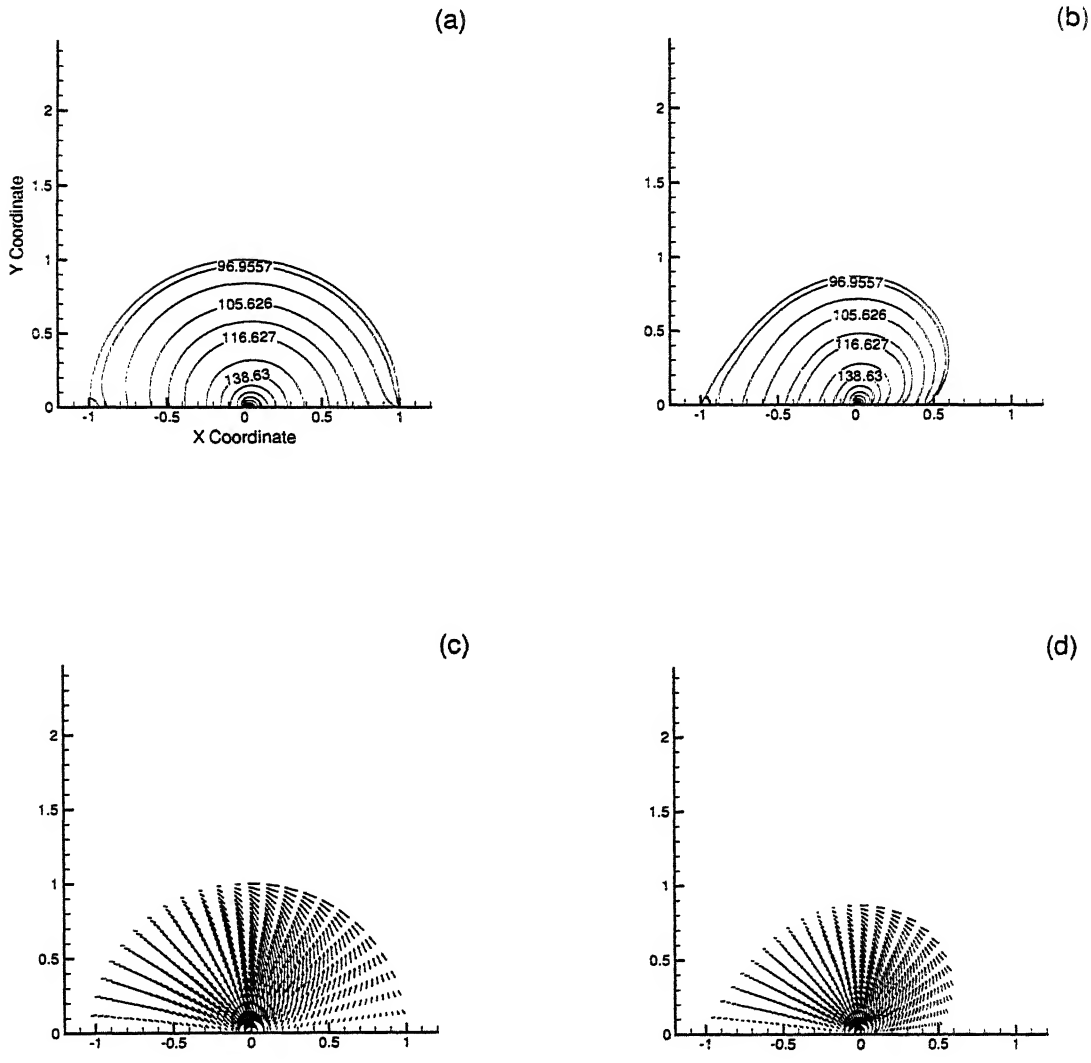

Figure 7.7: Pressure contours and velocity vectors (relative to the plate) for We=0.01 and Re=1.0. (a), (c): computational domain; (b), (d): physical domain.

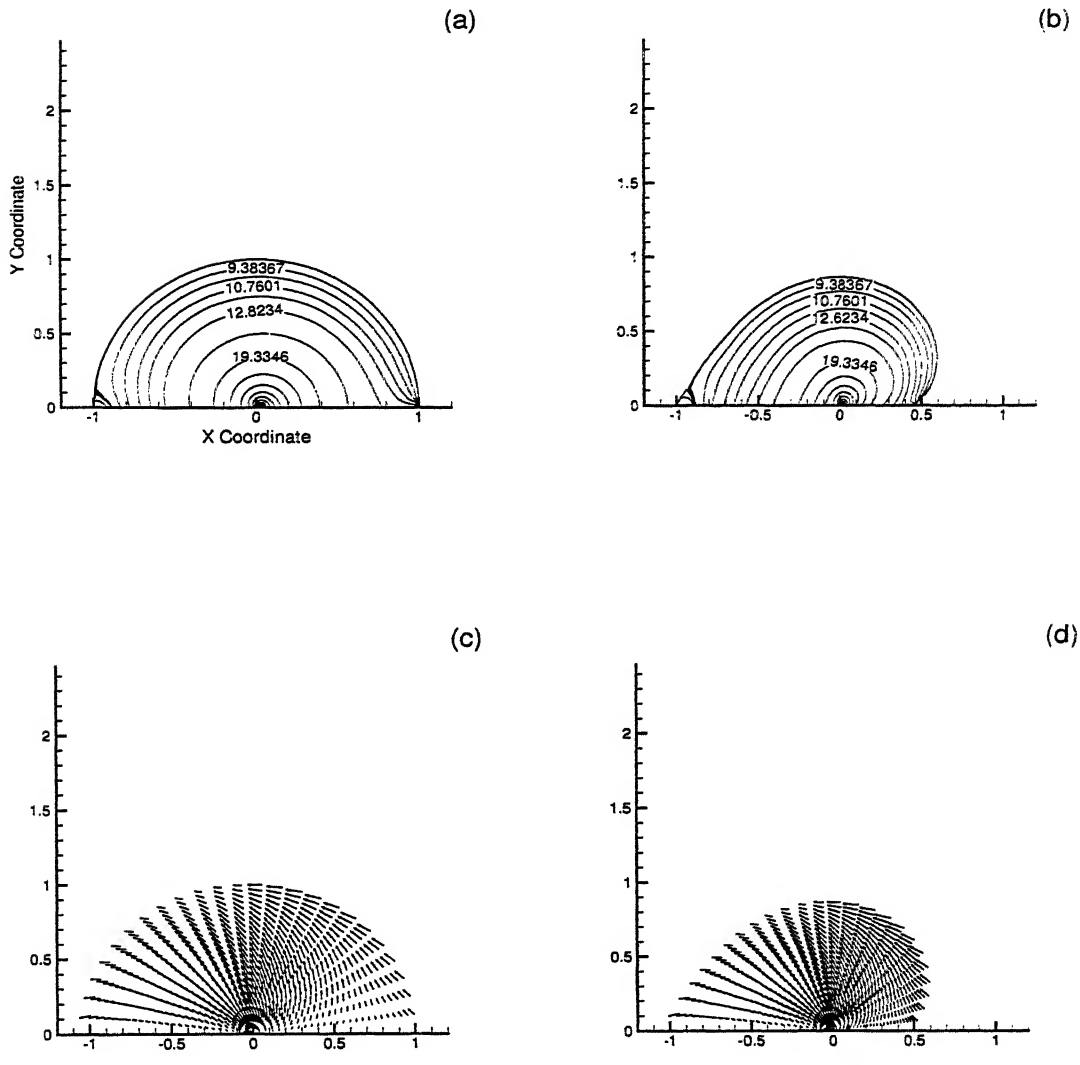

Figure 7.8: Pressure contours and velocity vectors (relative to the plate) for We=0.1 and Re=1.0. (a), (c): computational domain; (b), (d): physical domain.

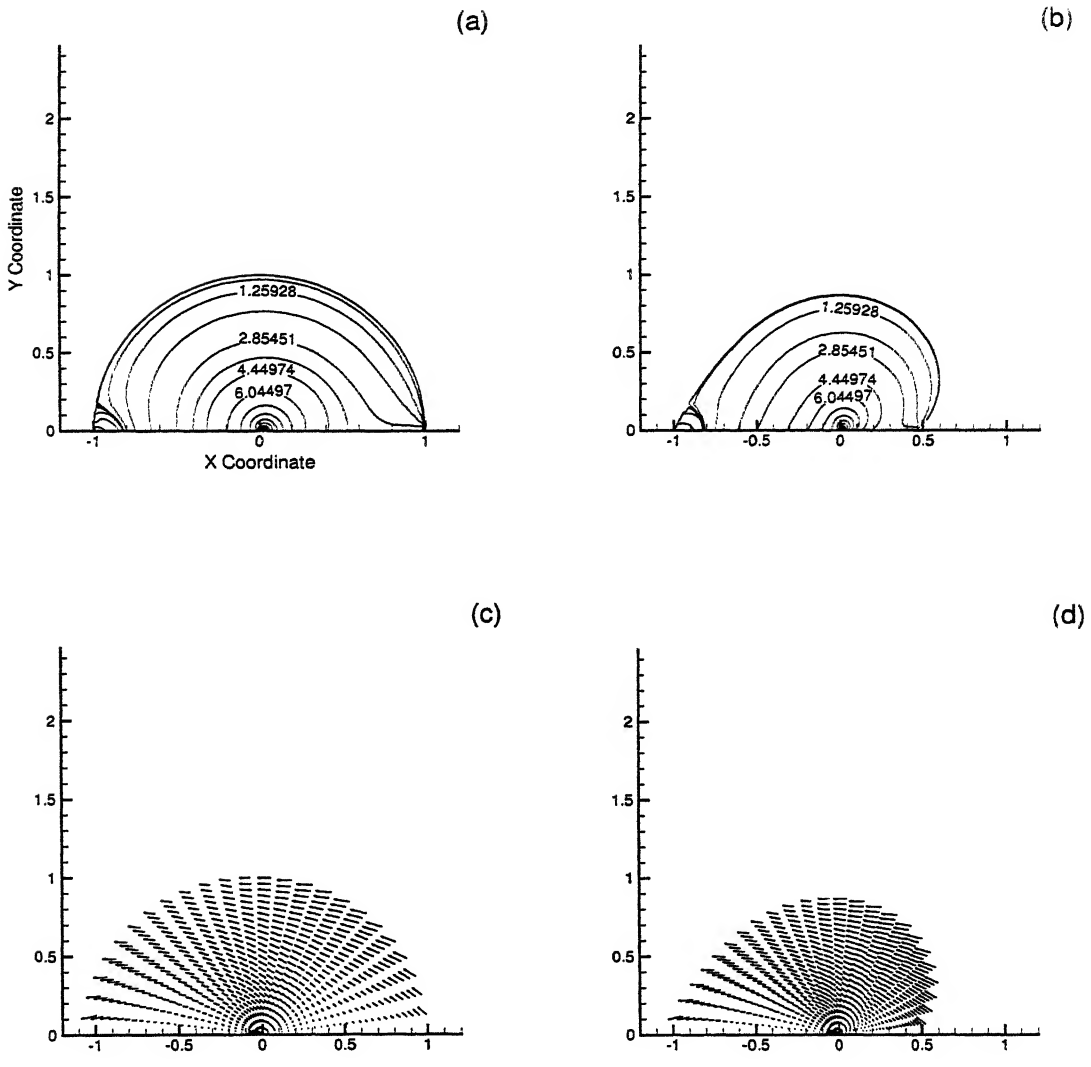

Figure 7.9: Pressure contours and velocity vectors (relative to the plate) for We=1.0 and Re=1.0. (a), (c): computational domain; (b), (d): physical domain.

Chapter 8

Proposal for studying flow fields at high Reynolds numbers and unsteady Temperature distribution

The stream function-vorticity formulation is a useful approach for solving two-dimensional incompressible flows. One of the main attractive features of this method is that it does not involve the solution of the pressure field. In the stream function-vorticity method, pressure is completely eliminated by cross-differentiation of the momentum equations.

8.1 Solution for flow fields at high Reynolds number

The mass balance equation is

$$\frac{u}{r} + \frac{\partial u}{\partial r} + \frac{1}{r}\frac{\partial v}{\partial \theta} = 0 \tag{8.1}$$

r momentum equation is

$$u\frac{\partial u}{\partial r} + \frac{v}{r}\frac{\partial u}{\partial \theta} - \frac{v^2}{r} = -\frac{\partial p}{\partial r} + \frac{1}{\mathrm{Re}}\left[\frac{\partial^2 u}{\partial r^2} + \frac{1}{r}\frac{\partial u}{\partial r} + \frac{1}{r^2}\frac{\partial^2 u}{\partial \theta^2} - \frac{2}{r^2}\frac{\partial v}{\partial \theta} - \frac{u}{r^2}\right] \tag{8.2}$$

θ momentum equation is

$$v\frac{\partial v}{\partial r}+\frac{u}{r}\frac{\partial v}{\partial \theta}+\frac{uv}{r}=-\frac{1}{r}\frac{\partial p}{\partial \theta}+\frac{1}{\mathrm{Re}}\left[\frac{\partial^2 v}{\partial r^2}+\frac{1}{r}\frac{\partial v}{\partial r}+\frac{1}{r^2}\frac{\partial^2 v}{\partial \theta^2}+\frac{2}{r^2}u-\frac{v}{r^2}\right] \tag{8.3}$$

To obtain the stream function-vorticity ($\varphi-\omega$) equation, p is eliminated from Equation (8.2) and Equation (8.3) by differentiating Equation (8.2) with respect to θ and Equation (8.3) with respect to r and subtracting one from the other. The resulting equation is expressed with vorticity ω as the dependent variable which is defined by

$$\frac{\partial^2 \varphi}{\partial r^2}+\frac{1}{r}\frac{\partial \varphi}{\partial r}+\frac{1}{r^2}\frac{\partial^2 \varphi}{\partial \theta^2}=-\omega \tag{8.4}$$

The result is

$$u\frac{\partial \omega}{\partial r}+\frac{v}{r}\frac{\partial \omega}{\partial \theta}=\frac{1}{\mathrm{Re}}\left[\frac{\partial^2 \omega}{\partial r^2}+\frac{1}{r}\frac{\partial \omega}{\partial r}+\frac{1}{r^2}\frac{\partial^2 \omega}{\partial \theta^2}\right] \tag{8.5}$$

where the radial and tangential velocity components are

$$u=\frac{1}{r}\frac{\partial \varphi}{\partial \theta} \quad \text{and} \quad v=-\frac{\partial \varphi}{\partial r} \tag{8.6}$$

The boundary conditions for the velocity are
For $\theta=0$

$$u=1 \quad \text{and} \quad v=0 \tag{8.7}$$

For $\theta=\pi$

$$u=-1 \quad \text{and} \quad v=0 \tag{8.8}$$

For $r = 0$

$$u = \text{linear interpolation between -1 and 1} \quad \text{and} \quad v = 0 \tag{8.9}$$

At the interface

$$\mathbf{u} \cdot \hat{\mathbf{n}} = 0 \quad \text{and} \quad \frac{\partial(\mathbf{u} \cdot \hat{\mathbf{t}})}{\partial \hat{\mathbf{n}}} = 0 \tag{8.10}$$

From these boundary conditions for velocity components, the boundary condition for the stream function can be found.

Transforming the Equation (8.4) into computational domain

$$A\frac{\partial^2\varphi}{\partial\xi^2} + B\frac{\partial^2\varphi}{\partial\eta^2} + C\frac{\partial^2\varphi}{\partial\xi\eta} + D\frac{\partial\varphi}{\partial\xi} + E\frac{\partial\varphi}{\partial\eta} = 0 \tag{8.11}$$

where

$$\begin{aligned} A &= \xi_r^2 + \frac{\xi_\theta^2}{r^2} \\ B &= \eta_r^2 + \frac{\xi_\eta^2}{r^2} \\ C &= 2\left(\xi_r\eta_r + \frac{\xi_\theta\eta_\theta}{r^2}\right) \\ D &= \xi_{rr} + \frac{\xi_r}{r} + \frac{\xi_{\theta\theta}}{r^2} \\ E &= \eta_{rr} + \frac{\eta_r}{r} + \frac{\eta_{\theta\theta}}{r^2} \end{aligned} \tag{8.12}$$

Transforming the Equation (8.5) into computational domain

$$A\frac{\partial^2\omega}{\partial\xi^2} + B\frac{\partial^2\omega}{\partial\eta^2} + C\frac{\partial^2\omega}{\partial\xi\partial\eta} + D\frac{\partial\omega}{\partial\xi} + E\frac{\partial\omega}{\partial\eta} = 0 \tag{8.13}$$

where

$$\begin{aligned} A &= \xi_r^2 + \frac{\xi_\theta^2}{r^2} \\ B &= \eta_r^2 + \frac{\xi_\eta^2}{r^2} \\ C &= 2\left(\xi_r\eta_r + \frac{\xi_\theta\eta_\theta}{r^2}\right) \\ D &= \xi_{rr} + \frac{\xi_r}{r} + \frac{\xi_{\theta\theta}}{r^2} - \mathrm{Re}\left(u\xi_r + \frac{v}{r}\xi_\theta\right) \\ E &= \eta_{rr} + \frac{\eta_r}{r} + \frac{\eta_{\theta\theta}}{r^2} - \mathrm{Re}\left(u\eta_r + \frac{v}{r}\eta_\theta\right) \end{aligned} \tag{8.14}$$

8.2 Solution of Pressure Equation

In the stream function-vorticity method, to obtain pressure at each grid point for viscous flow, it is necessary to solve an additional equation for pressure. This equation is derived by differentiating Equation (8.2), r momentum equation, with respect to r and Equation (8.3), θ momentum equation, with respect to θ. Combining with Equation (8.1), mass balance equation, we finally get the governing equation for pressure. The boundary conditions can also be found in terms of stream function. Thus pressure can be solved for each grid point, knowing the value of stream function.

8.3 Solution of Unsteady Thermal Energy Equation

Dimensionless form of the unsteady thermal energy equation is

$$\frac{\partial T}{\partial t} + u\frac{\partial T}{\partial r} + v\frac{1}{r}\frac{\partial T}{\partial \theta} = \frac{1}{\mathrm{Pe}}\left(\frac{\partial^2 T}{\partial r^2} + \frac{1}{r}\frac{\partial T}{\partial r} + \frac{1}{r^2}\frac{\partial^2 T}{\partial \theta^2}\right) \tag{8.15}$$

where $\mathbf{u}$, T, t are the dimensionless form of velocity, temperature difference and

time scaled by u_o, ΔT and r_1/u_o respectively.
Initial condition is
At t=0

$$T = 1 \tag{8.16}$$

Boundary conditions are
For $\theta = 0$ and $\theta = \pi$

$$T = 0 \tag{8.17}$$

For $r = 0$

$$T = 0 \tag{8.18}$$

For $r = 1$

$$T = 1 \tag{8.19}$$

Transformation to the computational domain leads to the following dimensionless form of the governing equation in computational domain

$$\frac{\partial T}{\partial t} = A\frac{\partial^2 T}{\partial \xi^2} + B\frac{\partial^2 T}{\partial \eta^2} + C\frac{\partial^2 T}{\partial \xi \eta} + D\frac{\partial T}{\partial \xi} + E\frac{\partial T}{\partial \eta} \tag{8.20}$$

where

$$\begin{aligned}
A &= \frac{1}{\mathrm{Pe}}\left(\xi_r^2 + \frac{\xi_\theta^2}{r^2}\right) \\
B &= \frac{1}{\mathrm{Pe}}\left(\eta_r^2 + \frac{\eta_\theta^2}{r^2}\right) \\
C &= \frac{2}{\mathrm{Pe}}\left(\xi_r \eta_r + \frac{\xi_\theta \eta_\theta}{r^2}\right) \\
D &= \frac{1}{\mathrm{Pe}}\left(\xi_{rr} + \frac{\xi_r}{r} + \frac{\xi_{\theta\theta}}{r^2}\right) - u\xi_r - v\frac{\xi_\theta}{r} \\
E &= \frac{1}{\mathrm{Pe}}\left(\eta_{rr} + \frac{\eta_r}{r} + \frac{\eta_{\theta\theta}}{r^2}\right) - u\eta_r - v\frac{\eta_\theta}{r}
\end{aligned} \tag{8.21}$$

Discretizing Equation (8.16) by finite differences. we get

$$T_{i,j}{}^{1} = 1 \tag{8.22}$$

Discretizing the boundary conditions by finite differences. we get
For $\eta = 0$

$$T_{i,1}{}^{p} = 0 \tag{8.23}$$

where i goes from 2 to $n-1$
For $\eta = \pi$

$$T_{i,m}{}^{p} = 0 \tag{8.24}$$

where i goes from 2 to $n-1$
For $\xi = 0$

$$T_{1,j}{}^{p} = 0 \tag{8.25}$$

where j goes from 1 to m
For $\xi = 1$

$$T_{n,j}{}^{p} = 1 \tag{8.26}$$

where j goes from 1 to m, p denotes particular time step. Discretization variable in radial direction (ξ) is i, its value ranges from 1 to n. Discretization variable in angular direction (η) is j, its value ranges from 1 to m.
There are three popular schemes available for solving initial value unsteady problems. These are

1. Euler method (or explicit method)

2. Crank-Nicholson method

3. Pure implicit method

Of these three methods, Crank-Nicholson is the most accurate and pure implicit is the most stable. To make an optimum choice out of these three, pure implicit method is usually preferred over the other two. In the pure implicit method, the time derivative at the new time is used to move ahead in time. Thus

$$T^{p+1} = T^p + \left.\frac{\partial T}{\partial t}\right|^{p+1} \Delta t \tag{8.27}$$

Here $\left.\frac{\partial T}{\partial t}\right|^{p+1}$ is substituted from Equation (8.20) in Equation (8.27), hence we get an expression in T^{p+1} which can then be solved iteratively using the Gauss-Seidel method.

8.4 Drop Cluster and Coalescence

When a single drop is surrounded by many drops, then there is much probability that this drop will coalesce with one or more of its surrounding drops. Thus in the study of multiple drops, the phenomena of coalescence becomes significant.

When two drops of radius R touch surface tension drives an initially singular motion which joins them into a bigger drop with smaller surface area. Eggers *et al.* (1999) showed that this motion is always viscously dominated at early times. They focused on the early-time behavior of the radius r_m of the small bridge between the two drops. The flow is driven by a highly curved meniscus of length $2\pi r_m$, and width $\Delta \ll r_m$ around the bridge, from which it can be concluded that the leading-order problem is asymptotically equivalent to its two-dimensional counterpart. For the case of inviscid surroundings, an exact two-dimensional solution (Hopper, 1990) shows that $\Delta \propto r_m^3$ and $r_m \sim (t\gamma/\pi\eta)ln[t\gamma/(\eta R)]$; and the same is true in three dimensions. (Hopper, 1990) also studied the case of coalescence with an external viscous fluid. A significantly different structure is found in which the outer-fluid forms a toroidal bubble of radius $\Delta \propto r_m^{3/2}$ at the meniscus and $r_m \sim (t\gamma/4\pi\eta)ln[t\gamma/(\eta R)]$. This basic difference is due to the presence of the outer-fluid viscosity, however small.

When a droplet of radius r_1 touches or overlaps a droplet of radius r_2, a new droplet is formed, centered on the center of mass of the two original drops. If this

droplet overlaps one or more other droplets, they are coalesced and this procedure continues until no overlaps remain.

8.5 Results and Discussion

Results for the unsteady temperature problem are shown in Figure 8.1. Figure (a), (b), (c), (d) shows the temperature contours (Pe=0.01) in a deformed drop at 11^{th}, 23^{th}, 35^{th}, 47^{th} time steps and Figure (e) shows temperature contours at 47^{th} time step in the computational domain. Figure (f) shows the temperature evolution for a particular grid point. Steady state was reached in 47^{th} time step.

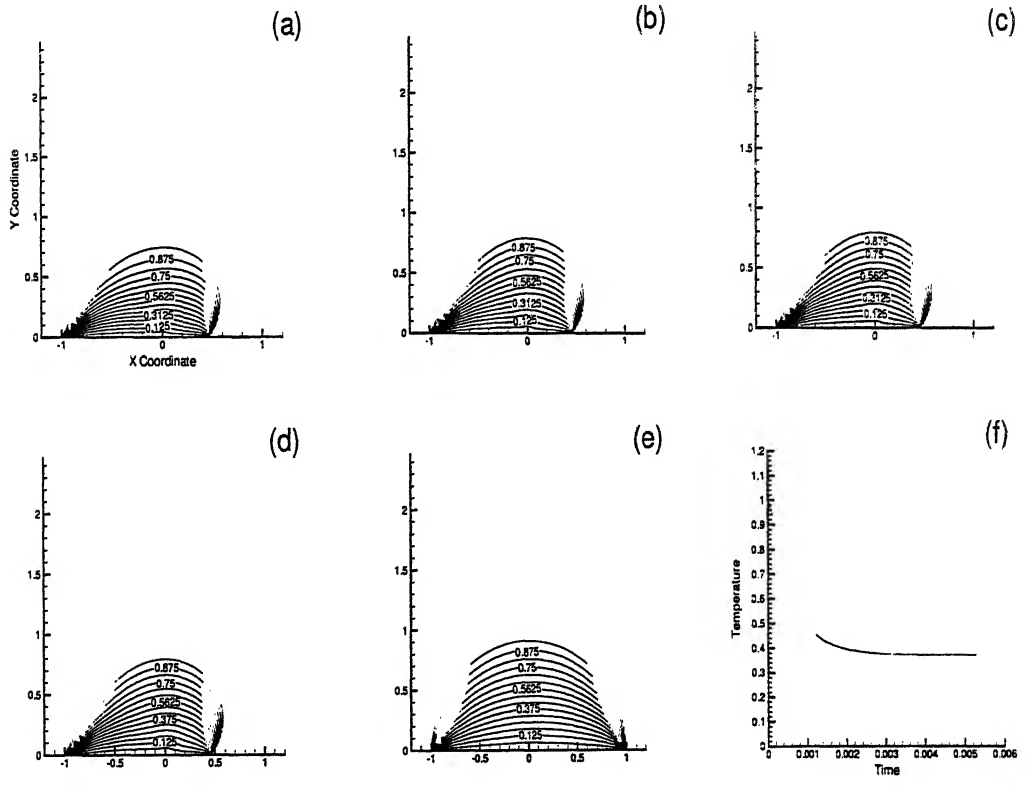

Figure 8.1: Temperature contours (Pe=0.01) in a deformed drop (a) at 11^{th} time step, (b) at 23^{rd} time step, (c) at 35^{th} time step, (d) at 47^{th} time step, (e) in the computational domain (semi-circular region) at 47^{th} time step, (f) temperature evolution for a particular grid point with time.

Chapter 9

Conclusions and Scope for Future Work

Drop shapes above and below an inclined and horizontal flat plate, are generated. Stability analysis of sessile and pendant drops were carried out for different plate inclinations. It was observed that with increasing plate inclination, the drop becomes more unstable. Three liquids were considered namely, mercury, bismuth and water, besides having different densities and coefficient of surface tension, their contact angles are also different. The plate inclination was varied from 0 to 30^0. A formulation for the moment generated by forces that slide the drop down the incline is also presented.

Numerical solution for pressure, velocity are obtained for a semi-circular drop. The results are reported for three orders of magnitude variation, of Weber number and Reynolds number. For a deformed drop, the grids are mapped from the physical domain to computational domain. The governing equations and boundary conditions are then transformed in the computational domain. After obtaining the solution for pressure and velocity in the computational domain, then using transformation relations, solution for pressure and velocity in the physical domain is obtained. Unsteady temperature contours have also been obtained for a deformed drop.

The numerical solutions obtained are for a two dimensional geometry and for Stokes flow. A proposal for solving pressure and velocity for Reynolds number greater than one, and drop coalescence has also been provided.

Results show that the coefficient of friction increases as Reynolds number and Weber number decreases. The effect of deformation is seen in the local pressure

and velocity fields, but the overall impact on the coefficient of friction is small.

Scope for future work consists of obtaining pressure and velocity fields for Reynolds number greater than unity. Pressure and velocity solution for three dimensional drop is also recommended for future work. Modeling for coalescence is required both for two dimensional and three dimensional drops.

References

[1] Beysens, D., The formation of dew, *Atm. Res.*, Vol. 39, pp. 215-237. 1995.

[2] Brown, R. A., Jr., Orr F. M., and Scriven, L. E., Static Drop on an inclined plate: Analysis by the Finite Element Method, *J. Colloid Interface Sci.*, Vol. 73, pp. 76-87, 1980.

[3] Burnside, B. M., and Hadi, H. A., Digital computer simulation of dropwise condensation from equilibrium droplet to detectable size, *Int. J. Heat Mass Transfer*, Vol. 42, pp. 3137-3146, 1999.

[4] Dimitrakopoulos, P., and Higdon, J. J. L., On the gravitational displacement of three-dimensional fluid droplets from inclined solid surfaces. *J. Fluid Mech.*, Vol. 395, pp. 181-209, 1999.

[5] Dussan, V., E. B., and Chow, R. T.-P., On the ability of drops or bubbles to stick to non-horizontal surfaces of solids, *J. Fluid Mech.* Vol. 137, pp. 1-29, 1983.

[6] Dussan, V., E. B., On the ability of drops or bubbles to stick to non-horizontal surfaces of solids. Part 2. Small drops or bubbles having contact angles of arbitrary size, *J. Fluid Mech*, Vol. 151. pp. 1-20, 1985.

[7] Eggers, J., Lister, J. R., and Stone, H. A., Coalescence of liquid drops.*J. Fluid Mech.*, Vol. 401, pp. 293-310, 1999.

[8] Eggers, J., Coalescence of spheres by surface diffusion, *Phys. Rev. Lett.*, Vol. 80, pp. 2634-2637, 1998.

[9] Elyousfi, A. B. A., Chesters, A. K., Cazabat, A. M., and Villette, S., Approximate Solution for the Spreading of a Droplet on a Smooth Solid Surface, *J. Colloid Interface Sci.*, Vol. 207, pp. 30-40, 1998.

[10] Family, F., and Meakin, P., Kinetics of droplet growth processes: Simulation, theory, and experiments, *Phys. Rev. A*, Vol. 40. pp. 3836-3854. 1989.

[11] Furmidge, C. G. L., Studies at Phase Interfaces 1. The sliding of liquid drops on solid surfaces and a theory for spray retention, *J. Colloid Sci.*. Vol. 17, pp. 309-324, 1962.

[12] Hopper, R. W., Plane Stokes flow driven by capillarity on a free surface. *J. Fluid Mech.*, Vol. 213, pp. 349-375, 1990.

[13] Huh, C., and Scriven, L. E., Hydrodynamic Model of Steady Movement of a Solid/Liquid/Fluid Contact Line. *J. Colloid Interface Sci.*, Vol. 35. pp. 85-101, 1971.

[14] Iliev, S. D., Static Drops on an Inclined Plane: Equilibrium Modeling and Numerical Analysis, *J. Colloid Interface Sci.*, Vol. 194, pp. 287-300. 1997.

[15] Karmakar, D., Modeling of Drop Shapes Above and Below Horizontal and Inclined Surfaces, M. Tech. thesis, Indian Institute of Technology Kanpur. kanpur, 2001.

[16] Kim, H.-Y., Lee, H. J., and Kang, B. H., Sliding of Liquid Drops Down an Inclined Solid Surface, *J. Colloid Interface Sci.*, Vol. 247. pp. 372-380. 2002.

[17] Liu, H., *Science and Engineering of Droplets*, Noyes Publications. United States of America, 2000.

[18] Muralidhar, K., and Sundararajan, T., *Computational Fluid Flow and Heat Transfer*, Narosa Publishing House, New Delhi. 1995.

[19] Pozrikidis, C., *Introduction to Theoritical and Computational Fluid Dynamics*, Oxford University Press, New York, 1997.

[20] Rother, M. A., Zinchenko, A. Z., and Davis, R. A., Buoyancy-driven coalescence of slightly deformable drops, *J. Fluid Mech.*, Vol. 346, pp. 117-148. 1997.

[21] Wang, H., and Davis, R. H., Collective Effects of Gravitational and Brownian Coalescence on Droplet Growth, *J. Colloid Interface Sci.*, Vol. 178. pp. 47-52, 1996.

[22] Yiantsos, S. G., and David, R. H., Close approach and deformation of two viscous drops due to gravity and van der Waals forces, *J. Colloid Interface Sci.*, Vol. 144, pp. 412-433, 1991.